ABSTRACT

Title of Dissertation: DEVELOPMENT OF A DECISION/DEPLOYMENT SUPPORT TOOL FOR VARIABLE SPEED LIMITS IN RECURRENT CONGESTION

Mark Louis Franz, Doctor of Philosophy, 2015

Dissertation Directed by: Professor Gang-Len Chang

Department of Civil and Environmental Engineering

Traffic demand increases are pushing aging ground transportation infrastructures to their theoretical capacity. The result of this demand is traffic bottlenecks that are a major cause of delay on urban freeways. In addition, the queues associated with those bottlenecks increase the probability of a crash while adversely affecting environmental measures such as emissions and fuel consumption. With limited resources available for network expansion, traffic professionals have developed active traffic management systems (ATMS) in an attempt to mitigate the negative consequences of traffic bottlenecks. Among these ATMS strategies, variable speed limits (VSL) and ramp metering (RM) have been gaining international interests for their potential to improve safety, mobility, and environmental measures at freeway bottlenecks.

Though previous studies have shown the tremendous potential of variable speed limit (VSL) and VSL paired with ramp metering (VSLRM) control, little guidance has been developed to assist decision makers in the planning phase of a congestion mitigation project that is considering VSL or VSLRM control. To address this need, this study has developed a comprehensive decision/deployment support tool for the application of VSL and VSLRM control in recurrently congested environments. The decision tool will assist practitioners in deciding the most

appropriate control strategy at a candidate site, which candidate sites have the most potential to benefit from the suggested control strategy, and how to most effectively design the field deployment of the suggested control strategy at each implementation site. To do so, the tool is comprised of three key modules, (1) Decision Module, (2) Benefits Module, and (3) Deployment Guidelines Module. Each module uses commonly known traffic flow and geometric parameters as inputs to statistical models and empirically based procedures to provide guidance on the application of VSL and VSLRM at each candidate site. These models and procedures were developed from the outputs of simulated experiments, calibrated with field data.

To demonstrate the application of the tool, a list of real-world candidate sites were selected from the Maryland State Highway Administration Mobility Report. Here, field data from each candidate site was input into the tool to illustrate the step-by-step process required for efficient planning of VSL or VSLRM control. The output of the tool includes the suggested control system at each site, a ranking of the sites based on the expected benefit-to-cost ratio, and guidelines on how to deploy the VSL signs, ramp meters, and detectors at the deployment site(s).

This research has the potential to assist traffic engineers in the planning of VSL and VSLRM control, thus enhancing the procedure for allocating limited resources for mobility and safety improvements on highways plagued by recurrent congestion.

DEVELOPMENT OF A DECISION/DEPLOYMENT SUPPORT TOOL FOR VARIABLE SPEED LIMITS IN RECURRENT CONGESTION

By

Mark Louis Franz

Dissertation submitted to the Faculty of the Graduate School of the
University of Maryland, College Park in partial fulfillment
of the requirements for the degree of
Doctor of Philosophy
2015

Advisory Committee:
Professor Gang-Len Chang, Chair
Professor Martin Dresner
Associate Professor Cinzia Cirillo
Associate Professor David Lovell
Dr. David Yang

Dedication

To my beautiful wife Jennifer whose love and support keeps me focused and motivated. To my father, William, mother, Susan, my sister, Heather, my brother, Sean, for their encouragement and love, and to my in-laws Joe, Al, and Mona for always believing in me. I love you all from the bottom of my heart.

Acknowledgements

This great achievement would not have been possible without the support and guidance from my family, friends, colleagues, and committee members.

Thank you to my advisor, Dr. Gang-Len Chang for his persistence in encouraging me to challenge myself to achieve goals I never thought possible. His guidance has molded me into a professional researcher and will be very valuable in my future career.

I would also like to express my sincere gratitude to my dissertation committee members, Dr. Cinzia Cirillo, Dr. Martin Dresner, Dr. David Lovell, and Dr. David Yang for their valuable and constructive comments to improve the quality of my research. I would also like to thank Dr. Lei Zhang for his patience and understanding while I completed my degree.

Next, I would like to thank my friends and colleagues, Sung-Yoon Park, Jean-Michel Tremblay, Yang (Karl) Lu, Hyeonmi Kim, Dr. Xianfeng Yang, Dr. Woon Kim, Dr. Chen-Lun Lan, Yao Chen, Dr. Lei Zhang, Hyoshin Park, and Dr. Carlos Carrion for all of their support.

Lastly, I would like to express my deepest appreciation to my wife Jennifer, father, William, mother, Susan, sister, Heather, brother, Sean, and my in-laws Joe, Al, and Mona for their love and support through all of ups and downs of attaining my doctoral degree. Without them, this dissertation would not have been possible.

Table of Contents

List of Figures

List of Tables

Chapter 1: Introduction and Background

1.1 VSL and Ramp Metering Background

Traffic demand increases are pushing aging ground transportation infrastructures to their theoretical capacity. The result of this demand is traffic bottlenecks that are a major cause of delay on urban freeways. In addition, the queues associated with those bottlenecks increase the probability of a crash while adversely affecting environmental measures such as emissions and fuel consumption. With limited resources available for network expansion, traffic professionals have developed active traffic management systems (ATMS) in an attempt to mitigate the negative consequences of traffic bottlenecks. Among these ATMS strategies, variable speed limits (VSL) and ramp metering (RM) have been gaining international interests for their potential to improve safety, mobility, and environmental measures at freeway bottlenecks.

VSL are speed limits that can change based on real-time traffic and/or weather conditions. The changed speed limits are communicated to road users in a number of ways, such as overhead gantries, variable message signs (VMS) and electronic roadside speed limit signs. The activation of the VSL system and the control logic for updating the VSL may be controlled manually by a traffic management center (TMC) or by using real-time traffic data as part of an intelligent transportation system (ITS). In either case, the primary objective of VSL is to harmonize the traffic flow upstream of a bottleneck. This harmonization is most commonly accomplished by gradually reducing the speed limit on the segment upstream of the bottleneck location. In doing so, the shockwaves associated with vehicle deceleration are suppressed, resulting in improved traffic safety. Interestingly, an inherent consequence of reducing speeds upstream of a congested segment is inflow control. Thus, a properly executed VSL control system will not only improve safety but

may also improve measures of mobility by delaying the onset of the bottleneck formation and reducing the duration and severity of the congestion period.

Another ATMS strategy that is more commonly used in practice is ramp metering. Ramp metering is a traffic inflow control strategy that restricts the number of vehicles entering a congested segment from nearby on-ramps. This ramp inflow control is typically achieved by installing traffic signals on the on-ramps within the vicinity of the recurrently congested segment. Similar to VSL, when properly applied to a congested segment, the duration and severity of the congestion may be reduced. This benefit is achieved by shifting some of the mainline delay to the associated on-ramps. While this strategy may increase the travel time for some road users, the total time spent for all road users may be reduced relative to the no-control scenario.

Recognizing the potential for VSL and ramp metering to mitigate congestion, several researchers have investigated the integration of these two strategies. As will be discussed in Chapter 2, VSL control with integrated ramp metering (VSLRM) can enhance the benefits of either of the independent control strategies. These benefits result from the coordination of inflow control offered by this hybrid strategy. The scope of this study will analyze the use of VSL and VSLRM in recurrently congested environments.

1.2 Critical Issues Related to VSL and Ramp Metering

Interestingly, most of the previous work on this topic focused on the evaluation of VSL or VSLRM control at a specific site suffering from the ill effects of a bottleneck. Although this methodology is useful for testing control strategies and estimating the site-specific benefits of these control strategies, it does not directly assist decision-makers in the planning process of a congestion mitigation project considering the utilization of VSL or VSLRM control.

The first step in the planning process is to determine which if either of these control strategies is the most appropriate for a candidate site. In addition, though VSLRM control generally outperforms independent VSL or ramp metering control, little guidance has been developed on which conditions warrant the use of VSLRM over independent VSL.

The next step in the planning process is to evaluate the potential benefit resulting from the implementation of the control strategy at a given candidate site. As will be discussed in Chapter 3, there is a range of methods available to perform such investigations. Here, over-simplified methods such as applying engineering judgement may result in an inaccurate estimation of benefits, resulting in improper deployment decisions and wasted resources. On the other hand, more rigorous evaluation methods such as the use of traffic simulation require significant time and effort from trained traffic simulation experts, further restricting limited resources. Moreover, it is reasonable to assume that a given traffic agency will have several candidate sites for congestion mitigation efforts and will not likely have enough resources to intervene at each of them. Therefore, it is necessary to investigate the potential benefits at each candidate site for prudent resource allocation. Thus, there is a need to develop a tool that can efficiently and accurately estimate the expected benefits from VSL or VSLRM control at multiple candidate sites. The associated outputs can then be used to target limited resources at sites with the most potential benefit.

Upon determining which sites have the most potential to benefit from VSL or VSLRM intervention, the list of deployment sites can be generated. The final step of the planning process is to determine the control area and locations of the critical control infrastructure, including VSL signs, ramp meters, and the associated detectors needed for real-time system control at each deployment site.

To summarize, the following critical issues/research questions are identified:

1. What conditions warrant the implementation of VSL control?
2. What conditions warrant the addition of supplemental ramp metering to VSL control?
3. What conditions do not warrant the use of either of these ATMS?
4. Upon selecting either of these two ATMS at a given site, what is the expected overall benefit?
5. When considering multiple sites, which site(s) have the greatest potential for benefit?
6. At each deployment site, what is the control segment under the selected control strategy?
    a. Where should the VSL signs be located?
    b. Which ramps should be metered?
    c. Where should the detectors be located to control the system logic?

Recognizing these issues, there is a need to develop a comprehensive planning tool that can assist in determining the most appropriate control strategy, estimate the expected benefits resulting from the suggested control strategy, and provide guidance on how to deploy the suggested control strategy at a given candidate site.

1.3 Research Objectives and Critical Tasks

In light of the aforementioned research needs, this section describes the specific objectives and associated key tasks of this research. The focus of this research is the planning process for VSL and VSLRM on recurrently congested freeways. However, many of the methodologies and contributions presented in this dissertation may be relevant to other ATMS applications. In any case, the goals of this research are to address some of the crucial issues in VSL/VSLRM research by establishing the following objectives:

1. Describe the state of the practice in VSL and VSLRM research.
2. Create a VSL control system that reflects the underlying parameters of commonly applied real-time VSL control logic.
3. Design a supplementary ramp metering control algorithm that reflects common parameters of real-time ramp metering logic.
4. Design an experiment to generate a robust dataset of potentially congested environments to evaluate the benefits of VSL and VSLRM control across a multitude of traffic environments.
5. Develop and evaluate a comprehensive decision/deployment support tool for the planning of VSL and VSLRM control in recurrent congestion. This tool must provide guidance on the control decision, efficiently and accurately estimate expected benefits, assist in deployment site selection, and assist in locating the critical control system components at each deployment site.
6. Demonstrate the usefulness of the developed tool to traffic operation practitioners/decision-makers.

To accomplish the above mentioned objectives, this research is guided by the following key tasks:

Task 1: Present a thorough literature review of existing studies of VSL and VSLRM. This task will illustrate the various VSL/VSLRM control algorithms, commonly used performance measures, VSL impact on traffic flow, and results of VSL/VSLRM implementation in both field and simulated environments.

Task 2: Create a VSL control algorithm designed to reflect the underlying logic of common VSL control systems. The VSL system must create a safe speed transition zone from free-flow conditions down to the desired control speed. Using real-time traffic data, the system can adapt to the evolution of the congestion. However, the activation, updating, and deactivation of the target control segment and control speed must be subject to safety constraints.

Task 3: Develop a ramp metering control algorithm designed to complement VSL control while reflecting the logic of common ramp metering systems. The inputs of the ramp metering control system will share many of the same data inputs as the VSL control system.

Task 4: Using data from a VSL field deployment, calibrate a VSL simulation environment to be used as a basis for developing a robust dataset to develop the planning module. Starting with the calibrated simulation, alter traffic flow parameters, road geometry features, and driver behavior variables to develop a diverse sample of possible VSL and VSLRM candidate sites. This set of variables is considered the control variables in this experiment. These simulations represent the “No Control” (i.e., base) scenarios. Next, the proposed VSL and VSLRM control strategies must be implemented and evaluated in each of the simulated environments. The

effectiveness of each control system will be evaluated via changes in safety and mobility relative to the no-control case.

Task 5: Develop and evaluate several decision models for VSL/VSLRM control selection using the outputs of the simulated experiments. These models will use the control variables as inputs with hypothetical decisions based on the overall benefit of the associated control strategy. Here, four mutually exclusive decisions are possible, under-congested (i.e. control not needed), VSL control implementation, VSLRM control implementation, or over-congested (i.e. consider other congestion mitigation strategies).

Task 6: Develop and evaluate an estimated benefits model for each control strategy. These models will also use the control variables as inputs to estimate the overall benefit of a given control strategy.

Task 7: Establish guidelines for the deployment of VSL and VSLRM control. These guidelines will establish the location of traffic detectors, VSL signs, and ramp meters needed for efficient VSL and VSLRM control.

Task 8: Describe the step-by-step procedures of applying the tool to real-world data. This illustrative example will highlight the key functions of the tool, including control decision assistance, benefit estimation, site ranking, and finally, field deployment of the critical control system parameters at a real-world bottleneck location.

Task 9: Discuss future research paths for the use of VSL and VSLRM in recurrent congestion conditions.

1.4 Dissertation Organization

Based on the above mentioned objectives and critical tasks, this dissertation consists of eight chapters, summarized in Figure 1.1. The following chapter presents an in-depth review of VSL and VSLRM control. This review includes the application of VSL control, the impact of VSL control on traffic flow, VSL control algorithms, impact of driver compliance to VSL control, and results of both field and simulated VSL studies. The potential for pairing VSL with ramp metering is also presented. Chapter 3 presents the overall structure of the proposed decision/deployment support tool. Here, the data needs, key functions, and interrelations of those functions are described. Next, Chapter 4 presents experiment design, including the description of the control algorithms. This chapter discusses the effort in calibrating and building the simulation dataset used in the subsequent development of the decision/deployment support tool. Chapter 5 discusses development and results of the decision and benefits modules of the tool, including the calculation of the performance measures and theoretical background on the applied statistical models. Next, Chapter 6 explains the development of the operation guidelines for VSL and VSLRM control. Topics covered include the development of a procedure for determining the control segment, and the location of VSL signs, ramp meters, and detectors. Chapter 7 presents a real-world application of the developed decision/deployment support tool. The paper concludes with Chapter 8, which summarizes the contributions of this research and future research paths.

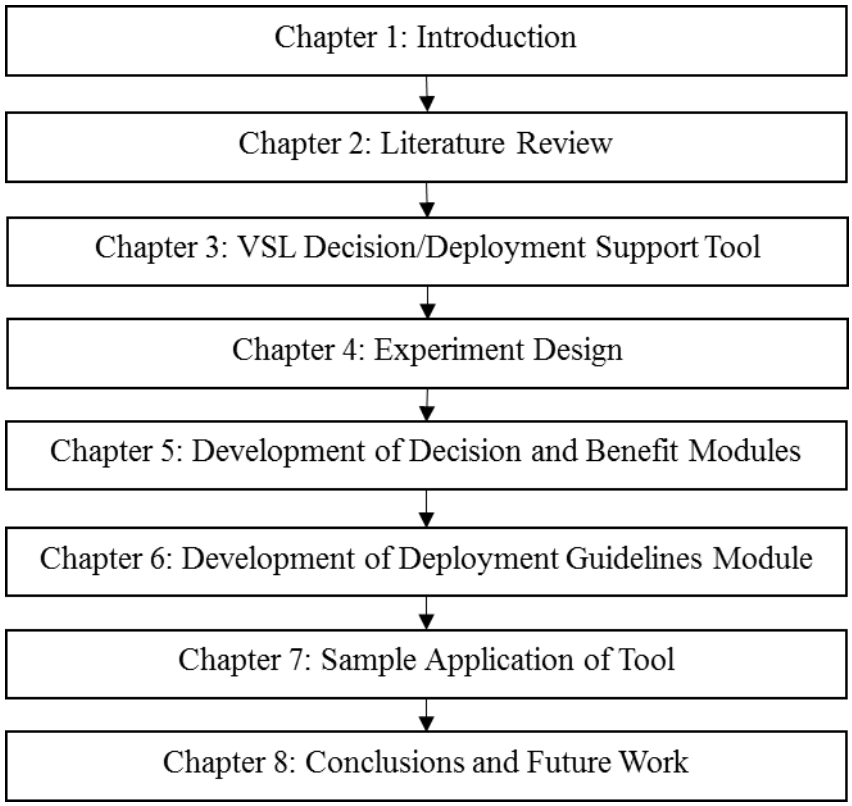

Figure 1.1: Dissertation Organization

Chapter 2: Literature Review

2.1 Chapter Organization

This chapter presents the existing research on the VSL control. First, a summary of the studies describing the impact of VSL control on traffic flows is presented. Second, the common applications of VSL control are discussed. The next section describes a variety of VSL control algorithms, followed by a summary of the results from both simulated and field-deployed studies of VSL in recurrent congestion. Next, the studies on the potential effectiveness of VSL paired with ramp metering control are presented. The chapter concludes by summarizing the existing research on VSL control and discusses the ongoing research needs used to guide this analysis.

2.2 VSL Effect on Traffic Flow

Several researchers have investigated the impact of VSL on the traffic flows over the past decades. Papageorgiou et al. (2008) explored the effects of VSL on traffic flows by comparing the flow-occupancy curves for different speed limits. The authors found that at under-critical densities VSL can flatten the slope of the flow-occupancy diagram and shift the critical occupancy to a higher value. Heydecker and Addison (2011) analyzed the relationship between speed and density for freeways under VSL control. Using one-minute aggregated data, a speed-density relationship was created using log-likelihood value comparisons. The study discovered that capacity increased when speed control was implemented. In relation, the research by Nissan and Koutsopoulos (2011) evaluated the effectiveness of VSL using level of service under several control scenarios. Interestingly, the study found that the definition of level of service E was dependent on the implemented traffic controls. A similar finding was discovered by Wang and Ioannou (2011), reporting

that the change in speed limit for a long period, such as in the case of inclement weather or long-term work zones, can change the shape of the fundamental diagram. Kononov, et al. (2012) investigated the relationship between flow/density, speed, and crash rate using neural networks to calculate a Flow Crash Potential Indictor under various conditions. The study found that crash rates remain constant until a critical threshold of speed and density is achieved. Further research on the effect of VSL on traffic flow was conducted by Kianfar et al. (2013), who investigated the operational impacts of a field-deployed VSL system on I-270 in the state of Missouri. Statistical tests showed that the flow-occupancy diagram changed significantly under VSL control in seven of eight congested locations. The slopes of the flow-occupancy function at over-critical occupancies were steeper under VSL control, which demonstrates a more rapid approach to jam density under VSL control. The study also found inconsistencies in the impact of VSL on the congestion duration and throughput under VSL control. The authors noted that the control algorithm and associated control parameters can affect the observed benefits of a VSL system.

The study of Lu et al. (2014) showed that a properly implemented VSL control system could help postpone bottleneck formation and expedite recovery from congestion. Lastly, the work of Carlson et al. (2011) showed the impact of VSL on fundamental traffic flow relationships, as illustrated in Figure 2-1. As shown in Figure 2-1(a), at under-critical densities, VSL will reduce the flow rate. However, Figure 2-1(b) shows that at densities beyond the critical density, VSL control can increase traffic flow rates. In Figure 2-1(b), each curve represents the fraction of the original speed limit (e.g., b= 0.8 represents 80 percent of the original speed limit). Thus, for a given over-critical density, there exists a speed limit that can maximize the flow rate.

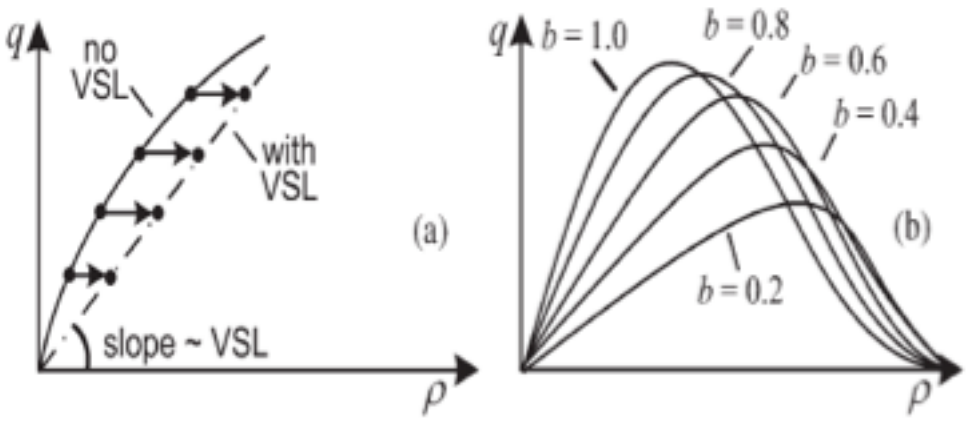

Figure 2-1: Effect of VSL on the Flow-Density Diagram (Carlson et al. 2011)

2.3 VSL Applications

With the potential for VSL to curtail the adverse consequences of traffic bottlenecks and the associated shockwave formation, several specific applications have been developed. The most prevalent VSL applications that have emerged from the literature are for use in inclement weather conditions, work zones, and in recurrent congestion.

2.3.1 Inclement Weather

Several safety studies have shown a correlation between adverse weather conditions and increased crash frequencies (Caliendo et al., 2007, Malyshkina et al., 2009, and Yu and Abdel-Aty, 2013). To address this issue, several traffic studies have experimented with VSL control to improve traffic safety.

In the U.S., several states such as Nevada, New Mexico (Robinson 2000), New Jersey, Alabama, Tennessee (Goodwin and Pisano, 2003), and Washington (Ulfrasson and Shankar, 2005) have investigated VSL systems that are activated based on precipitation, visibility, and pavement conditions. In addition, the work of Buddemeyer et al. (2010) and the associated study by Layton and Young (2011) investigated the use of regulatory VSL

in Wyoming winter weather. These studies found that, in general, VSL was effective at reducing the speeds of vehicles in inclement weather conditions. However, speed variation was sometimes increased under VSL control, potentially explained by compensatory behavior of drivers.

The use of VSL in poor weather has also been applied in other countries. For example, Australia and the Netherlands have deployed an advisory VSL system to prevent rear-end crashes in foggy conditions (Robinson, 2000). Further applications of VSL in poor weather were studied in Germany (Jonkers and Klunder, 2008), Finland (Rämä, 1999), and Canada (Steel a 2005).

2.3.2 Work Zones

Temporary traffic control caused by work zones inherently create bottlenecks by reducing or removing shoulders as well as travel lanes. While such measures are needed to build and maintain traffic infrastructure, work zones often reduce the mobility and safety of workers and motorists. Such scenarios are suspect to improvement by advanced warning systems and speed control. In fact, several studies have been conducted to assess the potential benefits of VSL control in work zone applications.

Several studies such as Park and Yadlapati (2003), Kang et al. (2004), Kang and Chang (2007), Lin et al. (2004), Fudala et al. (2010) and Radwan et al. (2011) have explored the potential of VSL to improve safety and mobility in work zone applications. The results of these simulated studies show that VSL has the potential to increase throughput while improving surrogate measures of safety in work zone environments.

In general, the results from the simulated studies were realized by several field deployments of VSL in work zones. The study by Lyles et al. (2004) in Michigan found that average speeds increased and travel times decreased, while speed variation did not significantly change. Kwon et al. (2007) analyzed an advisory VSL system in Minnesota that showed increased throughput and reduced speed variance during the analysis period. A similar finding of reduced speed variance was observed by McMurtry et al. (2009) in Utah. The study by Nicholson et al. (2011) in Virginia found no significant change in measures of speed, but some improvement in travel times. Outside the U.S., VSL is used to manage work zone traffic in Copenhagen, Denmark (Mirshahi et al., 2007).

2.3.3 Recurrent Congestion

Due to the frequent and predictable occurrence of peak-hour congestion in many of the world's urban networks, applications of VSL in recurrent congestion have become one of the most researched ATMS strategies in recent years. In fact, researchers from across the globe have investigated the potential for VSL control to improve mobility, safety, and environmental considerations. The remainder of this chapter is dedicated to presenting a thorough review of existing studies of VSL applications in recurrent congestion. This review includes sections on the control algorithms, results from simulated and field studies, analysis of VSL paired with ramp metering, and human factors related to VSL implementation.

2.4 VSL Control Algorithms

Algorithms for VSL system control vary in their objectives and their levels of sophistication. The simplest algorithms are those that are pre-timed or activated based on engineering judgment. However, most modern control algorithms are based on ITS

applications using real-time data. Within the realm of ITS-based control algorithms, three general control strategies can be distinguished: basic traffic flows, shockwave detection/mitigation, and traffic prediction. Though these strategies differ in objective and underlying logic to activate and update the VSL system, all are based on real-time traffic data as inputs into a traffic model calibrated for local traffic conditions**.**

2.4.1 Basic Traffic Flow Algorithms

The report by McLawhorn (2003) documented that a VSL system on I-90 in Washington State and on the New Jersey Turnpike used average speeds from roadway detectors to set the displayed VSL. Next, Chien et al. (1997) developed an automated highway system that calculated the desired speed to achieve an optimum traffic flow rate. In this simulated study, the system was able to resolve instabilities in the traffic flows and thus alleviate congestion. Similarly, Van den Hoogan and Smulders (1994) formulated a VSL control algorithm in the Netherlands with the objective of reducing the speed variance, both within and across lanes. The system was activated when the detected volumes approached the capacity of the study segment. The analysis showed the VSL system was effective in reducing the variance and thus improved the overall safety of the corridor.

The work of Nissan (2010) and Nissan and Koutsopoulos (2011) created an advisory speed limit system in Stockholm, Sweden by using two threshold speeds to decide when to activate the VSL control system. Moreover, the research of Lee et al. (2010) analyzed a density-controlled VSL model using the demand-supply method of the cell transmission model originally proposed by Daganzo (1994). In yet another ITS-based control algorithm, Hellinga and Allaby (2007) tested five different VSL control algorithms using occupancy,

volume, and the number of VSL signs on the control segment. Assuming high driver compliance, the study found that, in the peak and near-peak conditions, all five algorithms improved safety at the cost of increased travel times. Later work by Allaby et al. (2007) used PARAMICS in a study of the Queen Elizabeth Way near Toronto, Canada. The VSL system was controlled by real-time measures of volume, speed, and occupancy. Finally, the research by Waller et al. (2009) developed a VSL control algorithm on motorway A2 in the Netherlands based on one-minute averages of speed and volume. The system also had a default VSL of 50 km/hr when an incident was detected.

In a study by Alessandri et al. (1999), an extended Kalman filter was used to estimate the nonlinear traffic density that activated a speed signaling (i.e., VSL) system. The authors found that the proposed system could prevent congested conditions and produce a more stable traffic flow and higher speeds through the congested segment. Abdel-Aty et al. (2010) applied the findings of Cunningham (2007). Here, a speed difference of 7 mph between the upstream and target station activated the VSL control system. Next, the work by Placer et al. (1998) and Placer (2001) developed a fuzzy logic for variable speed limit control for the state of Arizona. The system was designed to determine the appropriate speed limit at a given location under certain conditions such as wind speed and various road surface conditions. The system was designed for I-40 but was suspended due to legal complications involving system implementation and enforcement. In the field-deployed VSL control study, Bham et al. (2010) also used the basic measures of speed, flow rate, and density to control their algorithm. Future improvements from this study suggest the use of traffic conditions both upstream and downstream of the bottleneck.

Several studies have gone beyond basic ITS-controlled algorithms to optimize specific measures of effectiveness. The work by Deryushkina (2012) developed and tested a VSL control algorithm in PARAMICS using data from probe vehicles. The results showed that the algorithm was effective in reducing speed variance and typically needed less data than traditional point detector-based VSL control algorithms. Yang et al. (2013B) developed a tri-objective, bi-level programming model to optimize link-specific speeds with the goal of minimizing the system travel time, the number of expected crashes, and emissions. The study found that, in general, reducing the speed limits improves safety at the cost of congestion and emissions. Interestingly, the authors claimed that a carefully designed speed limit scheme can improve mobility, safety, and emissions simultaneously. Lastly, Zegeye et al. (2010) incorporated the VT-micro model developed by Ahn et al. (1999) into a VSL control algorithm using METANET simulation. The proposed algorithm used a multi-criteria objective weighted function, including emissions, fuel consumption, and total time spent. The study found that the proposed algorithm reduced emissions and fuel consumption while improving traffic flows.

Lastly, several ITS-based control algorithms consider driver behavior. The study by Wang and Ioannou (2011) constructed a dynamic VSL control model based on a car-following model that considered driver behavior. The researchers argued that changing the speed limit for long periods can change the shape of the fundamental diagram. This research was compared with the METANET model developed by Carlson et al. (2010B) and was shown to be more effective in both the free-flow and ten-minute incident scenarios. Next, Pan et al. (2010) and Chang et al. (2011) actualized the dual module algorithm developed by Lin et al. (2004). Model 1 was designed to smooth the transition from free-

flow to congested states while considering the response of motorists to set the control speeds. Module 2 was used for updating the display speed at each location based on differences between the detected and the target control speeds. Similarly, the work of Lu et al. (2015) developed a VSL control algorithm to maximize flow using a feedback loop that considers the difference in posted speed limit and observed speeds. Finally, the study by Fang et al. (2015) derived a dynamic driver response model that embodies the relationship between posted speed, desired speed, and traffic conditions.

2.4.2 Shockwave Detection and Mitigation Algorithms

Several researchers have investigated methods of shockwave detection and mitigation as the basis for VSL control. Here, Kwon et al. (2011A) and Kwon et al. (2011B) generated an algorithm to mitigate the propagation of shockwaves associated with bottlenecks by reducing the speeds of approaching vehicles in the Twin Cities, Minnesota. The acceleration/deceleration rates between adjacent detectors were estimated and used to determine the VSL control boundaries as well as the advisory speed limits for each sign within the control zone. In addition, the study by Hegyi and Hoogendorn (2010) created the Speed Controlling Algorithm using the Shockwave Theory (SPECIALIST) dynamic speed limit algorithm for use on the Dutch A12 freeway. This algorithm is based on the shockwave theory to resolve significant perturbations detected in the traffic flows using a four-phase approach. Phase one is for shockwave detection while phase two activates the dynamic speed limits upstream of the detected shockwave to dissolve the shockwave. This process is illustrated in Figure 2-2. The study found that 80 percent of all detected shockwaves were resolved using the algorithm. In doing so, on average the system saved 35 vehicle hours per prevented shockwave.

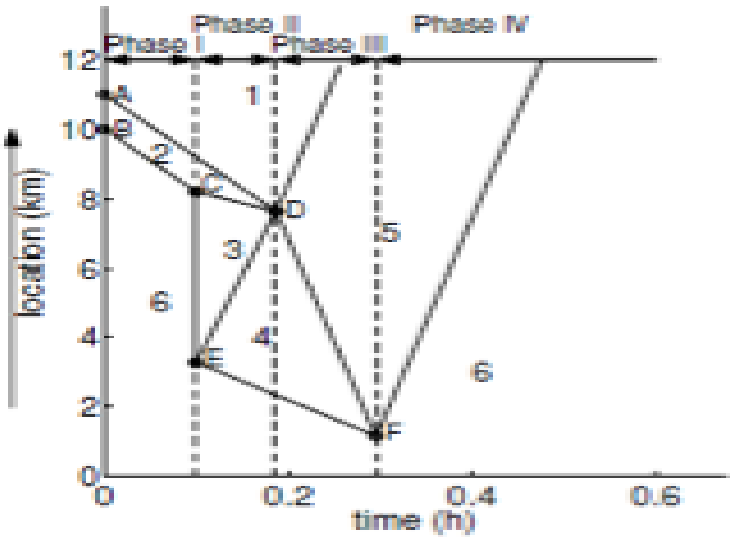

Figure 2-2: The Four Phase SPECIALIST Algorithm (Hegyi and Hoogendorn 2010)

Finally, Chen et al. (2014) developed models based on kinematic wave theory to increase throughputs. The proposed control algorithms worked to resolve the queues near the bottleneck, then shifted to address the associated upstream queues. This strategy starved the bottleneck while smoothing upstream transition speeds, resulting in significant delay savings.

2.4.3 Predictive Control Algorithms

The final category of advanced VSL control algorithms includes those featuring their prediction capability or proactive function. Lenz et al. (1999 and 2001) formulated a VSL control algorithm to prevent the breakdown of traffic flows by intervening before a critical density is reached. Using an anticipative control model, speed limits were set as a function of defined density ranges. Next, Breton et al. (2002) created a predictive control system to minimize the total time spent in the study network. Using a modified METANET model,

the developed model was able to reduce congestion by improving throughput and reducing the total time spent. Likewise, Carlson et al. (2011) used a predictive traffic model using METANET developed in Carlson et al. (2010B). Their proposed model used fundamental traffic flow relationships to select the best display speed with the objective of minimizing a cost function, dominated by the total time spent (TTS) by all vehicles. Next, Harbord (1998) evaluated the field deployment of a mandatory VSL control system, deemed the Motorway Incident Detection and Automatic Signaling (MIDAS) system. The MIDAS system was installed on England's M25 with the objective of reducing peak period crashes. To do so, a model was developed to predict when flow breakdown was about to occur and to display a reduced mainline speed before it occurs. The model inputs were traffic data collected from detectors at a spacing of 500 meters, updated every minute. The results showed a 28 percent reduction in injury crashes and a 25 percent drop in damage-only incidents. In another application of predictive modeling, Hegyi et al. (2005A) developed a coordinated VSL control model with the goal of shockwave mitigation/elimination. The system was activated in under-critical conditions based on model predictive controls developed in Hegyi (2004), with the objective of minimizing the total travel time under several safety constraints. The authors concluded that the VSL control system was effective at suppressing and, in some scenarios, eliminating shockwaves while improving the total time spent by 17.3 percent. Furthermore, (Hadiuzzaman and Qiu 2012) created a VSL control system by generating a predictive flow model based on modifications of the cell transition mode (Daganzo 1994). The objective of the system was to minimize the total travel time and the distance traveled by maximizing the bottleneck flows. Using VisSim simulation, the authors were able to show that the proposed control system was able to

significantly increase the throughput while reducing the travel times. Lastly, the study by Kattan et al. (2014) developed and tested a model predictive control VSL algorithm using vehicle probe-based data. The study showed that the control system was sensitive to information update frequency and probe-vehicle penetration rate.

2.5 VSL in Recurrent Congestion Studies

The performance measures used to evaluate VSL control typically correspond with the objective(s) of the control algorithm. Common VSL performance measures include changes in safety (e.g. crash probability, speed variance), mobility (e.g. average travel time, total time spent, queueing/stopping), and/or environmental impact (e.g. emissions and fuel consumption) relative to the no-control scenario. As presented in the following sections, these studies are conducted in either simulated or field environments.

2.5.1 Field VSL Studies

Field tests of VSL control in recurrent congestion are rarer than the previously discussed simulated studies. This realization indicates that observations from field tests of VSL in recurrent congestion are critical to understanding the potential and limitations of this method.

From an international perspective, Germany installed an enforceable VSL system on the A3, A5, and A8 motorways to improve safety and reduce environmental impact. The system has reduced the crash rate by 20-30 percent (Mirshahi et al., 2007). Another study in Germany by Bertini et al. (2005) found that the VSL system dampened the congested conditions on the Autobahn. In a follow-up analysis, Bertini et al. (2006) when the system was activated, upstream speeds were reduced and flows into the bottleneck were reduced. As a result, the dense traffic continued to flow through the bottleneck. Next, the

Netherlands has experimented with a photo-enforced (during some periods) VSL system to relieve congestion. The system has been effective in reducing shockwaves associated with bottlenecks (Mirshahi et al., 2007). In the UK, the Highway Agency (2007) reported on the costs and benefits of a mandatory VSL system installed on the M25 Controlled Motorway. The study found that injury crashes were reduced by 15 percent, and emissions were decreased by 2-8 percent; however, few differences were found in travel times. In yet another European application, Hegyi and Hoogendorn (2010) proposed and field tested the SPECIALIST VSL control algorithm on the Dutch A12 freeway. The study found that the system saved 35 vehicle hours per resolved shockwave. Further research by Hoogendoorn et al. (2013) assessed the impact of VSL on traffic operations, air quality, noise, and traffic safety on A20 in the Netherlands. The study found that VSL improved vehicle hours by 20 percent by increasing the capacity by 4 percent at the bottleneck area. Interestingly, VSL was found to increase emissions and noise levels with little impact on safety. Finally, as mentioned previously, the work of Papagergio et al. (2008) on a European Motorway found that VSL can produce increased flows in over-critical densities.

Few highway agencies in the U.S. have evaluated field-deployed VSL control in recurrent congestion. Interestingly, the first documented attempt of U.S. VSL implementation occurred in Michigan in the 1960s. Here, advisory speed limits were tried on M-10 and I-94. However, the system was found to have little impact on vehicle speeds (Robinson, 2000). More recent field studies of VSL in the U.S. were conducted in St. Louis, Missouri, and Hanover, Maryland. The work of Bham et al. (2010) evaluated the safety and mobility impacts of VSL on I-270/I-255 in St. Louis. In analyzing four independent segments, the study found that safety was improved by 4.5-8 percent. However, the

mobility results were less convincing, with two of the segments showing increased travel times of 3.1 percent, and 13.6 percent, while the other two segments showed decreased travel times of 5.6 percent, and 19.1 percent.

Next, the analysis by Chang et al. (2011) investigated the effects of an advisory VSL and a VMS traveler information system on travel time and throughput on a recurrently congested freeway near the Baltimore-Washington International Airport. The study evaluated the effect of three different ATMS strategies, including VSL control only, a travel time display only, and VSL control paired with a travel time display. All three of these strategies showed an improvement in the average travel time of 7.5 percent, 5.1 percent and 26.4 percent, respectively. These travel time improvements were paired with modest increases to the total throughput relative to the No Control case. Additionally, the study showed that VSL and VSL paired with a travel time display increased the average speeds in the control segment by 1.2 mph and 15.0 mph, respectively, thus reducing the spatial speed variance of the study section.

2.5.2 Simulated VSL Studies

Recognizing the limited field deployments of VSL, many researchers have turned to traffic simulation to explore the potential benefits of VSL control. Several studies led by Abdel-Aty (Abdel-Aty et al., 2006, and Abdel-Aty et al., 2007) utilized PARMAICS (Quadstone Limited, 2015) simulation software and showed that VSL could improve safety by using real-time data under medium- to high-speed traffic conditions. However, no significant improvement was found in the low-speed scenarios. A later study by Abdel-Aty et al. (2008) investigated the safety via an overall risk change index derived from neural networks. The study found that VSL reduced both rear-end and lane-changing crashes

under the 60 percent and 80 percent loading conditions. However, the VSL system did not have a significant positive effect under 90 percent loading. In relation, Fang et al. (2015) studied a predictive VSL control algorithm that considered driver response a safety-based VSL control algorithm. The study found that VSL can reduce crash probability by 32 percent.

Next, Lee et al. (2004) used the real-time crash prediction model developed in Lee et al. (2002) and Lee et al. (2003) to evaluate the safety benefits of VSL on a Canadian freeway. Using PARAMICS simulation, the study found that lower VSL system activation thresholds reduced the overall crash potential, the greatest reduction in crash potential was discovered at segments with high turbulence, and that updating the VSL system too frequently can actually decrease measures of safety. In a related study, the team of Allaby et al. (2007) investigated the potential effects of VSL on safety and travel time using PARAMICS micro-simulation on a Canadian freeway. The analysis showed that the average safety benefit for all stations were 40 percent in peak conditions, 20 percent in near-peak conditions, and an 11 percent decrease in safety in off-peak conditions. The increases in travel times under peak, near-peak and off-peak demand were 11 percent, 25 percent, and 1.3 percent, respectively. In 2008, Lee and Abdel-Aty collaborated to assess the impact of speed change warning messages (via VMS) and VSL on driver speeds and compliance with posted speed limits. The study found that when the messages and VSL were displayed, speeds tended to be more uniform with less speed variation along the study segment. The authors concluded that such a VSL control system can not only improve safety but can improve the mobility of a freeway.

In a VisSim simulated experiment, Kwon et al. (2011A) investigated a VSL control system on I-35 in the Twin Cities, Minnesota, geared toward suppressing shockwave propagation. Assuming 50 percent driver compliance, results showed that the average maximum deceleration was reduced 15-48 percent paired with 3-15 percent increases in travel time. Likewise, Liu et al. (2014) investigated the impact of VSL on a hypothetical morning commute using derived travel time, travel cost, and queuing models. The results showed that, while VSL can reduce schedule delay costs and emissions, it would not likely improve total travel time or overall costs in the analyzed scenario.

The work by Grumert et al. (2013) used Simulation of Urban Mobility (SUMO) software (Krajzewicz, 2010) to assess the effect of a cooperative VSL system. The results showed that the cooperative VSL system harmonized traffic flow and reduced emissions. Using a METANET simulation framework, Hegyi et al. (2005A) used model predictive control (MPC) developed in Hegyi (2004) to predict network evolution under VSL control with the objective of improving total travel time. Under safety constraints that limited the frequency of the speed limit change, the system showed a 17.3 percent reduction in total travel time. The work of Carlson et al. (2011) also used METANET to evaluate a predictive VSL control algorithm with the objective of minimizing a cost function that was dominated by travel time. The results showed that the algorithm was able to reduce total time spent (TTS) by approximately 15 percent in each of the five unique application scenarios.

The Australian researchers, Jiang et al. (2011), investigated the impact of VSL control algorithms under high flows and queuing scenarios in an AIMSUN (Transportation Simulation Systems, 2015) simulation environment. The results showed that when ramp flows were small, VSL control improved travel time, speed deviation, fuel consumption,

and emissions of CO_2. However, when ramp flows were high, measures of mobility increased under VSL control. In another AIMSUN based study, Lu et al. (2015) investigated speed variation, total number of stops, total travel distance, bottleneck flow, and total delay under VSL control. The control algorithm for bottleneck flow maximization produced improved measures of safety and mobility at compliance levels of 10, 25, and 50 percent. This work also developed and tested VSL control in a connected vehicle environment. Additional connected vehicle VSL control studies were conducted by Wang et al. (2015) and Grumert et al. (2015). Using MOTUS simulation, Wang et al. (2015) showed that a connected vehicle-based VSL system can reduce TTS and fuel consumption. Similarly, the work of Grumert et al. (2015) showed that a connected vehicle VSL control strategy can harmonize speeds and reduce emissions.

Chen et al. (2014) evaluated several VSL control algorithms based on kinematic wave theory. The results showed that, in a hypothetical environment, VSL can produce significant delay savings. In relation, Kattan et al. (2014) evaluated a probe-based VSL system in PARAMICS. The results showed that, with high penetration rates, the probe-based control system was comparable to traditional detector-based systems and in some cases, even outperformed legacy control strategies. These conclusions were based on the ability of the probe-based system to reduce mainline delay and speed variance.

2.6 VSL with Integrated Ramp Metering Studies

In addition to VSL control, ramp metering has become another popular tool in the ATMS realm. Much like VSL, ramp metering is not a new traffic control method but has been receiving growing interest for it potential to alleviate recurrent congestion. Studies illustrating the benefits of ramp metering are plentiful, such as Hadj-Salem et al. (1990),

Papageorgiou et al. (1991), Papageorgiou et al. (1997), Smaragdis et al. (2004), Abouaissa et al. (2012), Saidi and Kattan (2010), Wang et al. (2010), and Ying and Chow (2015). However, the focus of this research applies to the potential for ramp metering paired with VSL to improve traffic conditions.

In light of the tremendous potential for VSL and ramp metering to independently alleviate recurrent congestion, several researchers have explored the impacts of a VSL control system with integrated ramp metering. To date, such studies have only been conducted in simulated environments. Early work on the analysis of VSL paired with ramp metering was presented in Alessandri et al. (1998). The results showed that the proposed control system could improve throughput while reducing mean travel times. Next, Hegyi et al. (2005B) explored an optimal coordination of VSL and ramp metering using model predictive control in METANET simulation. In comparing the benefits of VSL, ramp metering, and coordinated control, the study recommended a system that had the capability to use both strategies and also switch between the two, as it would provide the most benefits. Moreover, Hou et al. (2007) generated an iterative learning control (ILC) approach for density control using ramp metering and speed regulation (i.e., VSL). Similar to other studies, three scenario strategies were tested — VSL alone, ramp metering alone, and integrated VSL paired with ramp metering. The study showed that while the independent control systems were able to control densities, the best density control was achieved by the coordinated control system. Next, the work of Carlson et al. (2010A) developed a second-order traffic flow model using VSL as a supplement to ramp metering in METANET. The analysis showed that while both VSL and ramp metering are independently effective in mitigating the ill effects of traffic bottlenecks, combining the

two traffic control strategies can produce enhanced benefits. Likewise, the work led by Lu et al. (2010A, 2010B, 2011) showed that VSL with coordinated ramp metering control can improve travel times and increase bottleneck throughput. Furthermore, the study by Su et al. (2011) introduced a VSL and ramp metering traffic control algorithm to improve the traffic flow while reducing delay. Upon testing the algorithm in AIMSUN (TSS, 2015), the results showed that the total time spent and the delay can be improved at 30 percent or 100 percent driver compliance.

The work by Dhindsa (2005) used PARAMICS micro-simulation to explore the potential of a VSL combined with a ramp metering system to improve safety conditions on congested freeways. Both strategies were also tested independently to determine the individual effects of VSL and ramp metering. While the independent control strategies showed both safety and mobility benefits, the coordinated strategy showed the highest benefits by increasing average speeds while improving safety by up to 56 percent and network travel time 21 percent. Similar safety benefits of a coordinated control system were reported by Haleem (2007), and Abdel-Aty et al. (2007). Finally, the work by Lu et al. (2014) investigated the potential benefits of VSL, RM, and VSL with integrated RM using CORSIM. The study found that while VSL and ramp metering can ease congestion, the coordinated control system produces significant reductions in the duration and severity of the congested period (Figure 2.2).

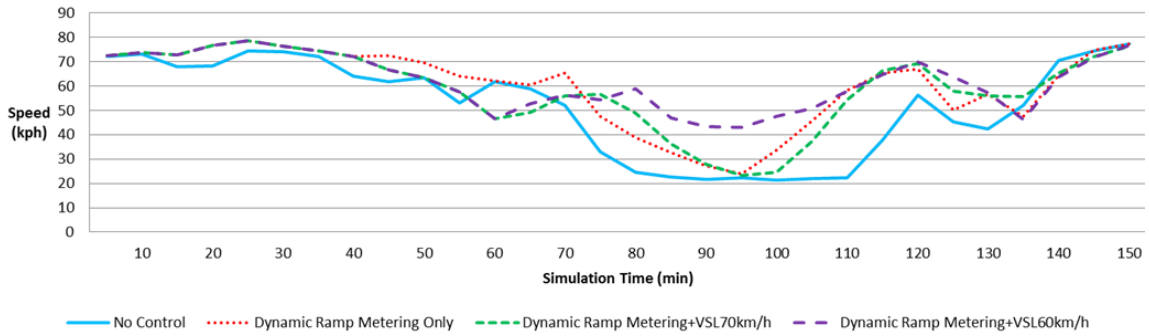

Figure 2-3: Bottleneck Speed vs Time under Various Controls (Lu et al., 2014)

2.7 Summary of Review Findings

Several researchers and highway agencies have investigated the potential benefits of VSL and VSL paired with ramp metering control to alleviate recurrent congestion. The primary differences of these studies are the logic and objectives of the control algorithms. Though there has been a multitude of VSL control algorithms developed, all are based in estimating the current or short-term future traffic conditions based on traffic flow models using real-time data inputs.

While Europe has been more progressive than the U.S. in performing field studies, most of the investigations of VSL control have been conducted in simulated environments. A *nearly* universal finding was that VSL control can harmonize traffic speeds and thus improve measures of safety and environmental impact in mild to heavy congestions. However, the positive impacts of VSL control on mobility have been less convincing. Studies such as Chang et al. (2011), Carlson et al. (2011), Lu et al. (2015), and Wang et al. (2015) showed that VSL control can indeed simultaneously improve safety and mobility. In contrast, the evaluations by Kwon et al. (2011A), Bham et al. (2010), and Allaby et al.

(2007) showed instances in which VSL control decreased measures of mobility in the form of increased travel times.

Realizing the potential benefits of pairing VSL control with the proven ATMS strategy of ramp metering, several researchers have investigated the potential benefits of pairing these control strategies. The results of these studies showed that a VSL with integrated ramp metering control can outperform either independent control system.

Despite the tremendous progress on the use of VSL control in recurrent congestion over the past decade, many critical issues remain:

1. There is a need for guidance on the selection of the appropriate control strategy for a given site.

2. There are limited tools available to estimate expected benefits from a VSL or VSLRM control system at a given site.

3. There is a shortage of guidance on how to deploy a VSL or VSLRM control at a given site.

Though it is clear that combining VSL with ramp metering control can enhance benefits, there is little guidance on when it is prudent to use combined control; there is also no guidance on when a given traffic environment cannot be significantly improved using either of these ATMS strategies. Next, it is likely that a given highway agency will have multiple candidate sites for congestion mitigation but not enough resources to intervene at all of them. Thus, a support tool that could suggest the most appropriate control strategy (if any) for each candidate site and the expected benefit resulting from the suggested strategy could assist traffic operation decision-makers in effectively allocating limited

resources for congestion mitigation. Lastly, there is little guidance on how to effectively deploy a VSL or VSL paired with ramp metering control algorithm. Such guidance should be based on the expected impact area resulting from VSL or VSL paired with ramp metering control.

The focus of this research is to address the aforementioned critical issues related to developing a comprehensive planning tool for VSL and VSLRM control. In doing so, a better understanding of how crucial traffic environment parameters impact the benefits of either of these ATMS strategies will be discovered. These results will offer valuable insight into understanding the conditions that warrant the use of either of these strategies, and the expected benefits, as well as guidance on how to deploy such as control system at a candidate site.

Chapter 3: VSL Decision/Deployment Support Tool

3.1 Motivation for Tool Development

Recognizing the widespread impact of the issue, researchers and traffic operations professionals have developed a multitude of strategies to contend with recurrent congestion. These strategies fall into the three general categories of ATMS (VSL, ramp metering, hard shoulder running, etc.), demand management (teleworking, flex hours, etc.), and capacity expansion.

In addition to the various strategies available for congestion mitigation, it is reasonable to assume that a given highway agency often has multiple candidate sites for congestion mitigation projects but not the resources to intervene at each of them. Given the various options for congestion mitigation and concerns for allocating limited resources, a decision-maker may encounter the following questions:

1. For each candidate site, is mitigation justified? If so, which mitigation strategy is feasible and the most appropriate?
2. If there are multiple candidate sites in which congestion mitigation is indeed justified and feasible, how should the limited resources be allocated?
3. For each site onto which a congestion mitigation strategy will be applied, how should the strategy be implemented and evaluated?

The natural sequence of these critical questions suggests a three-step procedure for congestion mitigation project planning. First, a decision must be made regarding which, if any, mitigation strategy is appropriate for each candidate site. Next, when multiple sites are found to be eligible for intervention, resources must be targeted at the sites expected to benefit most from congestion mitigation. This process must take into consideration the costs and challenges associated with

implementing the desired strategy. Finally, guidance on how to properly implement the suggested mitigation strategy must be provided. This guidance should offer sufficient information to assist decision-makers in defining the control boundaries and location of the control infrastructure components.

Unfortunately, there are few methods that can comprehensively address these crucial considerations in the planning phase of a congestion mitigation project. Perhaps the most common method of evaluating a given congestion mitigation strategy in the planning phase is traffic simulation software. Though traffic simulation is a proven method for estimating the impacts of a congestion mitigation strategy, there are several challenges associated with employing this powerful planning tool. First, building a traffic simulation environment that reflects field conditions requires significant data input. These inputs include details of the network geometry, temporal and spatial traffic flow patterns, and driver behavior parameters. Next, the simulation environment must be calibrated to reflect field conditions. Calibration often requires significant effort from experienced engineers. Once the environment is calibrated, the desired congestion mitigation strategy must then be implemented. Even more, sophisticated congestion mitigation strategies often require coding for real-time traffic control. Finally, the simulation outputs are used to compute performance measures that are compared to the base scenario (No Control). This process must be repeated for each candidate site and control strategy.

More importantly, many traffic agencies lack the resources and/or detailed data inputs to effectively utilize traffic simulation. In such cases, the planning phase decisions rely heavily on engineering judgment. Decision-makers assess the potential effectiveness of various congestion mitigation strategies by analyzing available field data such as traffic flow patterns and the evolution of the congested conditions. While such strategies provide insight on the general nature

of congested conditions, the underlying complex interrelations between network geometry, traffic flow, and driver behavior may be overlooked. As such, the decision-maker may initiate an inappropriate control strategy that can contribute to several negative consequences including wasted resources, road-user frustration and reduced trust in innovative traffic control systems, and exacerbated costs of congestion including delay, secondary crashes, emissions, and fuel consumption.

Acknowledging the tremendous efforts needed to employ traffic simulation and the potential pitfalls of engineering judgment, it is essential to develop a convenient, efficient, and reliable tool for analyzing congestion mitigation strategies in the planning phase. Such a tool should have the following functions:

1. Minimize the data inputs and effort needed for decision-makers to identify the congestion mitigation strategies of interest.
2. Assist in selection of the most appropriate congestion mitigation strategy (if any) at each candidate site.
3. Estimate the expected benefits from deploying the most appropriate strategy at each candidate site.
4. Provide guidance on how to properly deploy the most appropriate congestion mitigation strategy at each site.

The scope of this research is to develop a decision/deployment support tool for investigating the use of independent VSL control and VSL paired with ramp metering (VSLRM) control in the planning phase. However, a similar methodology can be followed to include additional congestion mitigation strategies.

3.2 Framework of the Decision/Deployment Support Tool

The objective of the proposed tool is to provide a convenient and reliable alternative in assessing VSL and VSLRM control in the planning phase of a congestion mitigation project. Additionally, the tool provides guidance on how to deploy an ITS-based VSL or VSLRM control system at each target site. Based on the inherent sequence of planning for a congestion mitigation project, the proposed VSL decision/deployment support tool is comprised of three modules that utilize minimal user inputs to assess and provide guidance on the use of VSL and VSLRM control at a list of candidate sites.

The first module is the Decision Module, which provides guidance on which, if either of these strategies, is recommended for each candidate site under user-defined objectives and constraints. The second model is the Benefits Module, which estimates the expected benefits from the recommended control strategy.

Note that candidate sites that are not expected to benefit from VSL or VSLRM control are not passed onto the benefits module. The output of this module is a ranked list of candidate sites eligible for VSL or VSLRM strategy, based on the control objective and constraints. This list may be used as guidance in allocating limited resources for congestion mitigation.

The third and final module is the Deployment Guidelines Module, which provides guidance on the placement of traffic control devices (i.e. VSL signs, ramp meters, and detectors) based on the expected impact area of the employed control system for each candidate site. The overall structure of the VSL decision/deployment support tool is presented in Figure 3-1. A detailed discussion on the user inputs and each of the three modules is presented in the following sections.

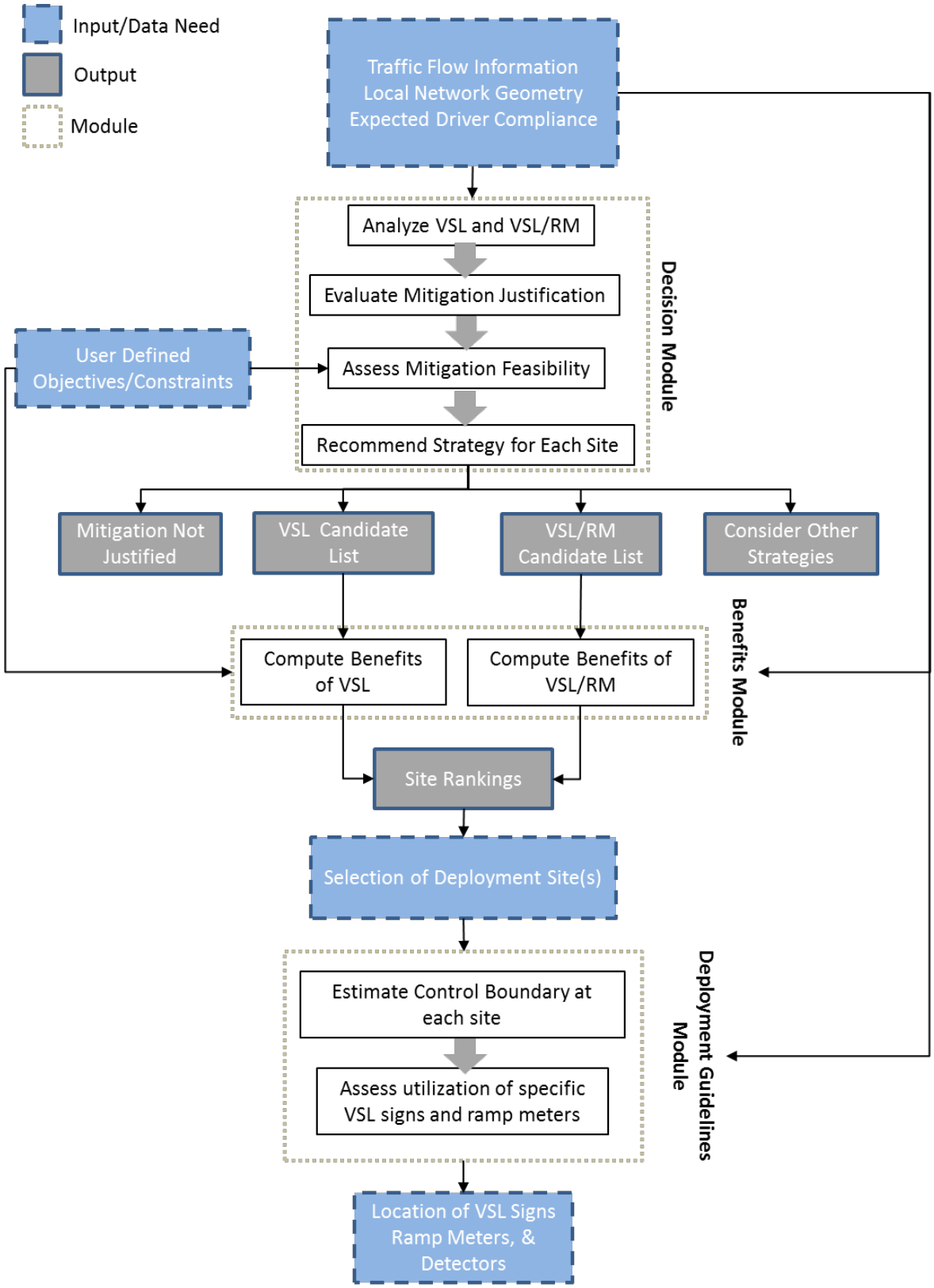

Figure 3-1: Structure of the VSL Decision/Deployment Support Tool

3.2.1 User Inputs/Data Needs

As shown in Figure 3-1, the decision/deployment support tool requires inputs from users. The input fields include information about the candidate sites, assumed compliance levels to VSL, control objectives, and constraints. The information associated with the candidate sites includes parameters related to the geometry and traffic stream characteristics. Next, the user must input an expected compliance level to the VSL control system. This percentage can vary from zero to 100 percent. Next, the decision-maker/user must also define the objective and constraints for the congestion mitigation project. In this analysis, the mobility and safety benefits are considered. Thus, the user can define the weighted values associated with each of these potential benefits (e.g. safety is twice as important as mobility) to assess the control strategies based on specific objectives and constraints. The details of calculating the mobility and safety performance measures are discussed in Chapter 4.

3.2.2 VSL Decision Module

The Decision Module provides guidance on which, if any, control strategy is most appropriate for each candidate site. The nature of this decision suggests the use of a discrete choice model or a rules-based tool. As will be discussed in Chapter 5, several choice models were analyzed for the Decision Module. In any case, the Decision Module first determines if either of the control strategies is justified based on user inputs. Though such sites are less likely to be on a candidate site list, the model is able to determine when such control strategies will provide minimal benefits (based on user inputs) due to light congestion. If congestion mitigation is indeed warranted, the module analyzes the impacts of VSL and VSLRM control. Though these strategies are proven to alleviate congestion, some severely congested scenarios may not provide sufficient expected benefits to justify their implementation. While such scenarios justify congestion mitigation, the

module may determine that VSL and VSLRM control are not feasible strategies. In such cases, alternative traffic control and demand management strategies should be explored before resorting to network capacity expansion. On the other hand, the module may find that one or more candidate sites can benefit from a VSL or VSLRM control. If a given candidate site is determined to significantly benefit from a VSL or VSLRM control, it is passed to the Benefits Module. Those sites that are determined to lack congestion mitigation justification or feasibility are removed from further analysis.

3.2.3 VSL Benefits Module

The candidate sites that are recommended for either VSL or VSLRM control are further assessed in the Benefits Module. This module quantifies the direct benefit resulting from the application of the recommended control strategy. The benefit function is a weighted sum of the safety and mobility benefits relative to the no-control scenario. The ratio scale of measure of the total benefits function implies the use of continuous prediction model such as ordinary least squares (OLS) regression. Chapter 5 discusses the analysis of such model structures, including an advanced model that considers the correlation of errors between the Decision Model and the Benefits Model. At any rate, output of the Benefits Module is a ranked list of sites based on the user-defined objectives and constraints. Such a list provides valuable insight on the sites expected to benefit the most from the suggest control strategy. The user may use this list to select the sites in which to deploy the suggested mitigation strategy. The down-selected sites are then passed to the Deployment Guidelines Module.

3.2.4 VSL Deployment Guidelines Module

The final module in the decision/deployment support tool is used to provide guidance on placement of the control infrastructure, based on the expected impact area and utilization of traffic

control devices. The first critical function of this Module is used to assess the impact area under and associated control boundaries of the suggested control strategy. This function is derived from the expected maximum mainline queue lengths under the suggested control strategy. The second key function of this module determines the locations to place VSL signs within the impact area. The developed method assesses the maximum speed drop in the target control sub-segment based on the dynamic evolution of the mainline queue. This speed drop is then used to determine the number of VSL signs needed to safely transition approaching vehicles to the desired speed. In a similar fashion, the third key function evaluates the placement of ramp meters based on the evolution of the mainline queue. In addition, a procedure for assessing the operational mode of each ramp meter. The final function on this Module provides guidance on the placement of the traffic sensors used to feed the control system with real-time data. Here, general guidelines are presented to reduce system malfunction caused by inaccurate data inputs.

3.3 Summary of Decision/Deployment Support Tool

Based on the intrinsic structure of the planning tasks associated with a congestion mitigation project, the proposed support tool is comprised of three coordinated modules. The first module provides guidance on selecting the appropriate control strategy. The output of this module is then used to assess the expected benefits from the suggested control strategy under user-defined objectives and constraints. Upon selecting the deployment sites, the final module provides guidance on the deployment of the critical infrastructure components needed to effectively implement the suggested strategy. The remainder of this dissertation will describe the details relating to the development of this tool. Chapter 4 will present the development of the dataset used to generate the various models considered in each of the modules of the tool. Chapter 5 discusses methodology, results, and analysis of the decision and benefits estimation models that were

considered in this study. Next, Chapter 6 presents the development of the deployment guidelines module. Finally, the developed tool will be demonstrated on set of real-world candidate sites defined in the Maryland State Highway Mobility Report (2014) in Chapter 7.

Figure 3-2 presents the structure and relationships between the contents of Chapters 4-7. The dataset created in Chapter 4 will be used to develop and test the decision and benefits modules of the proposed tool presented in Chapter 5. In addition, the dataset will be used to establish the deployment module of the decision/deployment support tool and associated field calibration guidelines in Chapter 6. The application of the final models developed for each of the tool modules are illustrated in chapter seven. This demonstration will provide valuable insight into how a decision-maker can utilize this tool in the planning phase of a congestion mitigation project.

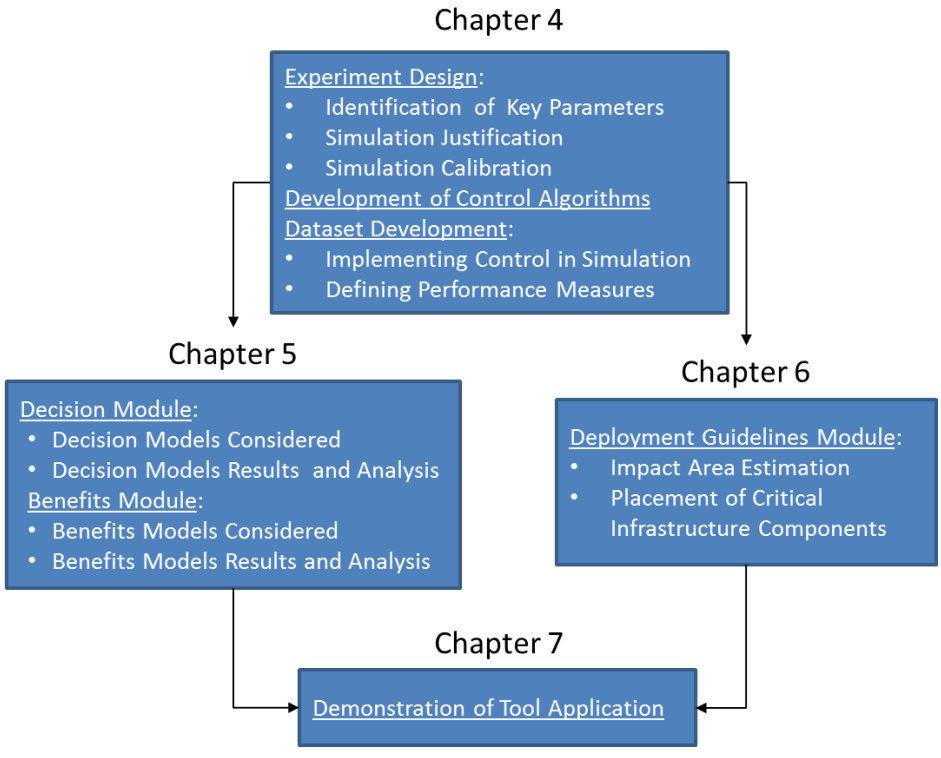

Figure 3-2: Framework for Main Topics of Dissertation

Chapter 4: Experiment Design

4.1 Overview of the Experiment Design for Tool Development

As described in Chapter 3, the structure of the VSL-VSLRM control decision/deployment support tool requires sufficient observations and measurements of these control strategies' performance in congested environments. The dataset for such a tool development shall contain the following information:

1. Driver responses to the deployed control system
2. A variety of possible recurrently congested traffic scenarios
3. The impact of traffic conditions under typical VSL and/or ramp metering control strategies
4. Changes in safety and mobility due to the deployment of VSL or VSL/RM control

To generate a reliable dataset, this study utilizes VisSim traffic simulation. The use of simulation for such needs is justified for the following reasons. First, as evidenced in the literature review, there have been limited field deployments of VSL and VSLRM control, and the results of those studies are not sufficient for model calibration. Next, simulated experiments can be calibrated with field data to ensure reasonable representation of critical traffic flow parameters and driver behaviors, thus meeting data requirement number one. In this research, a base simulation environment is calibrated using field data from the Chang et al. (2011) VSL control study. Next, related to data requirement number two, a simulation-based experiment allows for the generation of multiple potentially congested environments by altering key geometric, traffic flow, and driver behavior parameters suspected to influence the performance of VSL and VSLRM control. Moreover, in connection with the third data requirement, simulation allows for the integration of ITS-based control strategies. As evidenced by the literature review, there is no shortage of VSL

and VSLRM control algorithms from which to choose. It should be noted that one of the objectives of this research is to create a *robust* decision/deployment support tool, thus the outputs of the tool should not be overly sensitive to the details of the implemented control strategy.

Interestingly, nearly every ITS-based VSL and ramp metering control strategy is founded on traffic flow modeling utilizing real-time detector data. To incorporate this observation, this study aimed to apply VSL and VSLRM control logic that reflects the framework of commonly used VSL and VSLRM control algorithms. The details of these algorithms are presented in sections four and five, respectively. Lastly, simulation allows for the direct comparison of VSL and VSLRM control at identical sites. It should be noted that, even if field data was available for VSL and VSLRM at an identical site, care would have to be taken to ensure that the observations were not biased by uncontrollable factors such as fluctuations in the demand pattern, differences in driver behavior and changes in vehicle composition. In addition, the critical parameter of driver compliance is challenging to accurately estimate in the field using traditional aggregated traffic detector data. Fortunately, simulation allows for complete control of the traffic environment, thus removing such biases and meeting data requirement number three. As a result, driver compliance is precisely known and the observed results can be positively attributed to the employed traffic control strategy.

Figure 4-1 shows the procedure for analyzing VSL and VSLRM control in a simulated environment. As will be described in Chapter 5, the results of the experiments will be used to approximate the performance measures of these control strategies.

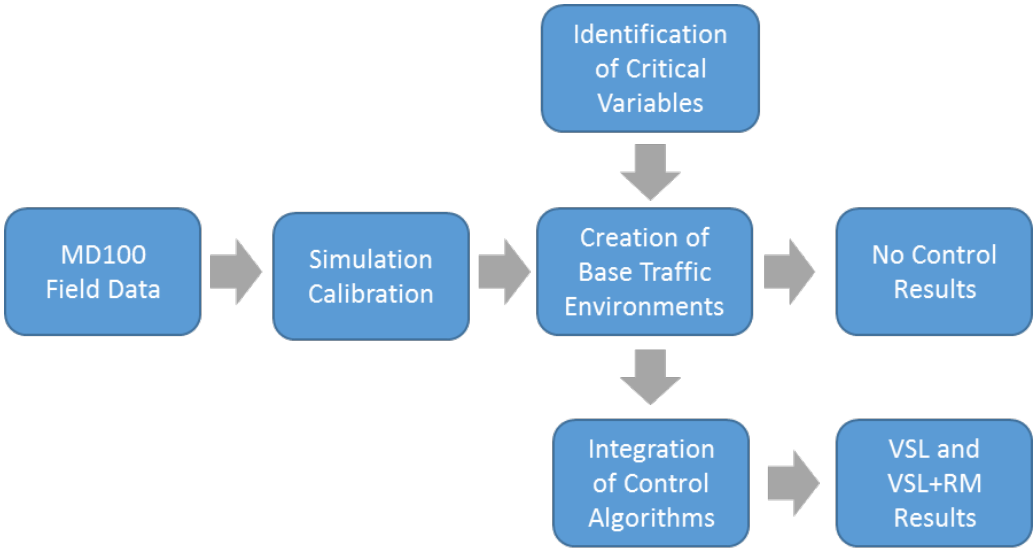

Figure 4-1: Experiment Design Flow Chart

4.2 Development of Base Environments

4.2.1 Calibration of Base Scenario (MD-100)

The process of creating a set of base scenarios for evaluation of VSL and VSLRM control begins with the calibration of the base simulation environment. The field deployment of VSL control on westbound MD-100 at the interchange of Coca-Cola Drive referenced in the study by Chang et al. (2011) was used for calibration. Bottleneck speed and mainline travel times during the PM peak period were the parameters selected for calibration. Bottleneck speed reflects the severity of the bottleneck and is strongly correlated with speed variance. In relation, the mainline travel time reflects the mobility impact of the bottleneck on the local network. Furthermore, these two parameters comprise the foundation of the performance measures of safety and mobility that are described in detail in section 4-5. The bottleneck speeds and mainline travel times from simulation were averaged from simulation runs under ten different random seeds. Speeds and travel times were aggregated every five minutes and were tested at the 95 percent confidence interval derived from field observations from 10 week-day PM peak periods. The

results of this effort are shown in Figures 4-2 and 4-3.

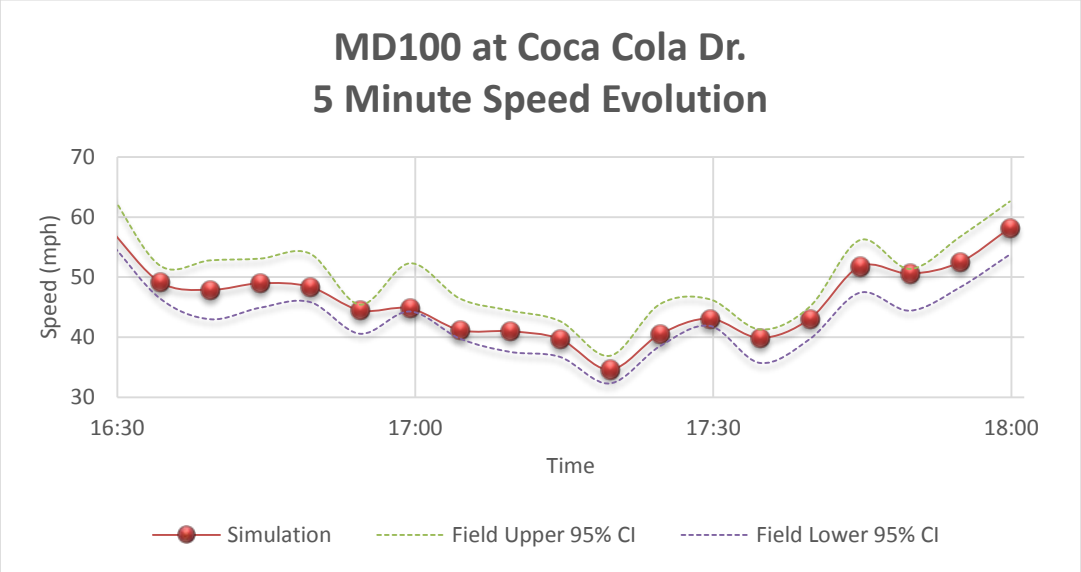

Figure 4-2: Calibration-Evolution of Bottleneck Speeds

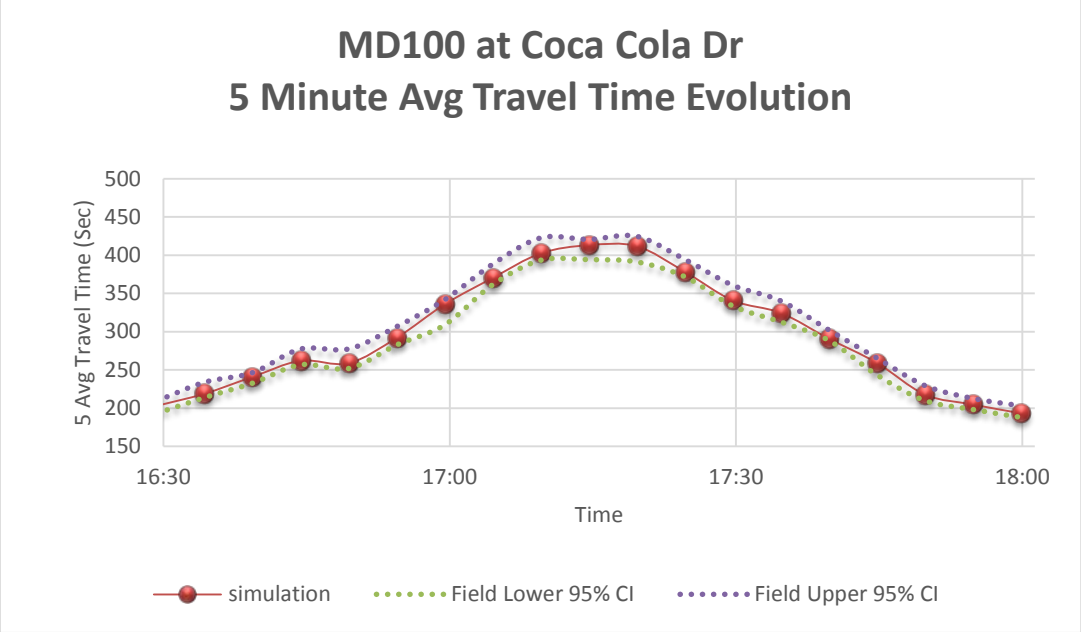

Figure 4-3: Calibration-Evolution of Mainline Travel Times

4.2.2 Design of Simulation Experiment for Recurrent Congestion

Having sufficiently calibrated the simulation environment, several hypothetical scenarios were created by altering parameters suspected to influence the effectiveness of VSL control. These parameters were the distance to the upstream on-ramp, truck percentage, volume to capacity (V/C) ratio at the bottleneck area, the percentage of the bottleneck V/C ratio coming from the associated on-ramp, and driver compliance to VSL. Upon investigating reasonable ranges for these parameters in recurrent congestion conditions, each parameter was assigned four levels. These levels are summarized in Table 4-1.

Table 4-1: Control Variables for Dataset Development

Control Variable	**Variable Levels**			
Distance to upstream on-ramp (miles)	0.5	1	1.5	2
% Trucks	2.5	5	10	15
V/C at Bottleneck	0.85	0.9	0.95	1
% V/C from Bottleneck Ramp	10	15	20	25
Driver Compliance (%)	25	50	75	100

A full factorial experiment design was employed to cover all 1,024 possible combinations of the variable levels in Table 4-1. Each of the 1,024 scenarios where simulated under no-control, VSL control, and VSL with integrated ramp metering control, resulting in 3,072 control environments. To eliminate stochastic biases, each simulation was tested under three random speeds, resulting in a total of 9,216 simulations. The following section describes the VSL and ramp metering control algorithms that were incorporated in the VisSim simulation environments via COM interface.

4.3 Data Needs for Control Algorithms

The control parameters of the proposed VSL and VSL with integrated ramp metering system are based on examining the flows into and out of the congested segment, constrained by spatial and temporal speed changes. Recognizing that the severity and extent of congestion are dynamic, the overall congested segment is further divided into sub-segments. Each sub-segment uses detectors at each entrance/exit point of the sub-segment to monitor inflow/outflow rates (Figure 4-4). The advantage of the sub-segment control methodology is twofold. First, as the system monitors traffic conditions in each sub-segment, determinations on the severity and extent of the congestion can be made and used to define the dynamic control strategy. Second, the sub-segment control methodology allows for supplementation of ramp metering control. By defining the congested sub-segments, the appropriate supplemental ramp metering control strategy can be executed by adding a single detector at each metered ramp for ramp queue override (detector 5 in Figure 4-4).

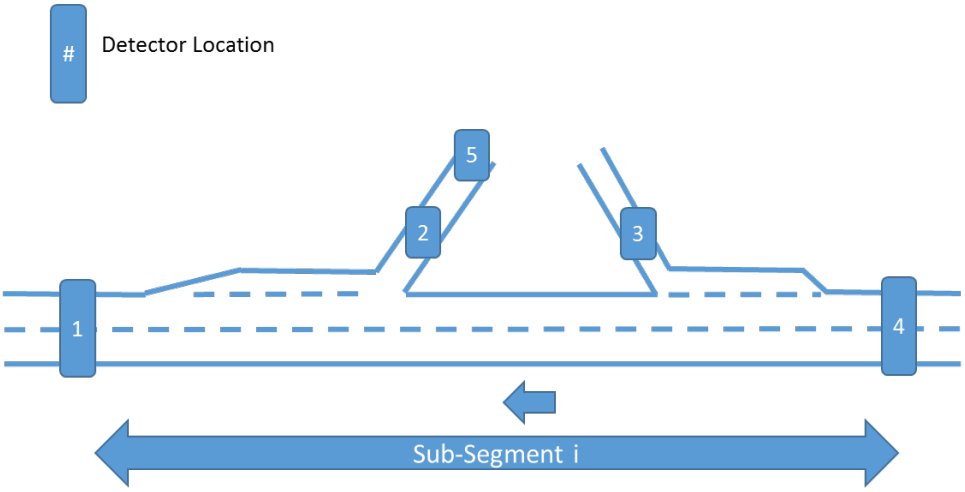

Figure 4-4: Detector Locations for ATMS Control

In Figure 4-4, the detectors are describes as:

Detector 1: Downstream Mainline Detector

Detector 2: On-Ramp Detector

Detector 3: Off-Ramp Detector

Detector 4: Upstream Mainline Detector

Detector 5: On-Ramp Queue Detector (for ramp metering)

Each simulated environment contained three sub-segments for these control strategies. The boundaries of each sub-segment were established between the interchanges within the simulation environment. The original congestion pattern and sub-segment control boundaries are shown in Figure 4-5.

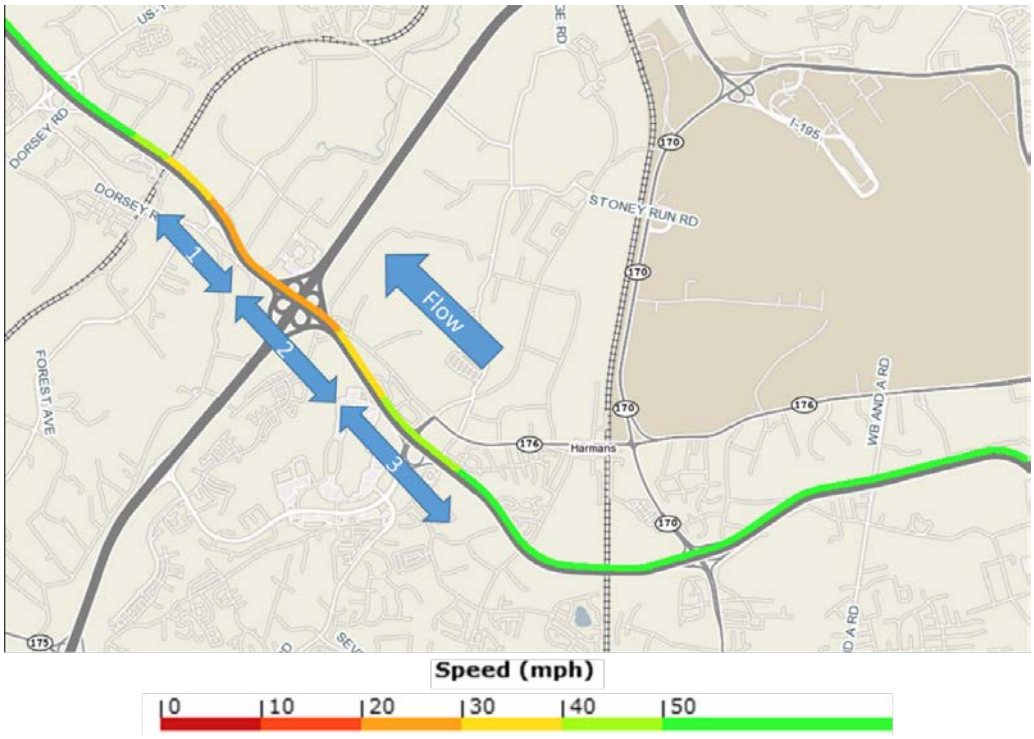

Figure 4-5: Control Sub-Segment Boundaries

4.4 VSL Control Algorithm

The primary objective of the proposed VSL control algorithm is to reduce queue formation by controlling inflow into the congested segment. Here, inflow is governed by reducing speeds approaching the congested segment. The target control speed is calculated from the fundamental diagram, based on real-time traffic conditions within the congested segment. The proposed VSL control algorithm is designed to incorporate supplemental inflow control via ramp metering. In light of the dynamic nature of the congestion pattern, safety constraints must be incorporated in the VSL control algorithm and deployment strategy.

It is worth noting that the foundation of the VSL control algorithm used in this study shares many features common in existing VSL control strategies, such as Chien et al. (1997), Van den Hoogan and Smulders (1994), Nissan and Koutsopoulos (2011), Hellinga and Allaby (2007), Allaby et al. (2007), and Abdel-Aty et al. (2010). The core of the VSL control algorithm in each of these studies utilized real-time traffic data to activate and update a VSL system to reduce the speeds of vehicles approaching the congested segment. Constructing a VSL control algorithm with the common logic of existing systems allows for a robust application of ATMS planning tools and guidelines that will be discussed in later chapters. The principal difference between the VSL control algorithm used in this study and those in existing studies is the data collection strategy. The use of multiple detectors allows for precise monitoring of inflow and outflow without relying on traffic flow modeling. In practice, this strategy would also offer a layer of redundancy to ensure reasonable system performance in the instance of a detector malfunction.

The VSL system was updated every five minutes using real-time data. In this study, detector data was recorded every 30 seconds. The target control speed was rounded to the nearest 10 mph using the original posted speed limit as the base speed. In each five-minute update interval, the

target speed limit was constrained to a maximum change of ± 10 mph. The spatial speed transition constraint was developed to create a speed transition zone from the free-flow speed down to the target control speed. The speed transition zone allows motorists to comfortably decelerate to the control speed as they approach the congested segment.

To effectively control the inflow of vehicles under VSL control, the structure of the proposed algorithm is based on three primary components:

System activation component: This component decides when to turn on the VSL control system based on threshold densities and spatial speed differences. Once activated, the associated infrastructure including VSL signs and advanced warning systems will be turned on to communicate the control speeds to motorists.

VSL control segment and speed updating component: Upon system activation, this component determines the extent and severity of the congested segment. This component is used to define the target control sub-segment and its respective control speed. Additional upstream VSL signs will be used to safely step down speeds to the target control speed. This component considers driver adherence to the posted VSL by comparing the target speed to the observed speed in a feedback loop.

System deactivation component: As congestion dissipates and the bottleneck dissolves, VSL will no longer be needed. This component controls the systematic deactivation of VSL to safely return the control segment back to the posted speed limit.

Each component uses real-time traffic data as inputs into the functions for VSL control logic. The operational flow chart of the VSL control system is presented in Figure 4-6, where the primary components are in bold text. The details of each component are presented in the following sections.

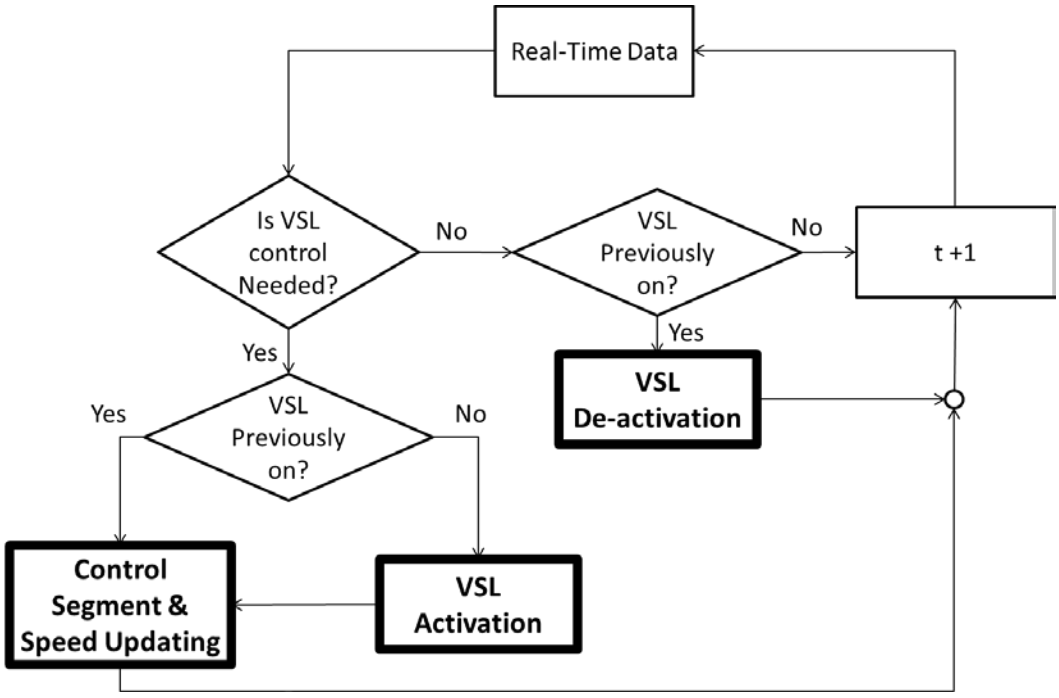

Figure 4-6: VSL Control Operational Flow Chart

4.4.1 VSL Activation Component

The activation of the proposed VSL algorithm and determination of the control sub-segment is based on observed speed differences between adjacent mainline detectors. In the pre-activation phase, traffic is monitored using 30-second aggregated data. If the downstream detector in a mainstream detector pair drops 10 mph or more below the speed at the upstream detector, the VSL system will be activated. Upon system activation, the control system must determine the target control sub-segment and the appropriate target control speed. This initial determination is performed using one-minute aggregate data, which activates the VSL control system. All subsequent target control speeds will be based on five-minute aggregated data from the target control sub-segment. In either case, the target control speed is derived from the fundamental equation using the observed flows into and out of the target control sub-segment and its length.

Since the system is constrained to speed updates of 10-mph increments from the original speed limit, the control speed is rounded to the nearest 10 mph:

$$v_c^i(t) = round\left[\frac{q_{down}^i(t-1)}{k_i(t)}, -1\right] \quad (4.1)$$

And

$$k_i(t) = k_i(t-1) + \frac{q_{in}^i(t-1) - q_{out}^i(t-1)}{L_i} \quad (4.2)$$

Where:

V_c^i (t) = target control speed into sub-segment i for time interval t (mph)

Q_{down}^i (t-1) = total mainline outflow out of sub-segment i in the previous time interval

Q_{in}^i (t-1) = total inflow into sub-segment i in the previous time interval

k_i(t) = density of sub-segment i at the start of time interval t

L_i = Length of sub-segment I (miles)

Once the target control speed is defined, the display speeds for the other VSL signs can be determined using the 10 mph step-down strategy. If the target control speed is more than 20 mph below the original speed limit, then multiple signs will be needed to create a safe speed transition zone.

4.4.2 VSL Control Segment and Control Speed Updating Component

The control speed can only change by ±10 mph in a consecutive update interval. Thus, if the control speed is calculated to be ±20 mph or more than the control speed in the previous update

interval, the system will select a ±10mph change and re-evaluate the required target control speed at the next five-minute update interval:

$$v_c^i(t) = \begin{cases} v_c^i(t-1), \ if \ v_c^i(t) - \ v_c^i(t-1) = 0 \\ v_c^i(t-1) - 10, \ if \ v_c^i(t) - \ v_c^i(t-1) \leq -10 \\ v_c^i(t-1) + 10, \ if \ v_c^i(t) - \ v_c^i(t-1) \geq 10 \end{cases} \quad (4.3)$$

Where:

$v_c^i(t) =$ target control speed for the current time interval t (mph)

$v_c^i(t-1) =$ target control speed for the previous time interval t-1 (mph)

If congestion continues to build from the bottleneck, the original control segment may become entirely queued. When this situation arises, the control system must shift to control inflow in the upstream control segment. To do so, an estimate of the queue length is needed. Here, the moving queue equation developed by Ramezani et al. (2011) was utilized:

$$Q_i(t) = \frac{n}{l} * \frac{s}{5280} \quad (4.4)$$

Where:

$$n = \sum_{t-1}^{t} [q_{in}^i(t) - q_{out}^i(t)] \quad (4.5)$$

$$s = \frac{\bar{v}}{Capacity} * 5280 \quad (4.6)$$

$Q_i(t)$= queue length at end of time interval t in segment i (mile)

$n =$ number of vehicles in queue

$l =$ number of lanes

$\bar{v}$ = average speed (mph)

s = average spacing of vehicles (ft)

In the proposed control algorithm, a conservative control segment threshold of 85 percent of the segment length is employed. This logic is based on the five-minute update constraint and the observed shockwave propagation from the MD-100 field study. In any case, the target control speed calculation is performed using the data from the new (upstream) target control sub-segment.

4.4.3 VSL Deactivation Component

Eventually, the peak period demand will diffuse and the need for inflow control will be reduced until it is no longer needed. The control system deactivation component uses real-time traffic conditions within the target control segment to determine when to start the decommissioning of VSL control. It is worth noting that the maximum severity of the speed drop within a given sub-segment is a function of the distance from the bottleneck. Farther upstream sub-segments will typically return to free-flow conditions earlier than downstream sub-segments. However, shockwave theory explains that upstream conditions cannot improve until the downstream bottleneck begins to dissolve. As the conditions at the bottleneck improve, the associated queues will dissipate, and the previously required upstream VSL signs will no longer be needed.

The updating component of the control system can effectively adjust to improving conditions. However, eventually the target control sub-segment will need to shift back towards the bottleneck (in the downstream direction) as conditions improve. Thus, the primary function of the deactivation component is to provide this shift and to update the unneeded VSL signs to display the original posted speed limit. Once the speeds at the downstream boundary of the most upstream sub-segment are within 10 mph of the posted speed limit, flows into this sub-segment will no

longer need to be regulated. Thus, the control system will shift the target control sub-segment to the next most upstream sub-segment:

$$S_{Control} = \begin{cases} I,\ if\ v_{up}^{I} - v_{down}^{I} \geq 10 \\ I-1,\ if\ v_{up}^{I} - v_{down}^{I} < 10\ and\ v_{down}^{I} \geq PSL - 10 \\ I-2,\ if\ v_{up}^{I-1} - v_{down}^{I-1} < 10\ and\ v_{down}^{I-1} \geq PSL - 10 \\ \vdots \\ i,\ if\ v_{up}^{i+1} - v_{down}^{i+1} < 10\ and\ v_{down}^{i+1} \geq PSL - 10 \\ System\ Off, if\ v_{up}^{i} - v_{down}^{i} < 10\ and\ v_{down}^{i} \geq PSL - 10 \end{cases} \quad (4.7)$$

Where:

$S_{Control}$ = Target control sub-segment

i = bottleneck sub-segment identifier

I = total number of sub-segments

v_{up}^{i} = Five minute average speed at the upstream boundary of sub-segment i (mph)

v_{down}^{i} = Five minute average speed at the downstream boundary of sub-segment i (mph)

PSL = Original Posted Speed Limit (mph)

As upstream VSL signs are no longer needed to control inflow, they will return to displaying the original speed limit under the same identical constraints in the updating component. That is, each sign can only change by ±10 mph for each update interval and the maximum speed change between consecutive signs is 10 mph. This process is repeated until the bottleneck sub-segment returns to un-congested conditions. At this point, the VSL control will terminate by turning off all VSL signs and advanced warning messages.

4.5 Supplemental Ramp Metering Control Algorithm

The basis of any ramp metering strategy is to govern inflow into a congested segment by controlling the vehicle entrance rate from on-ramps. As described in the literature review section, there are varying objectives and levels of control algorithm sophistication to activate the system and to estimate the appropriate ramp metering rate.

In the proposed ramp metering control algorithm, ramp metering is activated once a critical cumulative difference in inflow and outflow is detected. This difference in inflow and outflow is based on the critical density established from field data on the proposed control segment. The associated ramp metering rate is determined by calculating the difference between observed cumulative differences between inflow and outflow and the critical value. If the calculated ramp metering rate is below the pre-determined minimum ramp metering rate, the immediate upstream ramp metered may be activated for supplementary inflow control (if an upstream meter exists). In such instances, metering equity is considered based on real-time demand patterns on each respective on-ramp.

Similar to the development of the VSL control algorithm, the ramp metering control algorithm was designed to incorporate several features of common existing ramp metering systems. The foundation of many ramp metering control strategies is the monitoring of the bottleneck area (flow or occupancy/density) to activate and update the ramp metering system. This general control logic was investigated by Papageorgiou et al. (1997), Smaragdis et al. (2004), Abouaissa et al. (2012), Saidi and Kattan (2010), and Wang et al. (2010). In many applications, the metering rate is constrained by a maximum ramp queue. These key features are reflected in the supplemental ramp metering control algorithm used in this study. Using common control parameters gives

practitioners the ability to select and modify a ramp metering strategy to meet their needs, assuming it is based on similar core control logic.

As will be presented in the following sections, the overall ramp metering control logic can be segregated into four primary components:

1. Activation Component- Responsible for determining when ramp metering should be turned on for a given on-ramp based on cumulative differences in observed inflow and outflow into a given sub-segment within the pre-defined congestion segment.
2. Upstream Ramp Supplementation Component- When the calculated ramp metering rate exceeds the limits of a given ramp meter, the immediate upstream ramp meter may be activated for additional inflow control.
3. Ramp Queue Override Component- Before ramp metering activation and at each ramp metering rate update, the queue on the associated ramp is checked. If the maximum queue is detected, appropriate actions are taken to reduce the queue within the constraints of the control algorithm.
4. Deactivation Component- As congestion dissipates, ramp metering for inflow control is no longer needed. This component defines the criteria for shutting down ramp metering control.

The general ramp metering control algorithm flow chart can be visualized in Figure 4-7. The details of the ramp metering control algorithm are presented in the following sections.

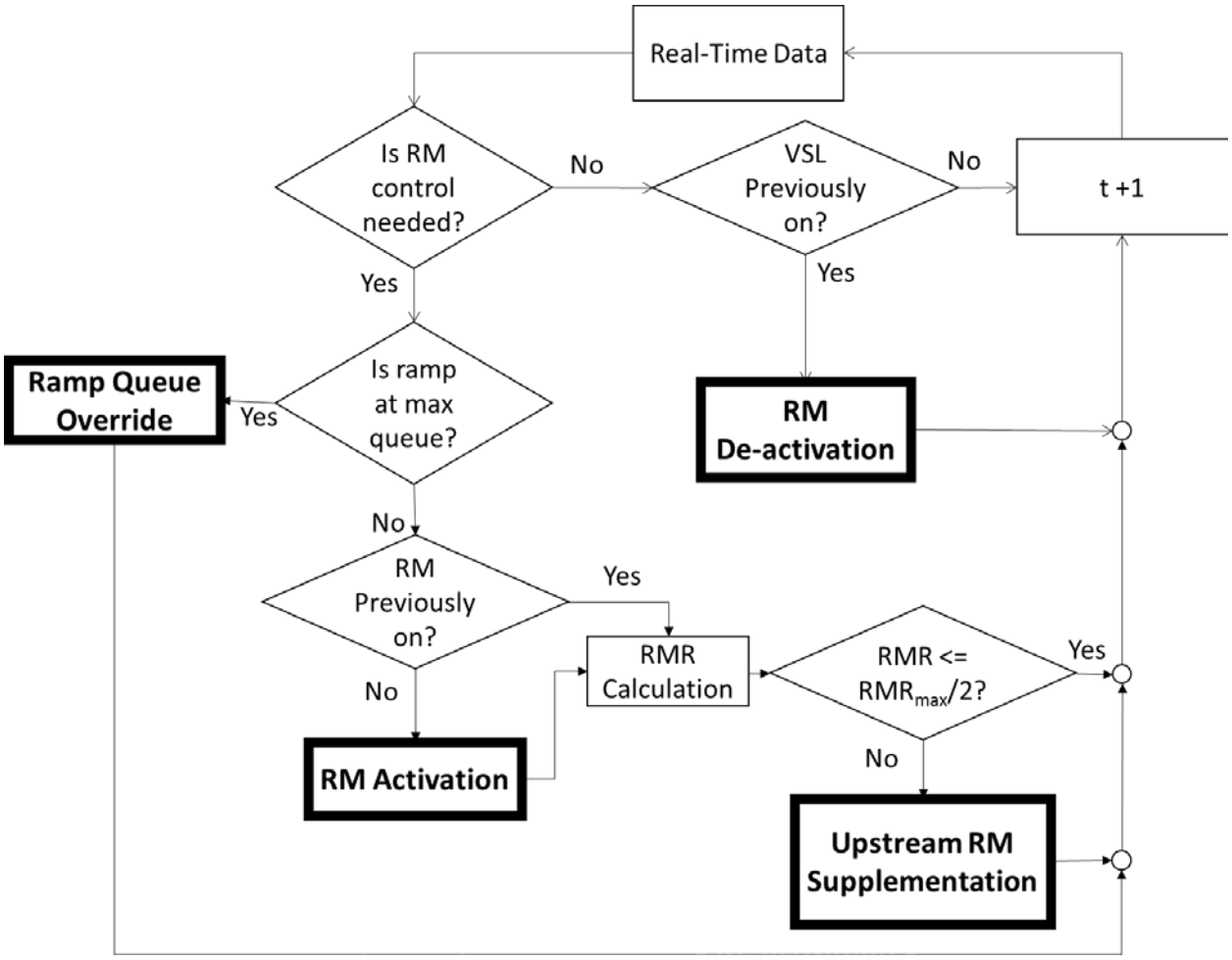

Figure 4-7: Ramp Metering Control Operational Flow Chart

4.5.1 Ramp Metering Activation

As described in the ramp metering deployment guideline section, several detectors are used to monitor real-time traffic flows into and out of each sub-segment. Total inflow is simply the sum of all entrance points into the sub-segment. In a similar fashion, total outflow from a sub-segment can be computed. As congestion builds, the cumulative difference in inflow and outflow will build up to a critical value. This critical difference in inflow and outflow can be derived from the flow-density relationship of the target sub-segment. The objective of the proposed ramp metering control is to intervene as conditions approach the critical density. In doing so, the inflow will be

throttled to keep the sub-segment in the stable flow regime of the flow-density diagram. Thus, applying a conservative estimate of the critical density will meet this need. Knowing the length of each sub-segment, the critical density can be converted into a critical cumulative difference in inflow and outflow using the following equation:

$$k_i^{crit} * L_i = X_i^{crit} \tag{4.8}$$

Where:

k_i^{crit} = critical density on sub-segment i

L_i = length of sub-segment i

X_i = critical cumulative difference in inflow-outflow on sub-segment i

In the proposed ramp metering control algorithm, this inflow and outflow data is sent to the system controller for ramp metering decisions every 30 seconds. Therefore, the cumulative difference in inflow-outflow can be computed as:

$$\beta_i(t) = \beta_i(t-1) + q_i^{in}(t) - q_i^{out}(t) \tag{4.9}$$

Where:

t = 30 second time interval step

β_i (t) = observed cumulative difference in inflow-outflow on sub-segment i at time t

q_i^{in} (t) = total inflow into sub-segment i during time interval t

q_i^{out} (t) = total inflow out of sub-segment i during time interval t

A few subtleties regarding equation two warrant further discussion. First, equation two assumes the sub-segment is empty during activation. If this condition cannot be satisfied in

practice, an estimate of vehicles with the sub-segment at activation will be needed. For instance, if the system is activated when 10 cars are within the boundaries of the target sub-segment, and assuming all 10 cars exit the downstream mainline boundary, then the system will have a 10-car outflow bias. Similarly, under non-congested conditions, some vehicles may enter the sub-segment at the end of the time interval and may not have sufficient time to traverse the entire sub-segment before the end of the time interval step. This condition would obviously bias the inflow count for that time interval. However, those vehicles that were counted as inflow for one time interval will be counted as outflow during the next time interval, assuming the sub-segment can be traversed in a single time interval. Thus, the cumulative difference in inflow and outflow will naturally stay below the critical value in non-congested conditions.

Finally, at the end of each time interval the result of equation two is compared to the pre-defined critical cumulative difference in inflow and outflow for each sub-segment. Once the cumulative difference in inflow and outflow exceeds the threshold, the ramp meter (or meters if the sub-segment has multiple on-ramps) will be turned on for that sub-segment. This process can be visualized in Figure 4-8. If a sub-segment with multiple on-ramps displays a cumulative inflow-outflow above the threshold value, then all ramps may be turned. The associated ramp metering rates will incorporate equity considerations based on recent demand patterns.

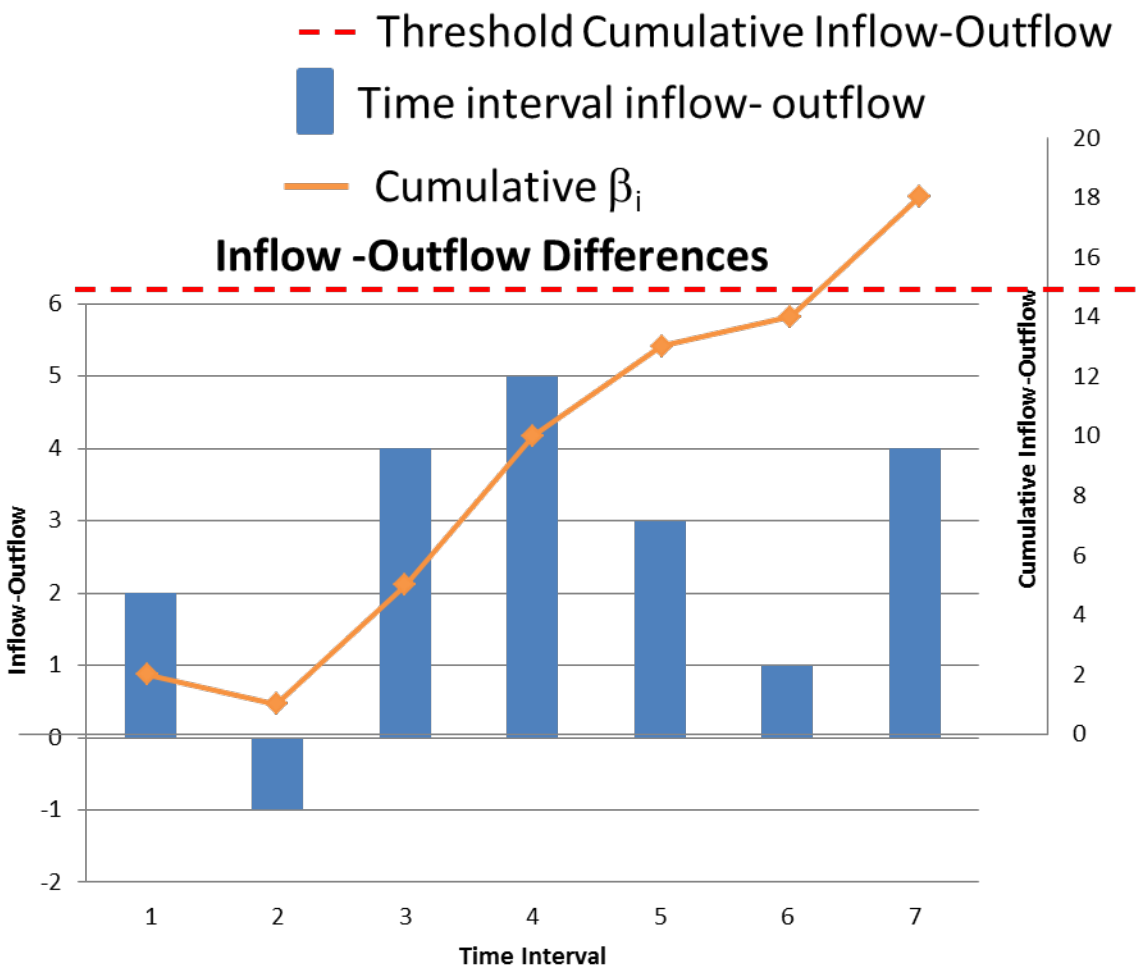

Figure 4-8: Ramp Metering Activation Visualization

As shown in Figure 4-8, the ramp meter would be activated at the start of time interval seven. The following section will describe how the metering rates are calculated.

4.5.2 Ramp Queue Override and Ramp Metering Rate

Recognizing that ramp metering seeks to mitigate congestion by controlling inflow from nearby on-ramps, the potential for causing excessive delay to the ramp vehicles exists. While several queue detection/estimation methods exist, the proposed control algorithm uses the

observed difference in ramp inflow and outflow to determine the queue length (number of vehicles) at the start of each time interval. This calculation is performed as follows:

$$\theta_{ramp\ i}(t) = \theta_{ramp\ i}(t-1) + q^{in}_{ramp\ i}(t) - q^{out}_{ramp\ i}(t) \quad (4.10)$$

Where: $\theta_{ramp\ i}(t)$ = queue on ramp i at the end of time interval t (number of vehicles)

$\theta_{ramp\ i}(t-1)$= queue on ramp i at the end of the previous time interval (number of vehicles)

$q_{ramp\ i}^{in}(t)$ = inflow onto ramp i during time interval t

$q_{ramp\ i}^{out}(t)$ = outflow from ramp i during time interval t

As done by Papageorgiou (2002), this study assumes a maximum acceptable on-ramp queue length of 20 vehicles. For freeway-to-freeway interchanges, the maximum acceptable queue length is 90 vehicles. This calculation requires an estimate of the average vehicle length. In the case where the on-ramp or interchange does not provide sufficient storage to meet the aforementioned acceptable queue lengths, an alternative method is suggested. This method is based on the findings of Hasan (1999), who found that on-ramp queue detectors placed at 75 percent of the physical ramp length outperformed detectors at 100 and 62.5 percent of the ramp length. In this application, the maximum acceptable queue length is defined to be 75 percent of the ramp length, given an average vehicle length. With this consideration in mind, the maximum acceptable queue length for an on-ramp is defined as:

$$\theta^{max}_{ramp\ i} = min\left[20\ vehicles, \frac{0.75L_{rampi}}{\overline{VL}}\right] \quad (4.11)$$

Where:

q^{max}_{rampi}= maximum acceptable queue on ramp i (number of vehicles)

$L_{ramp\ i}$= length of ramp i (ft)

VL = average vehicle length (ft)

In a similar fashion the maximum acceptable queue length for a freeway-to-freeway interchange ramp is:

$$\theta^{max}_{ramp\ i} = min\ \left[90\ vehicles, \frac{0.75 L_{rampi}}{\overline{VL}}\right] \quad (4.12)$$

Where:

q^{max}_{rampi}= maximum acceptable queue on ramp i (number of vehicles)

$L_{ramp\ i}$= length of ramp i (ft)

VL = average vehicle length (ft)

The maximum queue constraint is checked before ramp metering is activated and, each time, the metering rate is updated. Upon activation of a ramp meter(s), the associated ramp metering rate(s) needs to be established. This calculation is based on the magnitude in which the cumulative difference in inflow and outflow exceeds the threshold value. To keep the sub-segment operating in the stable regime of the fundamental diagram, the control system seeks to return the cumulative difference in inflow-outflow back to the threshold value in the next time interval. Thus, the appropriate ramp metering rate(s) will restrict the inflow of vehicles from the on-ramp(s) to achieve this goal. The ramp metering rate calculation is based on the assumption that this rate will stabilize the differences in inflow-outflow for the next time period. If the cumulative difference in inflow-outflow continues to grow for several consecutive intervals after supplemental ramp metering activation, this indicates that the current ramp metering strategy may not be sufficient for

the demand. Therefore, the immediate upstream ramp meter may be activated for supplementary inflow control. This topic is discussed later in this section.

For sub-segments containing a single on-ramp, the calculation for the initial ramp metering rate or metering rate updating is identical as it uses the observed ramp discharge rate from the previous time interval and the difference in cumulative inflow-outflow and the threshold value. Specifically,

$$q_{ramp\,i}(t-1) - [\beta_i\,(t-1) - X_i] = RMR_i(t) \tag{4.13}$$

Where:

$q_{ramp\text{-}i}(t\text{-}1)$ = ramp flow for the previous time interval

$\beta_i(t\text{-}1)$ = Cumulative inflow-outflow

X_i = Threshold inflow-outflow

$RMR_i(t)$ = Ramp metering rate for ramp i for time interval t

If the calculated ramp metering rate is above the maximum ramp metering rate, the maximum ramp metering rate will be selected. In a similar fashion, if the observed inflow-outflow drops below the threshold value while ramp metering is on, the maximum ramp metering rate will be selected. If the observed inflow-outflow remains below the threshold for five consecutive intervals, that ramp will be turned off.

On the other hand, if the calculated ramp metering rate is below half of the maximum ramp metering rate, then upstream ramps will be activated for supplementation. This strategy offers several advantages over waiting until the calculated ramp metering rate is below the minimum rate. First, this strategy reduces the likelihood of excessive ramp queues on a given ramp. Next,

this strategy allows for equity considerations as the upstream ramp flow enters the downstream sub-segment as mainline flow. Third, using the upstream ramp increases the capacity to control inflow rates. However, when no upstream ramps exist, the minimum ramp metering rate will be selected.

For sub-segments with more than one on-ramp, inflow may be controlled by multiple on-ramps. This control strategy recognizes that an increased number of inflow points can result in rapid increases in inflow-outflow. Additionally, this method allows for equity considerations for controlling flow into the target sub-segment. Here, the target ramp inflow rate for the next time interval is:

$$\sum_{n=1}^{N} q_n(t-1) - [\beta_i(t-1) - X_i] = F_{Total}(t) \quad (4.14)$$

Where:

n = number of metered on-ramps in the target sub-segment

q_n(t-1)= flow rate on ramp n within sub-segment i in the previous time interval

β_i(t-1) = Cumulative inflow-outflow

X_i = Threshold inflow-outflow

F_{Total}(t)= Target ramp inflow for the upcoming time interval

If F_{Total} is above half of the maximum ramp metering value, only the most downstream ramp will be activated. Once the target inflow is below this threshold, the next upstream ramp will be activated to supplement ramp inflow control. This process is repeated for the number of metered ramps within the sub-section. Each respective metering rate is based on recent demand observations. The ramp metering rate for each ramp is calculated as follows:

$$\frac{d_n(t-1)}{\sum_{n=1}^{N} d_n(t-1)} F_{Total}(t) = RMR_n(t) \quad (4.15)$$

Where:

$d_n(t\text{-}1)$ = demand on ramp n in the previous time interval

RMR_n = demand weighted ramp metering rate for on-ramp n within sub-segment

When the calculated ramp metering rate is below half of the maximum ramp metering rate for the target sub-segment, the immediate upstream ramp meter will be called on for inflow control supplementation if it is available. Since the sub-section upstream boundary was defined to be at the merge area of the upstream sub-section on-ramp, the effect of upstream ramp metering supplementation will be realized in the target control interval. In this study, only the immediate upstream ramp meter can be used for supplementation.

In such cases where upstream supplementation is possible, equity issues must be addressed. This process is similar to that which is used in the previous section for multiple ramp meters on a single sub-segment. First, the target ramp inflow rate for the next time interval must be calculated as:

$$\sum_{n=1}^{N} q_n(t-1) + q_{ramp\ j}(t-1) - [\beta_i(t-1) - X_i] = F_{Total}(t) \quad (4.16)$$

Where:

n = number of metered on-ramps in the target sub-segment i

$q_n(t\text{-}1)$= flow rate on ramp n, in the target sub-segment in the previous time interval

$q_{ramp\ j}(t\text{-}1)$ = flow rate on the upstream on ramp, in the previous time interval

$\beta_i(t\text{-}1)$ = Cumulative inflow-outflow

X_i = Threshold inflow-outflow

$F_{Total}(t)$= Target ramp inflow for the upcoming time interval

Again, the ramp metering rate for each meter is based on the recent demand observation. This consideration is similar to equation eight, except that the upstream on-ramp is included:

$$\frac{d_k(t-1)}{\sum_{n=1}^{N} d_n(t-1)+d_{ramp\ j}(t-1)} F_{Total}(t) = RMR_k(t) \quad (4.17)$$

Where:

k = total number of metered ramps (sum of sub-segment ramps and upstream ramp)

$d_k(t\text{-}1)$ = demand on ramp k in the previous time interval

RMR_k = demand weighted ramp metering rate for on-ramp k

It is worth noting that it is possible that a given ramp can be called for inflow control on the sub-segment for which it belongs and for supplemental inflow control for the immediate downstream sub-segment. In this case, the lower (more restrictive) ramp metering rate will be selected. Specifically, the ramp metering rate of the upstream ramp can be determined by:

$$RMR_{i+1}^{Final}(t) = \min[RMR_{i+1}(t), RMR_{i+1}^{*}(t)] \quad (4.18)$$

Where:

RMR_{i+1}^{Final}= selected ramp metering rate for the upstream meter

RMR_{i+1}= calculated ramp metering rate for the congested upstream sub-segment

RMR_{i+1}^{*}= calculated supplemental ramp metering for sub-segment i

As congested conditions dissipate, the cumulative inflow-outflow observation will begin to fall, as will the need to control inflow. Thus, the required ramp metering rates will gradually grow until metering is no longer needed. The sections above describe how ramp meters are activated and how the ramp metering rates are calculated and updated. The discussion now moves to the control logic for turning off ramp metering.

4.5.3 Ramp Metering Deactivation

When multiple ramps are activated to control the ramp flows into a congested sub-segment under the supplemental upstream on-ramp function, the ramps are turned off in a sequential order. Eventually, the required metering rate will be above half the maximum rate for the downstream meters. If this condition is observed for five consecutive intervals, the farthest upstream ramp will be turned off. Each of the remaining ramps will be turned off in a similar fashion until only the most downstream on-ramp on the sub-segment remains activated. Non-supplemental ramp meters will be deactivated if the observed inflow-outflow remains below the threshold for five consecutive intervals.

4.6 Chapter Summary

This chapter has presented the experimental plan to generate the dataset for developing the decision/deployment support tool for VSL and VSLRM control. The dataset aimed to cover a robust set of potentially congested traffic environments using a simulated experiment design. To ensure that the results reflected realistic conditions, a base environment was calibrated with field data. The incorporated VSL and VSLRM control algorithms were designed to reflect the common control logic of such ITS-based strategies. As will be described in Chapter 5, the outputs of these simulations were used to derive performance measures for the development of the tool.

Chapter 5: Development of Decision and Benefit Modules

5.1 Key Functions of Modules

The proposed decision/deployment support tool was designed for the general planning process of a congestion mitigation project. First, it must be determined which, if any, strategy is the most appropriate for a list of candidate sites. This decision should be based on the expected benefits of a given strategy relative to the cost of implementation. As will be described in section 5.2, these benefits are based on safety and mobility performance measures. While the expected benefits from a given strategy may be estimated from various methods including regression analysis, such methods do not capture the probabilistic essence of the decision-making process. Moreover, the distinct nature of the strategy selection process suggests the use of a discrete choice model (DCM). Upon selecting the appropriate mitigation strategy, additional guidelines are needed to ensure proper resource allocation. These guidelines are based on the estimation of the expected total benefit of the suggested strategy based on user-defined objectives and constraints. The continuous nature of the benefits estimation implies the use of regression methods that utilize user-defined benefit weights.

Recognizing the need to investigate the conditions that advocate the application of VSL or VSLRM control, this chapter first discusses the development and analysis of the Decision Module. To establish a "ground truth" for model comparison, control system performance criteria were defined to classify the data. The results of this analysis will provide valuable insight on the conditions that warrant VSL or VSLRM control, and the impact of specific critical variables on the expected benefits. For those conditions where the use of VSL or VSLRM control is not suggested, further guidance will be provided by determining the *general* cause of the less than desirable benefits yielded by these control strategies. Note that the VSL and VSLRM control

algorithms were designed to activate and update based on sustained levels of congestion. Therefore, the percentage of time that the control system was activated provides a surrogate measure of the duration and severity of the congested conditions. Thus, the level of sustained congestion was determined to be either too low or too high for significant benefits to be realized under these ATMS methods. This determination was made by evaluating the amount of time that the control system was active and the level of demand. Thus, the decision modeling is based on four possible choices: No Control, VSL control, VSLRM control, and Over-Congested. The Over-Congested choice suggests that additional or alternative congestion mitigation strategies are needed.

Next, the Benefits Module of the tool estimates the expected total benefits from the suggested control strategy, based on user-defined objectives and constraints incorporated in the mobility and safety weights. As described in section 5.3, total benefits were calculated using a weighted benefit for the relative change in total speed variance (safety) and total time spent (mobility), respectively. These weights were based on the estimated annual delay and crash savings relative to the initial capital cost of these control strategies. Similar to the decision model evaluation, the benefits module was compared to the observed benefits derived from the simulation outputs.

Several models were considered for both the Decision and Benefits Modules. Each model was labeled as either a base or advanced model. The base models were the independent statistical models that are commonly applied to decision or benefit estimation analysis. The base decision methods that were considered were decision trees and multinomial logistic regression (MLR). For the base benefits models, ordinary least squared (OLS) regression was evaluated. The advanced model employed in this study was a discrete-continuous model that considered the correlation in

the error terms between the decision and benefits models. Each model was compared to the "ground truth" dataset derived directly from the simulation results.

Before generating each of the considered models, the full dataset of 1,024 observations was randomly split, 80 percent (818 observations) for model calibration and 20 percent (206 observations) for model validation.

5.2 Performance Measures for ATMS Evaluation

5.2.1 Definition of Performance Measures

Upon the completion of the simulation runs under each control scenario, the outputs were used to evaluate the change in safety and mobility of VSL and VSLRM control relative to the "no control" case. Here, the surrogate measure of speed variance was used to assess safety while the total travel time for all vehicles in the network during the analysis period was used to evaluate mobility. Explicitly, these performance measures are defined as:

$$\%\Delta SV_i = \frac{SV_{No} - SV_i}{SV_{No}} \tag{5.1}$$

$$\%\Delta TTT_i = \frac{TTT_{No} - TTT_i}{TTS_{No}} \tag{5.2}$$

For decision-making purposes, the relative benefits are combined into a single metric, Total Benefit:

$$TB_i = \gamma_{SV}\%\Delta SV_i + \gamma_{TTT}\%\Delta TTT_i \tag{5.3}$$

Where:

TB_i = total benefit for ATMS i

$\%\Delta SV_i$= percent change speed variance for ATMS i

$\%\Delta TTT_i$= percent change total travel time for ATMS i

SV_{no} = speed variance under No Control

TTT_{no} = total travel time under No Control

SV_i= speed variance for ATMS i

TTT_i= total travel time for ATMS i

γ_{SV} = weight for safety benefit

γ_{TTT} = weight for mobility benefit

The relative changes in safety and mobility were calculated for each simulated scenario to estimate the total benefit of the control strategy. These results were used for the development of the decision and benefits models developed. The procedure for calculating the benefits weights is presented in the following section.

5.2.2 Determining Benefit Weights and Deployment Costs

To meet the needs of the decision-maker, the tool allows users to input objectives and constraints in the form of implementation costs and weighted safety and mobility benefits. To determine these weights, this study derived a procedure based on the monetized safety and mobility savings from the base environment of MD100. The relative differences in the monetary benefit from a relative unit change in speed variance (%ΔSV) and a relative unit change in total travel time (%ΔTTT) are used as safety and mobility weights, respectively. Note that the developed decision and benefits models are based on the sum of relative changes in speed variance and total travel time resulting from the implementation of VSL or VSLRM control. Therefore, it was necessary to monetize these relative changes, rather than raw changes in speed variance and total travel time.

The safety monetization procedure was structured around the estimation of reduced crash frequency and associated crash cost. The general safety monetization procedure can be summarized as a three-step process in Figure 5-1 below:

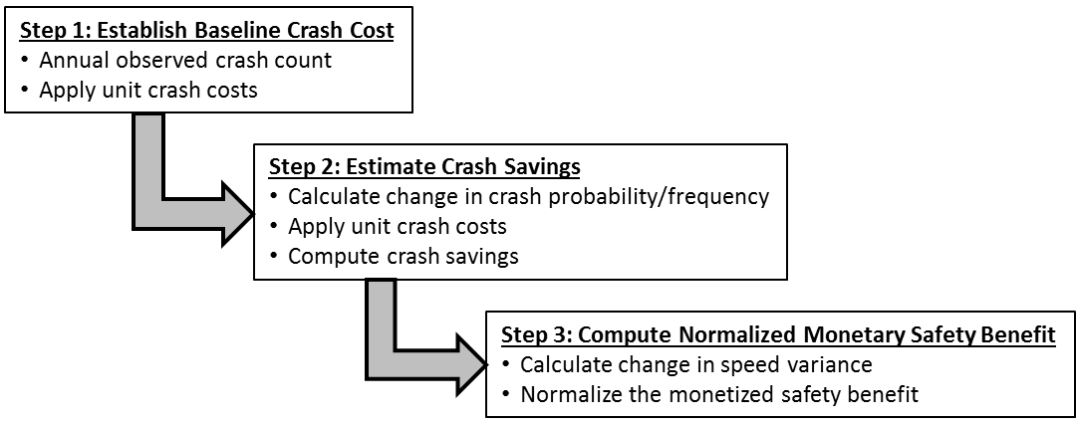

Figure 5-1: Procedure for Estimating Monetized Safety Benefit

The first step in monetizing the safety benefit was to establish the baseline (No Control) crash cost. To do so, a count of crashes with corresponding injury severity on the target highway segment was needed. Here, only crashes susceptible to correction by VSL control were considered (i.e. rear-end and side-swipe crashes). Further filtering was applied to consider only such crashes that occurred in the p.m. peak period, in the westbound direction of travel. The crash data for this analysis was accessed from the Maryland Automated Accident Reporting System (MAARS) for calendar-year 2013. Next, the total baseline crash cost was established by applying the National Highway Traffic Safety Administration (NHTSA) unit crash costs (2015). The summary of this step including the crash injuries and associated costs are shown in Table 5-1. Note that there were no fatal crashes on this segment in 2013.

Table 5-1: Summary of Baseline Crash Cost Calculation

Severity	*# Crashes in 2013	** Economic Cost	Crash Severity Cost
PDO	6	$ 42,298	$ 253,788
Injury	4	$ 127,768	$ 511,072
Possibly Incapacitating	1	$ 276,010	$ 276,010
Incapacitating	1	$ 1,001,208	$ 1,001,208
Total	**12**		**$ 2,042,078**

*****Obtained from MAARS Database (2015)

**Unit Crash Costs (NHTSA, 2010)

Step 2 covers the process of estimating the crash savings. This step is based on the expected crash reduction resulting from VSL or VSLRM control. In this study, the Bayesian Poisson-gamma models developed by Xu et al. (2013) were employed to estimate the change in crash frequency. This model was selected for two reasons. First, the model inputs were compatible with the available speed deviation and relative speed drop data. Next, the model was able to directly compute the expected crash frequencies of crash types susceptible to be reduced from VSL control, rear-end and side-swipe crashes. In any case, the relative change in crash frequency from the Xu et al. (2013) model was calculated to be 71.2 percent. Upon applying this crash reduction to the baseline crash cost, the total crash savings was found to be $1,458,043.

The third and final step was to normalize the crash savings by dividing the crash savings by the observed relative percentage change in speed variance. Using the field data from MD100, the relative change in speed variance was calculated as 15.1 percent. Therefore, the normalized unit

of crash savings per unit change in relative speed variance rounded to the nearest thousand was $92,000.

The monetization of the mobility savings was more straightforward. This process was founded on the estimation of annual delay for the base (No Control) condition. The formulation of the base delay estimation in hours per day was:

$$Base\ Delay\ Cost = \frac{(\overline{TT}_{Peak} - TT_{FF})}{3600} * Q_{Peak} * VT \quad (5.4)$$

Where:

$TT_{Peak} = Peak\ Period\ Average\ Travel\ Time\ (seconds)$

$TT_{FF} = Free\ Flow\ Travel\ Time\ (seconds)$

$Q_{Peak} = Peak\ Period\ Throughput\ (vehicles)$

$VT = Value\ of\ Time\ (\$/hr)$

Using field observations from the Chang et al. (2011) study, the free-flow travel time was 180 seconds, the p.m. peak period travel time was 460 seconds, and the peak period (4:30 p.m. – 6:00 p.m.) throughput was 5,615 vehicles. Next, the value of time for travelers in the Washington, D.C.-Baltimore region was $17.67 per hour (TTI, 2014). Finally, assuming 260 p.m. peak periods per year, the base delay cost was $2.2 Million. Therefore, a one-percent change in the base delay cost would result in $22,000 of annual delay savings. These estimated monetized benefits are used as the weights for the safety and mobility benefits.

Next, the costs to deploy the control systems were considered in the benefits module. To achieve this, VSL and ramp metering costs were employed from the U.S. DOT cost database (U.S.

DOT, 2015). This study assumed the cost to deploy the VSL system was $400,000 and the supplemental ramp metering cost was an additional $200,000. Therefore, adding ramp metering to the VSL system would increase the control system cost by 50 percent.

Using the above benefit weights and cost, a benefit-to-cost ratio (B/C) was determined for each control strategy under all 1,024 scenarios. As will be described in the following section 5.5, the B/C ratio was used as a critical parameter for benefits modules.

5.3 Base Decision Models

The base decision models evaluated were a decision tree and multinomial logic regression. Nested logistic regression was considered, but the correlation within the ATMS nest was too low for such a structure. Table 5-2 summarizes the variables used in the base decision models.

Table 5-2: Variables for the Decision Models

Variable Abbreviation	Variable Description	Variable Type
Decision	Decision	Dependent
Dist up	Distance to the upstream on-ramp	Independent
V/C 100	Volume to capacity ratio, multiplied by 100 for scaling purposes	Independent
Per ramp	Percentage of V/C ratio coming from the bottleneck on ramp	Independent
Per Truck	Percent trucks in traffic stream	Independent
DC	Driver Compliance	Independent

Note that the unweighted benefits are utilized for the choice logic to ensure observed benefits are beyond the simulation error. For each decision model, hypothetical choices were made based on three choice parameters derived by this study, described in Table 5-3.

Table 5-3: Criteria to Classify Simulation Benefits

Parameter	Description	Value
Minimum Benefit	Minimum benefit needed to consider VSL or VSLRM control	10
VSLRM Justification	Minimum benefit improvement to support VSLRM over VSL control	5
Minimum Activation	Used to determine cause of less than desirable benefits of VSL or VSLRM	50%

First, the minimum benefit for VSL or VSLRM implementation was set to 10. This value ensures that the observed total benefit is beyond the maximum simulation error set in the calibration effort. The next choice parameter is VSLRM justification. This parameter establishes a threshold of required additional benefits from the deployment of VSLRM over independent VSL control. This value was set to five based on the additional cost to deploy a supplemental ramp metering control relative to the minimum benefit parameter. The third and final choice parameter was the minimum activation parameter. When neither control strategy produced benefits beyond the minimum benefit parameter, this parameter was used to provide guidance on the cause of the less than desirable benefits. Recall that the control algorithms are activated based on sustained measures of congestion. Therefore, the percentage of time that VSLRM control was activated provides insight on the underlying cause of the limited benefits. The first explanation is that VSLRM control was not needed and thus the limited activation of the control system produced minimal benefits. In such cases, the percentage of time in which the control system was activated was limited. The second explanation was that the traffic demand was beyond the reasonable limits of these control strategies under the given compliance rate. Here, the percentage of time the control system was activated was relatively high. To determine the most appropriate value for the

minimum activation parameter, an ad-hoc sensitivity analysis was performed using activation parameter values of 25, 50, and 75 percent to assess the distribution of the "No Control" and "Over-Congested" choices. As shown in Figure 5-2, the differences in the distributions across these activation parameter values was minimal. These results suggest that in the environments that produced the "Over-Congested" choice, the control system was *generally* activated for at least 75 percent of the analysis period. On the other hand, in the environments that produced the "No Control" choice, the control system was *generally* activated for less than 25 percent of the study period. Recognizing the nominal impact of the minimum activation parameter on the distribution of choices, the median value of 50 percent was applied in this study. Note that each of these parameters could be changed to meet the needs of the end user.

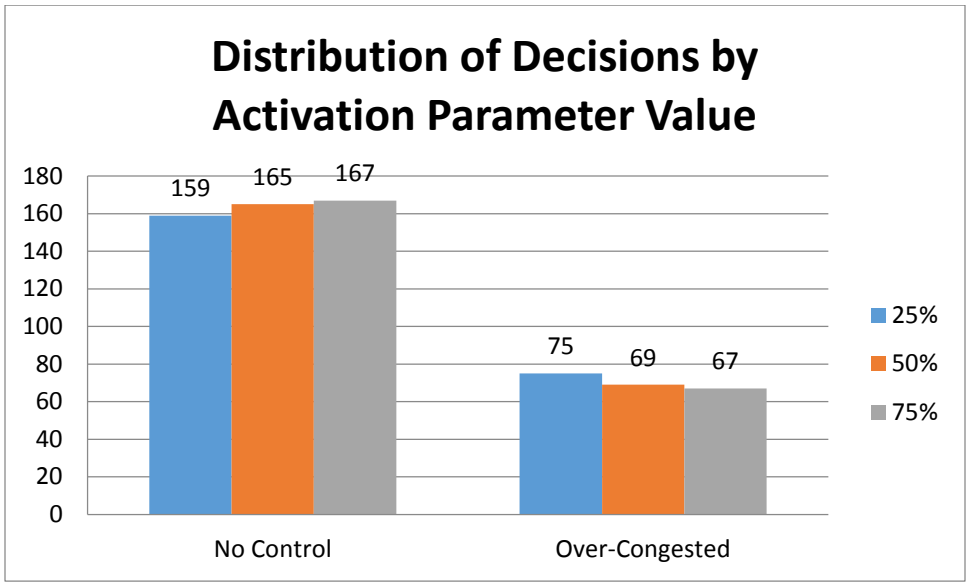

Figure 5-2: Distribution of "No Control" and "Over Congested" Decisions by Activation Parameter

In summary, this study uses a minimum benefit parameter of 10, a VSLRM justification parameter of five, and an activation parameter of 50 percent. Note that such criteria can be changed

to meet the goals of a given decision-maker. In any case, these parameters were used to establish the following criteria to classify the simulation benefits:

$$IF\ TB_{VSL} \geq 10\ AND\ TB_{VSL} + 5\ \geq\ TB_{VSLRM}\ THEN\ Choice = VSL \quad (5.5)$$

$$IF\ TB_{VSL} \geq 10\ AND\ TB_{VSL} + 5\ <\ TB_{VSLRM}\ THEN\ Choice = VSLRM \quad (5.6)$$

$$IF\ TB_{VSL} < 10\ AND\ \ AND\ \ TB_{VSLRM}\ \geq 10\ THEN\ Choice = VSLRM \quad (5.7)$$

$$IF\ TB_{VSL} < 10\ AND\ \ TB_{VSLRM} < 10\ AND\ ATMS_{ON} \leq 50\%\ THEN\ Choice = No\ Control \quad (5.8)$$

$$IF\ TB_{VSL} < 10\ AND\ \ TB_{VSLRM} < 10\ AND\ ATMS_{ON} > 50\%\ THEN\ Choice = Over\ Congested \quad (5.9)$$

Where:

TB_{VSL} = total benefit for VSL control

TB_{VSLRM} = total benefit for VSL paired with ramp metering control

$ATMS_{ON}$ = percent time at least one ATMS device was activated

Choice = Control Decision

The following sub-sections present the results and analysis of the base decision models.

5.3.1 Decision Tree

The decision tree was built using chi-squared automatic interaction detection (CHAID) procedures. This tree-growing algorithm relies on chi-square tests to evaluate the strength of the interaction of each independent (predictor) variable with the dependent (response) variable. The variable with the strongest interaction is used to create the branches and leaves of the tree. If

categories within an independent variable are not significantly different with respect to the dependent variable, they are merged (IBM, 2011).

The result of the CHAID tree analysis produced a calibrated tree with four branches, each with three levels as shown in Figure 5-3.

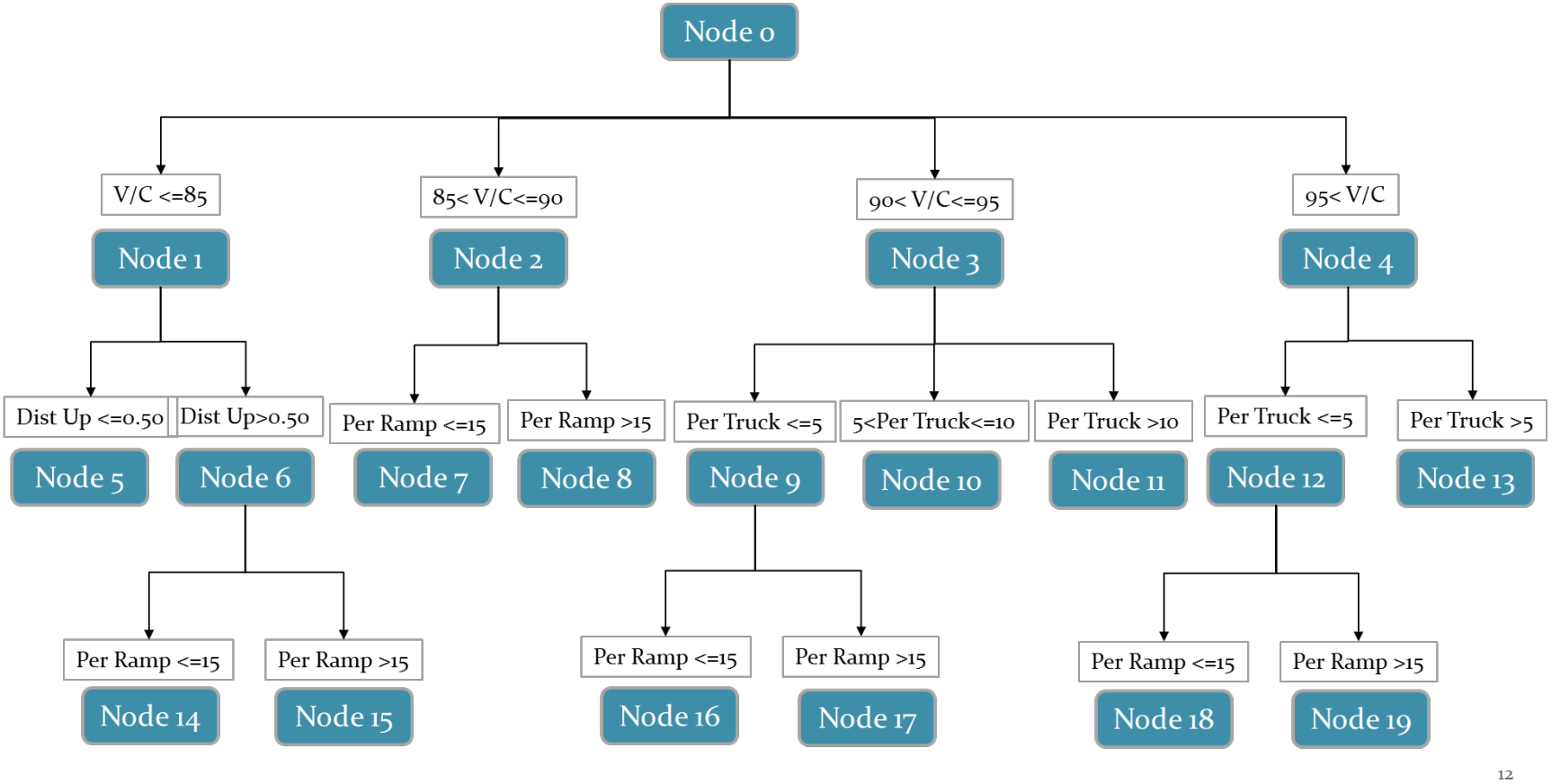

Figure 5-3: Decision Tree Results

To test the accuracy of the calibrated tree, the validation dataset was tested against the "ground truth" decisions. As shown in Table 5-4, the tree was able to accurately classify 64.6 percent of the control decisions. Note that degree of decision accuracy was 63.6 percent for "No Control," 78.2 percent for VSL, 60.7 percent for VSLRM, and 0 percent for "Over-Congested." These results indicate that the decision tree was not able to predict heavily congested conditions where VSL or VSLRM may have limited benefit. Failure to predict such situations can result in wasted resources and driver frustration.

Table 5-4: Decision Tree Validation Results

			TREE Prediction			**Total**
			No Control	VSL	VSLRM	
Decision	(1) No Control	Count	21	12	0	33
		% of Total	**10.2%**	5.8%	0.0%	16.0%
	(2) VSL	Count	10	61	7	78
		% of Total	4.9%	**29.6%**	3.4%	37.9%
	(3) VSLRM	Count	10	23	51	84
		% of Total	4.9%	11.2%	**24.8%**	40.8%
	(4) Over-Congested	Count	0	1	10	11
		% of Total	0.0%	0.5%	4.9%	5.3%
Total		Count	41	97	68	206
		% of Total	19.9%	47.1%	33.0%	100.0%

5.3.2 Multi-Nominal Logistic Regression Model

The next decision model considered was a MLR model. The response variable "Decision" can take one of four values, "No Control," VSL, VSLRM, or "Over-Congested," indexed as 1, 2, 3, and 4. The results of this model were probabilities of each "Decision" for a given set of independent variables (i.e. scenarios). Before presenting the results, a background on multinomial logit regression is warranted.

First, the definition of the probability function is:

$$\pi_{ij} = \Pr[Y_i = j] \tag{5.10}$$

Where: π_{ij} = Probability of i-th response falling into j-th category

Y_i = Random discrete variable (Decision)

Next, assuming a linear relationship between choice and the predictor variables, the "Decision" utility is:

$$\eta_{ij} = \alpha_j + \boldsymbol{X}_i\boldsymbol{\beta}_j + \varepsilon \tag{5.11}$$

Where: η_{ij} = the utility of i-th response in the j-th category

α_j = regression constant for j-th category

X_i = vector of observed predictor variables

β_j = vector of regression coefficients

ε = error of model

Therefore, the probability of the i-th observation falling into the j-th category becomes:

$$\pi_{ij} = \frac{\exp(\eta_{ij})}{\sum_1^J \exp(nij)} \tag{5.12}$$

Having provided a background on MLR, the discussion turns to the results of the model. Table 5-5 presents the analysis of parameters for the utility function of each of the choices, using the "No Control" choice as the reference category.

Table 5-5: MLR Model Parameters

Decision[a]		*B	Std. Error	Wald	Sig.	**Exp(B)	95% Confidence Interval for Exp(B)	
							Lower Bound	Upper Bound
VSL	Intercept	-67.232	7.725	75.754	.000			
	Dist up	-2.146	.340	39.892	.000	.117	.060	.228
	Per Truck	-.072	.035	4.147	.042	.930	.868	.997
	V/C 100	.823	.093	78.600	.000	2.277	1.898	2.731
	Per ramp	-.204	.033	38.419	.000	.815	.764	.870
	DC	.053	.007	55.946	.000	1.054	1.040	1.069
VSLRM	Intercept	-83.083	7.877	111.238	.000			
	Dist up	-2.131	.356	35.781	.000	.119	.059	.239
	Per Truck	-.267	.039	47.435	.000	.766	.709	.826
	V/C 100	.998	.094	112.049	.000	2.714	2.256	3.265
	Per ramp	-.062	.035	3.215	.073	.939	.878	1.006
	DC	.033	.007	19.639	.000	1.033	1.018	1.048
Over Congested	Intercept	-124.770	10.477	141.835	.000			
	Dist up	-1.779	.444	16.067	.000	.169	.071	.403
	Per Truck	-.065	.050	1.707	.191	.937	.849	1.033
	V/C 100	1.380	.117	140.285	.000	3.975	3.163	4.994
	Per ramp	-.027	.045	.377	.539	.973	.891	1.062
	DC	.031	.009	11.537	.001	1.031	1.013	1.050

a. The reference category is: No Control
*Regression Coefficient
**Exponential of Regression Coefficient

Interpreting the model parameter estimates in Table 5-5 reveals some interesting findings. First, the distance to the upstream on-ramp was negative and significant at the 95 percent confidence level in each of the utility functions. These results indicate that, as the distance to the upstream on-ramp increases, the need for traffic control or severe congestion decreases relative to the "No Control" choice. From a traffic flow perspective, these results made sense as increased interchange density produced less intense weaving and, therefore, better utilization of the available capacity. Next, the percent truck variable was found to be significant and negative only in the VSL and VSLRM choices. Therefore, within these choices, the probability of selecting a control strategy decreases with increasing truck percentage relative to the "No Control" choice. The V/C

ratio was positive and significant in each of the utility functions. In addition, the magnitude of the V/C ratio increases from VSL to VSLRM and then from VSLRM to the "Over-Congested" choice. These results are in sync with traffic flow logic. As the demand increases, additional inflow control is needed, but eventually the demand may exceed the capabilities of these control strategies.

Interestingly, the percentage of the V/C ratio originating from the bottleneck on-ramp was found to be significant at the 95 percent confidence interval in the VSL utility function, and at the 90 percent confidence interval for VSLRM. These results indicate that the ramp demand is important for creating the conditions that warrant the use of either of these control strategies. However, ramp percentage was found to be insignificant in the "Over-Congested" choice. This result was unexpected as increased ramp demand theoretically results in more intense weaving and thus, reduced capacity utilization. Lastly, driver compliance was found to be positive and significant in each of the utility functions, relative to the "No Control" choice. Interestingly, the magnitude of the driver compliance variable decreases from VSL to VSLRM and from VSLRM to "Over-Congested." These results suggest that the relative impact of driver compliance is strongest in the VSL choice, and becomes weaker in the VSLRM and "Over-Congested" choices.

Table 5-6: Multinomial Logit Regression Validation Results

			Predicted Group				**Total**
			No Control	VSL	VSLRM	Over-Congested	
Decision	No Control	Count	21	7	5	0	33
		% of Total	**10.2%**	3.4%	2.4%	0.0%	16.0%
	VSL	Count	3	63	12	0	78
		% of Total	1.5%	**30.6%**	5.8%	0.0%	37.9%
	VSLRM	Count	7	8	59	10	84
		% of Total	3.4%	3.9%	**28.6%**	4.9%	40.8%
	Over-Congested	Count	0	2	2	7	11
		% of Total	0.0%	1.0%	1.0%	**3.4%**	5.3%
Total		Count	31	80	78	17	206
		% of Total	15.0%	38.8%	37.9%	8.3%	100.0%

Upon testing the validation dataset with the devolved multinomial logit regression model, the total model accuracy was found to be 72.8 percent, an 8.2 percent increase over the decision tree. Here, the degree of choice accuracy was 63.6 percent for the "No Control" choice, 80.1 percent for the VSL choice, 70.2 percent in the VSLRM choice, and 63.6 percent within the "Over-Congested" choice. Therefore, the multinomial logit model outperforms the decision tree in terms of model accuracy.

5.4 Base Benefit Models

Based on the correlation between weighted safety and mobility improvements for both VSL (Figure 5-4) and VSLRM (Figure 5-5), the regression models omitted a regression constant. Note that for both control strategies, the general linear relationship between safety and mobility goes through the origin. Therefore, when the total benefit is assumed to be weighted sum of the safety and mobility benefits relative to the control costs, the regression constant for estimating total benefit should be close to zero.

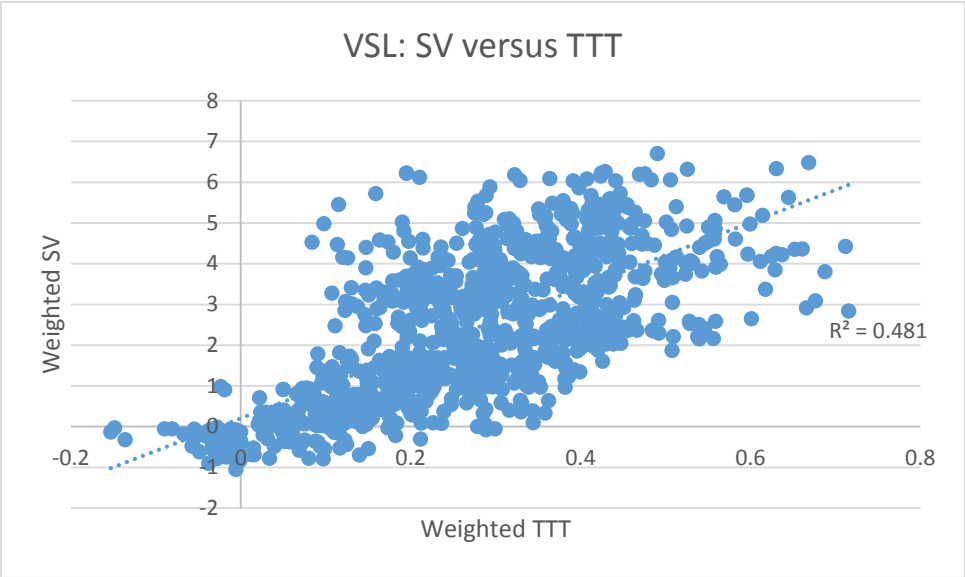

Figure 5-4: Correlation between Safety and Mobility Improvements under VSL Control

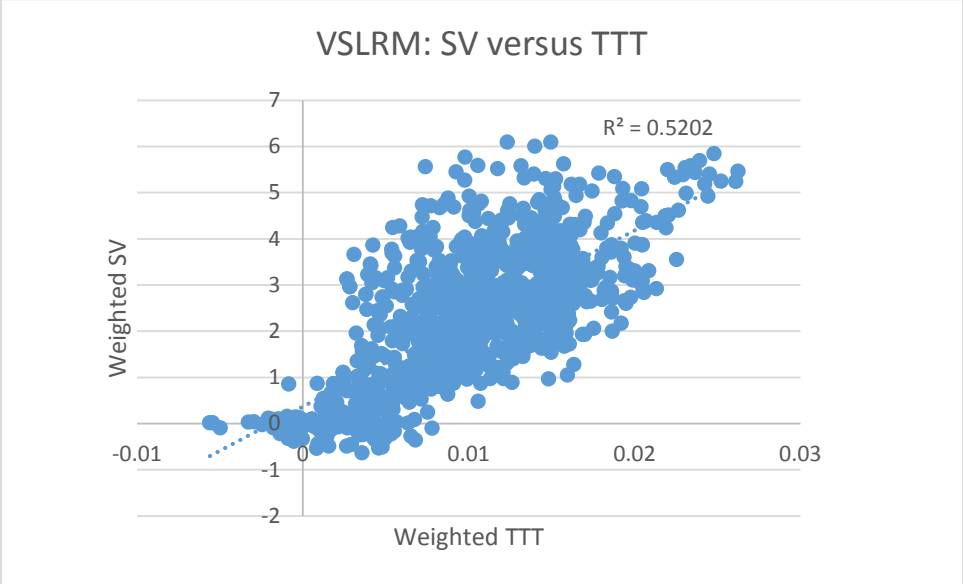

Figure 5-5: Correlation between Safety and Mobility Improvements under VSLRM Control

The variables for the base benefit models were very similar to those used in the base decision models. The only difference was the dependent variable, which became the total weighted benefit, a ratio scale variable. Thus, the total benefits for VSL and VSLRM were predicted from the five independent variables.

5.4.1 Linear Regression for VSL Benefit

As shown in Table 5-7, the linear regression model for total weighted benefit of VSL control found each of the five dependent variables to be significant at the 95 percent confidence level. First, the distance to the upstream on-ramp coefficient was found to be negative. This finding is supported by traffic flow theory in that increased interchange density would increase weaving intensity. Therefore, the benefits of VSL would be reduced. Next, the truck percentage coefficient was also negative. Again, this finding confirms that the inherent capacity consumed by commercial vehicles is essentially unaffected by VSL control. Thus, adding trucks to the traffic stream tends to reduce the overall benefits of VSL control.

The V/C ratio coefficient was found to be positive. This result was expected, as the V/C ratio increased the VSL control system is able to control inflow into the congested segment and produce increased benefits. Next, the ramp percentage coefficient was found to be negative. This result is in line with traffic flow theory; as the percentage of the bottleneck demand from the on-ramp increases, weaving intensifies. In addition, with increased ramp volumes, there is less inflow control into the congested segment under VSL control. Finally, as expected, the driver compliance coefficient was positive, meaning that as compliance to VSL control increases, the total benefit will increase. The adjusted R-squared value for this model was 0.733, meaning that about 73 percent of the variance in the data was explained by this model.

Table 5-7: VSL Benefit Linear Regression Model Parameters

Coefficients[a,b]

Model		Unstandardized Coefficients		Standardized Coefficients	t	Sig.
		B	Std. Error	Beta		
1	Dist Up	-.786	.092	-.335	-8.536	.000
	Per Truck	-.049	.011	-.145	-4.585	.000
	V/C	4.738	.262	1.366	18.096	.000
	Per Ramp	-.088	.009	-.503	-9.632	.000
	Driver Comp	.018	.002	.389	9.907	.000

a. Dependent Variable: Total Weighted Benefit

b. Linear Regression through the Origin

Model adjusted R^2= 0.733

Upon testing the model with the validation dataset, the standard error was found to be 2.18. This result shows that this model is able to estimate the benefits of VSL control using out-of-sample data, suggesting a fairly accurate estimation of VSL control benefits.

5.4.2 Linear Regression for VSLRM Benefit

Similar to the results found for the VSL model, the VSLRM model established that all five independent variables were found to be statistically significant at the 95 percent confidence level (Table 5-8). In addition, the signs of each of the coefficients were the same as the VSL model. One may have expected the ramp percentage coefficient to become positive in the VSLRM model; however, this was not the case. This observation may be explained by the underlying ramp queue override function that attempts to prevent ramp spillback at the cost of releasing more than the desired amount of vehicles onto the mainline. In any case, the model produced an adjusted R-

squared value of 0.749, suggesting that the model can explain nearly 75 percent of the variation in the data.

Table 5-8: VSLRM Benefit Linear Regression Model Results

Coefficients[a,b]

Model		Unstandardized Coefficients		Standardized Coefficients		
		B	Std. Error	Beta	t	Sig.
1	Dist Up	-.501	.075	-.255	-6.703	.000
	Per Truck	-.095	.009	-.334	-10.897	.000
	V/C	4.026	.213	1.385	18.916	.000
	Per Ramp	-.022	.007	-.147	-2.910	.004
	Driver Comp	.005	.001	.124	3.270	.001

a. Dependent Variable: Total Weighted Benefit
b. Linear Regression through the Origin
Model adjusted R^2= 0.749

The validation effort for the VSLRM model produced a standard error of 3.21. Therefore, the model was able to accurately predict the total benefits of VSLRM control system from an out-of-sample dataset.

5.5 Advanced Model for Decisions and Benefits

The advanced model employed in this analysis was a spinoff of the work by Cirillo et al. (2013). The DCM applied in this study consisted of an ordered probit discrete model for the control choice and a linear regression model to predict the total weighted benefit from a given control strategy. Ordered probit was selected for the discrete model as the choice parameter reflects the level of traffic control intervention for a given scenario. The primary advantage of using a discrete continuous model is that both discrete and continuous models are estimated simultaneously. In the model estimation process, the errors between the two models undergo a correlation analysis. If the

correlation of the error terms, ρ, is found to be statistically significant, this parameter may enter one of the models. Obviously, the error must be estimated in one model, then the result can be used to estimate the error correlation parameter in the second model. In this particular application, the error terms from the benefits model were utilized as inputs for the decision model.

Before discussion of the results of the advanced model, a background on the formulation of the employed discrete-continuous model is needed, as such a model may be foreign to traffic operation professionals. First, we define a surrogate variable (Z) to reflect the "Decision" variable. Z is computed as:

$$Z = X_C^T \beta_C + \varepsilon_C \tag{5.13}$$

Where: X_C^T = a transposed vector of the control decisions

β_C = a vector of model coefficients

ε_C = error of the choice model

This variable was then discretized as:

$$if\ Z \leq \alpha_0\ \ then\ Choice = No\ Control \tag{5.14}$$

$$if\ \alpha_0 < Z \leq \alpha_1\ \ then\ Choice = VSL \tag{5.15}$$

$$if\ \alpha_1 < Z \leq \alpha_2\ \ then\ Choice = VSLRM \tag{5.16}$$

$$if\ Z > \alpha_2\ \ then\ Choice = Over\ Congested \tag{5.17}$$

By default, the model sets α_0 to zero. Thus only, α_1 and α_2 were estimated. From these relationships, we assume that the error term follows the standard normal distribution, ε ~ N(0,1).

Z follows a normal distribution, $Z \sim N(X^T\beta, 1)$. To predict the change in the total benefit, linear regression was applied as:

$$Y = X_{TB}^T \beta_{TB} + \varepsilon_{TB} \tag{5.18}$$

Where: $Y \sim N(X^T\beta, \sigma^2)$

X_{TB}^T= a transposed vector of the total benefits

β_{TB} = a vector of model coefficients

ε_{TB} = error of the total benefit model

With both components of the DC model described, the joint model was developed by assuming that the error terms in both components follow a multivariate normal distribution with correlation ρ. Thus, the likelihood of a given observation is:

$$p(Choice, Y) = f(Y)p(Choice|Y) \tag{5.19}$$

Where:

$$f(Y) = \Phi(Y \,|\, X^T\beta, \sigma^2) \tag{5.20}$$

Given Y, the conditional probability for the error term of the ordered probit model is:

$$\varepsilon_{TB} \,|\, Y \sim N\left(\frac{\rho}{\sigma_{TB}}\varepsilon_{TB}, (1-\rho^2)\right) \tag{5.21}$$

Where: $\rho =$ correlation of error terms

Thus, conditional probability of Z given Y is:

$$p(Z|Y) = p(\gamma_i < N\left(X_C^T\beta_C + \frac{\rho}{\sigma_{TB}}\varepsilon_{TB}, (1-\rho^2)\right) < \gamma_{i+1}) \tag{5.22}$$

Where:

$$\gamma_i = \sum_{j=0}^{i} \alpha_j \tag{5.23}$$

Having sufficiently described the formulation of the discrete-continuous model, the discussion turns to the model formulation and results. Note that the inputs into the discrete-continuous model were identical to those in the base decision and benefits model. The resulting model estimated, including a regression constant for the ordered probit model (op const), and cut-points for discretizing the surrogate choice variable (α_1 and α_2) are provided in Table 5-9.

Table 5-9: Discrete-Continuous Model Results

Model	**name**	**beta_hat**	**SD**	**t**	**p**
Ordered Probit	Op const	-13.475	0.789	-17.075	0.000
	Dist up	-0.167	0.064	-2.632	0.009
	Per Truck	-0.042	0.007	-5.957	0.000
	V/C 100	0.162	0.009	18.971	0.000
	Per ramp	0.026	0.006	4.040	0.000
	Driver Comp	0.00	0.001	-0.379	0.704
	α_1	1.530	0.069	22.277	0.000
	α_2	1.921	0.099	19.494	0.000
Linear Regression	Dist_up	-0.711	0.094	-7.560	0.000
	Per_Truck	-0.072	0.011	-6.572	0.000
	V/C 100	0.047	0.003	17.510	0
	Per ramp	-0.064	0.009	-6.836	0.000
	Driver Comp	0.015	0.002	8.195	0.000
	sigma2	2.876	0.127	22.619	0.000
	rho	0.235	0.040	5.167	0.033
	maxLL :	-3885.68			

First, the model estimates for α_1 and α_2 were found to be significant. Thus, there was sufficient justification for creating the four “Decision” levels. Next, rho was found to be positive and statistically significant at the 95 percent confidence level. This finding suggests that the error term

in the continuous model for total benefits is positively correlated with the error term in decision model. The model estimates of the coefficients for the independent variables discrete-continuous model are similar to those produced in the base model in terms of significant parameters and their signs. However, there is one critical difference in that driver compliance became statistically insignificant in the ordered probit model. Though unexpected, this observation may be explained by the inclusion of the rho parameter. The variance explained by rho may explain a significant portion of the variance that was explained by the driver compliance parameter.

To test the accuracy of the model against the "ground truth" observations, the validation dataset was applied. As expected, the continuous model produced similar results as the independent models for total benefits resulting from VSL and VSLRM control. Here, the standard error was found to be 2.56, comparable with that of the base models. The summary of the ordered probit model validation is presented in Table 5-10. Here, the overall prediction accuracy was 79.6 percent, a 6.8 percent improvement over the multinomial logit model. Considering the performance within each "Decision," the ordered probit model showed with-group prediction accuracies of 72.7 percent, 85.9 percent, 76.2 percent, and 81.8 percent for "No Control," VSL, VSLRM, and "Over-Congested" choices, respectively. These results suggest that the advanced model outperforms the independent models.

Table 5-10: DCM Validation Results: Decision Given Total Benefit

			Predicted Group				**Total**
			No Control	VSL	VSLRM	Over-Congested	
Decision	No Control	Count	24	6	3	0	33
		% of Total	**11.65%**	2.91%	1.46%	0.00%	16.02%
	VSL	Count	3	67	8	0	78
		% of Total	1.46%	**32.52%**	3.88%	0.00%	37.86%
	VSLRM	Count	4	7	64	9	84
		% of Total	1.94%	3.40%	**31.07%**	4.37%	40.78%
	Over-Congested	Count	0	0	2	9	11
		% of Total	0.00%	0.00%	0.97%	**4.37%**	5.34%
Total		Count	31.00	80.00	77.00	18.00	206
		% of Total	15.05%	38.83%	37.38%	8.74%	100.00%

5.6 Conclusions of Decision and Benefits Model Findings

This chapter has presented the development, results, and analysis of several statistical models considered for use in the Decision and Benefits Modules of the decision/deployment support tool. Table 5-11 summarizes the performance of each model relative to the "ground truth" simulation results. The Decision Modules were analyzed via overall modeling accuracy while the continuous models for benefit estimation were evaluated with the R-squared value.

Table 5-11: Summary of Decision and Benefits Models

Model Type	Model Name	Accuracy	R^2	SE
Base Decision	Decision Tree	64.40%	-	
	MLR	72.80%	-	
Base Benefit	VSL Regression	-	0.799	2.18
	VSLRM Regression	-	0.812	3.21
Advanced Decision/Benefit	DCM	79.60%	0.823	2.56

For the Decision Module, two base models were developed, a decision tree and a MLR model. Upon evaluating the accuracy of each model with the validation dataset, the decision tree was found to accurately model 64.6 percent of the control decisions, while the MLR model had an accuracy of 72.8 percent. However, the advanced DCM model outperformed both base models by producing an accuracy of 79.6 percent.

Next, the benefits module considered two OLS linear regression models, one for VSL benefits and the other for VSLRM benefits. The standard error value for the VSL and VSLRM models were 2.18 and 3.21, respectively. Similar to the decision model results, the continuous portion of the advanced DCM surpassed the base models by generating a standard error of 2.56.

Though the base models produced acceptable results, these independent models could not consider complex interrelation between the decision and benefits module. As shown in the

comparison of the base and advanced models, this consideration allowed for better fitting decision and benefits models. In conclusion, the advanced DCM model outperformed the base models. This observation may be explained by the capability of the DCM to incorporate the correlated errors between the decision and benefits models.

Chapter 6: Deployment Guidelines Module

6.1 Overview of Deployment Guidelines Module

This chapter develops procedures to locate the control components based on the results of the simulated scenarios, consisting of four key components:

Component-A: Control Segment Boundary

Component-B: Number of VSL Signs Required

Component-C: Number of Ramp Meter Required (if any)

Component-D: Number of Detectors Required for System Control

Component-E: Placement of VSL Signs, Ramp Meters, and Detectors

The purpose of each of these components within the deployment guidance module is to define the control boundary and then to identify the number and locations of the VSL signs, ramp meters, and detectors required for congestion mitigation at the target site. The following sections of this chapter discuss the details of each of the components in this process.

6.2 Component-A: Control Segment Boundary

The first component of the deployment guidelines module determines the control segment boundary. Recall, the goal of VSL control is to harmonize speeds *approaching* the queue; thus, the VSL control boundary must extend upstream of the maximum queue length to allow for safe and comfortable transition to the congested conditions. To define the control boundary, the following steps must be completed:

Step 1: Estimate the maximum queue under the suggested control strategy.

Step 2: Identify the control sub-segment associated with the maximum queue.

Step 3: Set the control boundary to the location of the upstream boundary of the control sub-segment associated with the maximum queue.

Step 1 of Component-A requires the assessment of the expected maximum queue length. Here, OLS linear regression models were developed using the results of the simulated experiments to estimate the maximum queue length under VSL and VSLRM control, using the queue estimation method of Ramezani et al. (2011). For each model, the maximum queue length was estimated using the five independent variables of the distance to the upstream on-ramp (Dist Up), truck percentage (Per Truck), V/C ratio, percent of the V/C ratio originating from the bottleneck on-ramp (Per ramp), and driver compliance (Driver Comp) to VSL control.

Table 6-1 presents the results of the regression analysis for the maximum queue under VSL control. The model estimation resulted in an R-squared value of 0.804. Here, all variables were statistically significant at the 95 percent confidence interval except for the percentage of trucks. This observation may be explained by the contribution of truck percentage to the bottleneck V/C ratio. Using capacity analysis, the V/C ratio in the experiment design phase was derived by converting truck percentages to passenger car equivalents. In doing so, the impact of trucks on queuing was inherently considered in the statistically significant variable of V/C ratio. In analyzing the significant variables, the distance to the upstream on-ramp coefficient was found to be negative. This result agrees with traffic flow logic in that decreased interchange density results in less severe congestion. Second, the V/C ratio coefficient was positive. As expected, this finding suggests that increased V/C ratios result in longer queues. Next, the ramp percentage coefficient was discovered to be negative. This observation may be explained by considering the origin of the volumes entering the bottleneck. Here, increased ramp volumes shift a portion of the mainline queues to

the associated on-ramp. Finally, the driver compliance coefficient was discovered to be positive as increased driver compliance will mitigate the congested conditions by controlling mainline inflow.

Table 6-1: Continuous Model for VSL Maximum Queue Length

Coefficients[a]

Model		Unstandardized Coefficients		Standardized Coefficients	t	Sig.
		B	Std. Error	Beta		
1	Dist up	-975.286	268.284	-.222	-3.635	.000
	Per Truck	-50.011	39.769	-.061	-1.258	.210
	V/C	9728.779	708.079	1.684	13.740	.000
	Per ramp	-105.385	27.223	-.363	-3.871	.000
	Driver Comp	-19.697	5.711	-.234	-3.449	.001

a. Dependent Variable: VSL Total Maximum Queue

Adjusted $R^2 = 0.804$

The regression model for the maximum queue length under VSLRM control is shown in Table 6-2. The model produced an R-squared value of 0.786 and, similar to the VSL model, found that all but the truck percentage variable was statistically significant. In addition, the signs of the significant variable coefficients matched those of the VSL model. This result not only agrees with traffic flow logic, but can also be explained by the inherent similarities between the VSL and VSLRM control systems.

Table 6-2: Continuous Model for VSLRM Maximum Queue Length

Coefficients[a,b]

Model		Unstandardized Coefficients		Standardized Coefficients	t	Sig.
		B	Std. Error	Beta		
1	Dist up	-638.788	242.850	-.168	-2.630	.009
	Per Truck	-48.329	35.999	-.068	-1.343	.181
	V/C	7824.393	640.951	1.564	12.207	.000
	Per ramp	-72.456	24.642	-.288	-2.940	.004
	Driver Comp	-16.868	5.170	-.232	-3.263	.001

a. Dependent Variable: VSLRM Total Maximum Queue
Adjusted $R^2 = 0.786$

Next, Step 2 of Component-A requires determination of the control sub-segment that is associated with the estimated maximum queue from Step 1. As the congested conditions evolve and queue lengths grow, the VSL control system shifts to control traffic inflow upstream of the queue. Here, the length of the maximum queue is compared to location of each sub-segment boundary, relative to the bottleneck location. Note that the control logic shifts to the upstream control sub-segment if control segment becomes 85 percent queued. Thus, the control sub-segment associated with the maximum queue is computed as:

$$S_{max} = \begin{cases} i, if\ Q_{max} \leq 0.85L_i \\ i+1, if\ Q_{max} \geq 0.85L_i\ and\ Q_{max} \leq 0.85L_{i+1} \\ \vdots \\ I, if\ Q_{max} \geq 0.85L_{I-1} and\ Q_{max} \leq\ L_I \end{cases} \quad (6.1)$$

Where:

S_{max} = sub-segment associated with maximum queue

Q_{max} = estimated maximum queue length (ft)

L_i = length of sub-segment i (ft)

Finally, Step 3 of Component-A uses the result of Step 2 to establish the overall control boundary for the control system. Here, the upstream boundary of the control segment associated with the maximum queue is adopted as the overall control segment boundary.

6.3 Component-B: Number of VSL Signs

Once the control boundary is defined, the number of required VSL signs can be determined based on the following steps:

Step 1: Within the control boundary, determine the control sub-segment at each interval.

Step 2: Within each control sub-segment, determine the maximum speed drop.

Step 3: Use the maximum speed drop to determine the number of VSL signs needed at each control sub-segment.

Step 1 of Component-B analyzes the utilization of specific control sub-segments using the simulation results. Recall that this calculation was based on a modified version of the queue length estimation derived by Ramezani et al. (2011). Again, the VSL control algorithm shifted the control sub-segment once the queue length reached 85 percent of the sub-segment length. Therefore, the control sub-segment at each time interval is defined as:

$$S_{control}(t) =$$

$$\begin{cases} i, if\ \frac{\sum_{t-1}^{t}[q_{in}^{i}(t)-q_{out}^{i}(t)]}{l_i} * \frac{\bar{v}_i}{C_i} \leq 0.85L_i \\ i+1, if\ \frac{\sum_{t-1}^{t}[q_{in}^{i}(t)-q_{out}^{i}(t)]}{l_i} * \frac{\bar{v}_i}{C_i} \geq 0.85L_i\ and\ \frac{\sum_{t-1}^{t}[q_{in}^{i+1}(t)-q_{out}^{i+1}(t)]}{l_{i+1}} * \frac{\bar{v}_{i+1}}{C_{i+1}} \leq 0.85L_{i+1} \\ \vdots \\ I, if\ \frac{\sum_{t-1}^{t}[q_{in}^{I-1}(t)-q_{out}^{I-1}(t)]}{l_{I-1}} * \frac{\bar{v}_{I-1}}{C_{I-1}} \geq 0.85L_{I-1} and\ \frac{\sum_{t-1}^{t}[q_{in}^{I}(t)-q_{out}^{I}(t)]}{l_I} * \frac{\bar{v}_I}{C_I} \leq\ L_I \end{cases}$$

(6.2)

Where:

$S_{control}(t) =$ control sub-segment at time interval t

q_i^{in} (t) = total inflow into sub-segment i during time interval t (veh)

q_i^{out} (t) = total inflow out of sub-segment i during time interval t (veh)

$l_i =$ number of lanes in sub-segment i

$\bar{v}_i =$ average speed (mph)

$C_i =$ capacity of sub-segment i (veh/hr/lane)

$L_i =$ length of sub-segment i (miles)

Using the control sub-segment matrix generated by equation 6.2, the control sub-segment can be determined. This analysis provides insight on the expected evolution of congestion at the target site by assessing the control sub-segment for each system update interval.

Next, using the results from Step 1, Step 2 of Component-B analyzes the maximum speed drop within each control sub-segment. Here, the magnitude of the speed drop between the speed of the upstream and downstream boundaries of the control sub-segment was required to estimate the

number of VSL signs needed at each sub-segment boundary. To do this, the maximum speed drop within each control sub-segment must be determined.

$$\forall\, t \ni\ S_{control}(t) = i, \qquad \Delta v_{max}^{i} = \max\left[\ \bar{v}_{upstream}^{i}(t) - \bar{v}_{downstream}^{i}(t)\right],$$

$$\forall\, t \ni\ S_{control}(t) = i+1, \qquad \Delta v_{max}^{i+1} = \max\left[\ \bar{v}_{upstream}^{i+1}(t) - \bar{v}_{downstream}^{i+1}(t)\right],$$

$$\vdots$$

$$\forall\, t \ni\ S_{control}(t) = I, \qquad \Delta v_{max}^{I} = \max\left[\ \bar{v}_{upstream}^{I}(t) - \bar{v}_{downstream}^{I}(t)\right] \tag{6.3}$$

Where:

Δv_{max}^{i}= maximum speed drop for sub-segment i

$\bar{v}_{upstream}^{i}(t)$= 5 minute average speed for the upstream boundary of sub-segment i

$\bar{v}_{downstream}^{i}(t)$= 5 minute average speed for the upstream boundary of sub-segment i

Lastly, Step 3 of Component-B translates the maximum speed drop to the required number of VSL signs needed for safe transition from free-flow to the congested conditions. Note that if more than one on-ramp is contained within a control sub-segment, one additional VSL must be placed to inform merging motorists of the dynamic control speed. Thus, applying a 10 mph speed step-down strategy, the number of signs needed for each control sub-segment is:

$$\theta_i = \frac{\Delta v_{max}^{i}}{10} + \mu_i - 1 \tag{6.4}$$

Where:

θ_i= number of VSL signs required for sub-segment i

μ_i = number of on-ramps within sub-segment i

6.4 Component-C: Number of Ramp Meters

Similar to the VSL sign procedure, the number of required ramp meters was determined by analyzing each ramp meter during the congested period. Here, three distinct steps are defined:

Step 1: Evaluate the mode of operation for each ramp meter at each system update interval.

Step 2: For each ramp meter, analyze the time spent in each mode of operation.

Step 3: Determine the number of required ramp meters by assessing the utilization and operational efficiency of each ramp meter.

Step 1 of Component-C requires the analysis of the mode of operation for each ramp meter at each system update interval. Recall that the ramp metering control algorithm allows for three modes of operation. First was the regular mode (Reg), where the ramp meter operates to control ramp flows into the control sub-segment. Second was the upstream supplementation mode (Supp), where an upstream ramp meter was activated to assist inflow control. The third ramp meter operation mode was maximum queue-override (MQO). Here, the ramp meter operates at a maximum metering rate to allow for ramp queues to dissipate, thus mitigating the potential for ramp queue spillover. Using the outputs of the simulated experiments, the time-dependent mode of operation can be calculated as:

$$M_j(\mathrm{t}) = \begin{cases} 1, if\ Off \\ 2, if\ On - Reg \\ 3, if\ On - Supp \\ 4, if\ On - MQO \end{cases} \quad (6.5)$$

Where:

$M_j(t)$ = mode of operation for ramp j at time interval t

Next, Step 2 of Component-C uses the matrix derived in equation 6.5 to analyze the relative time spent in each mode of operation, for each ramp meter. Specifically:

$$\forall\ t \ni\ M_j(t) = m,\ \tau_{jm} = \frac{\left(\sum_{t=0}^{T} M_j(t) \Big/ m\right)}{T} \quad (6.6)$$

Where:

τ_{jm} = percent of time that ramp meter j operates in mode m

T = total number of time intervals in analysis period

Applying equation 6.6 allows for the analysis of ramp meter utilization and operational efficiency, Step 3 of Component-C. While the analysis for justifying the use of specific control devices was beyond the scope of this research, these results can be used to support device deployment decisions.

6.5 Component-D: Number of Detectors

Upon assessing the location of the VSL signs and ramp meters at a given deployment site, Component-D identifies the number of detectors required to feed the control system with real-time data. The procedure for identifying the locations of the detectors was derived from the employed system activation and updates methodology, and can be summarized as:

Step 1: Determine the number of ingress and egress points for each control sub-segment.

Step 2: For VSLRM control, add one additional detector to each metered ramp within each control sub-segment and two detectors for each supplemental ramp meter beyond the control boundary.

The determination of ingress and egress points in Step 1 of Component-D is based on the data needs for the employed control strategy. For each control sub-segment within the control area, detectors are required at each point of ingress and egress. Therefore, the number of required detectors for a given control segment is a function of the number of on- and off-ramps within the sub-segment boundary. Assuming one detector is needed for each lane, the total number of required detectors for VSL control is computed as:

$$D_{Total}^{VSL} \sum_{i}^{I}\left[\left(\sum_{\forall j \in J(i)} \sigma_j\right) + \left(\sum_{\forall k \in K(i)} \tau_j\right) + \varphi_i + \omega_i\right] \quad (6.7)$$

Where:

D_{Total}^{VSL} = total number of detectors required for VSL control

σ_j = number of lanes for on-ramp j, within sub-segment i

τ_j = number of lanes for off-ramp k, within sub-segment i

φ_i = number of lanes for the mainline downstream sub-segment boundary

ω_i = number of lanes for the mainline upstream sub-segment boundary

However, modern roadside detector technologies allow a single detector to cover multiple lanes. In such cases, equation 6.7 becomes:

$$D_{Total}^{VSL} = 1 + \sum_{i}^{I}[\mu_i + \pi_i + 1] \quad (6.8)$$

Where:

μ_i = number of on-ramps within sub-segment i

π_i = number of off-ramps within sub-segment i

As presented in equation 6.8, when using modern roadside detectors, the number of detectors needed is a function of the number of ingress and egress points plus two additional detectors to cover the upstream and downstream boundaries of the mainline control sub-segment. As the control sub-segment shifts under growing congestion, the former upstream boundary of the previous control sub-segment becomes the downstream boundary of the new control sub-segment.

Step 2 of Component-D considers the use of supplemental ramp metering control. Recognizing that the VSLRM control strategy was designed to utilize the detector infrastructure for the independent VSL control, the calculation for the number of detectors required for VSLRM control must consider the need for maximum queue detection at each metered ramp. Assuming use of modern roadside detectors, the number of detectors required for VSLRM control is defined as:

$$D_{Total}^{VSLRM} = 1 + \sum_i^I [\mu_i + \pi_i + \eta_i + 1] + 2\gamma \quad (6.9)$$

Where:

D_{Total}^{VSLRM} = total number of detectors required for VSLRM control

η_i = number of metered ramps within sub-segment

γ = number of on-ramps upstream of control boundary used for supplemental ramp metering control

6.6 Component-E: Location of VSL Signs, Ramp Meters, and Detectors

Having described the procedure for determining the number of required VSL signs, ramp meters, and detectors, the final step is to provide guidance on the specific locations for each of the control components. This procedure can be summarized in three steps:

Step 1: Place the VSL signs at each utilized control sub-segment, using spacing adopted from FHWA standards.

Step 2: Place the ramp meters on their respective on-ramps at a location that allows for safe acceleration-to-merge conditions.

Step 3: Place the detectors to allow for efficient system control.

For Step 1 of Component-E, the recommended spacing of the VSL signs and precise locations of the ramp meters on the on-ramps were based on FHWA standards. To ensure safe and comfortable speed transitions, the guidelines for advanced placement of warning signs (Table 2C-4 of the 2009 MUTCD) were adopted for the spacing of VSL signs. For Step 2 of Component-E, the location of a given ramp meter must allow enough distance for acceleration to safe merging speeds. Here, guidelines from the FHWA Ramp Management and Control Handbook (Jacobson et al., 2010) are suggested (Table 6-3).

Table 6-3: Ramp Acceleration Lengths (Jacobson et al., 2010)

Design Speed (mph)	Speed Reached (mph)	Accel length (ft) From stop condition
30	23	180
35	27	280
40	31	360
45	35	560
50	39	720
55	43	960
60	47	1200
65	50	1410
70	53	1620
75	55	1790

As described in the previous section, the detector deployment strategy, Step 3 of Component-E, was based on the control logic employed in this study. Thus, each point of ingress and egress within the utilized control sub-segments requires a detector to monitor the real-time traffic conditions for VSL or VSLRM control.

6.7 Deployment Guidelines Sample Application

To illustrate the application of the deployment guidelines module, the simulated experiment with a 1.0-mile distance to the upstream on-ramp, 2.5 percent trucks, V/C ratio of 0.95, a ramp percentage of 10 percent, driver compliance of 25 percent, and original posted speed limit of 55 mph was selected for demonstration. Here, VSLRM control will be deployed.

First, the process described for Component-A was applied. Upon applying the VSLRM maximum queue regression equation, the expected maximum queue was found to be 5,527 feet.

Next, equation 6.1 was applied to determine that sub-segment 2 was the sub-segment associated with the maximum queue. Thus, the control boundary was set to be equal to the upstream boundary of sub-segment 2, a distance of 7,240 feet from the bottleneck location.

Moving to Component-B, equation 6.2 was applied to determine the control segment at each update interval. This analysis showed that the VSL system was activated for 83.3 percent of the analysis period. Sub-segment 1 (VSL1) was the control sub-segment for 32.2 percent of the analysis period, while sub-segment 2 (VSL2) was the control sub-segment for 51.1 percent of the analysis period. This step can be visualized in Figure 6-1.

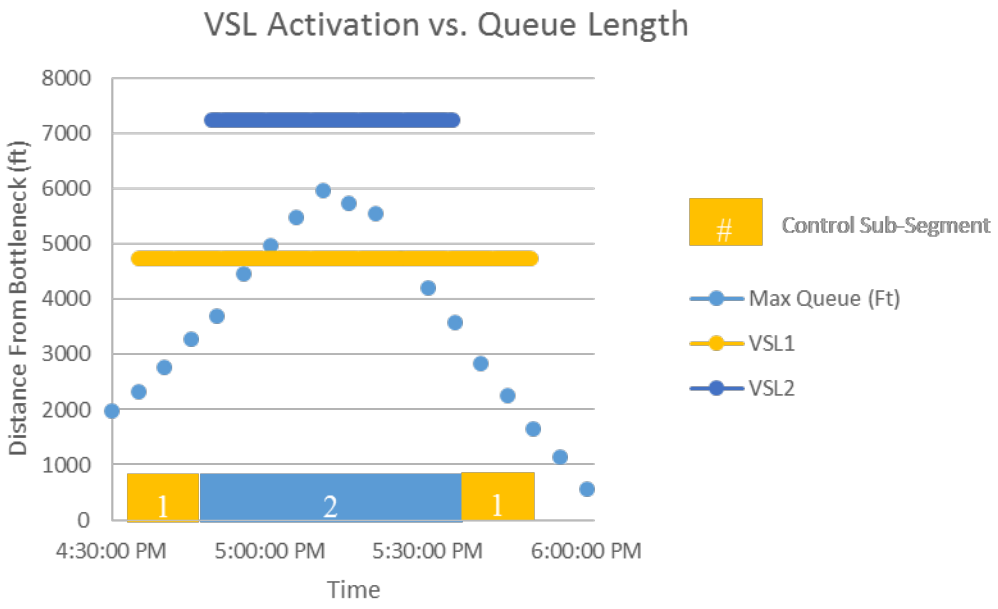

Figure 6-1: Visualization of VSL System Utilization

For Step 2 of Component-B, equation 6.3 was utilized to find that the maximum speed drop within each of the control-segments was 20 mph. Finally, equation 6.4 converted the speed drop and number of on-ramps within each control sub-segment to the number of required signs. Note

that sub-segment 1 had one on-ramp, while sub-segment 2 had two on-ramps. Thus, sub-segment 1 required two VSL signs, while sub-segment 2 required three VSL signs.

Next, Component-C commenced by analyzing the time dependent mode operation of each ramp meter, using equation 6.5. The resulting matrix was then used to determine the relative time spent in each mode of operation as described in equation 6.6. The result of this effort is summarized in Table 6-6.

Table 6-4: Summary of Ramp Meter Operation Modes

Control Device	TOTAL %TIME ON	%Regular	%Upstream Supplementation	%Ramp Queue Override
RM1	72.2%	49.4%	-	22.8%
RM2	36.7%	20.0%	16.7%	0.0%
RM3	12.2%	12.2%	0.0%	0.0%
RM System	72.2%	-	-	-

As presented in Table 6-4, this particular environment utilized the VSL control component for 83.3 percent of the analysis period, of which the second sub-segment was control sub-segment for a majority (62.0 percent) of the VSL control period. Meanwhile, the RM control component was on for 72.2 percent of the analysis period. Here, RM1 operated in regular mode for 49.4 percent of the analysis period and was in ramp queue override mode for 22.8 percent of the time. Next, RM2 was activated for 36.7 percent of the analysis period, of which 54.5 percent was in the regular mode with the remainder in the upstream supplementation mode. Finally, RM3 was activated for just 12.3 percent of the analysis period, all of which was regular mode. This step can also be visualized in Figure 6-2.

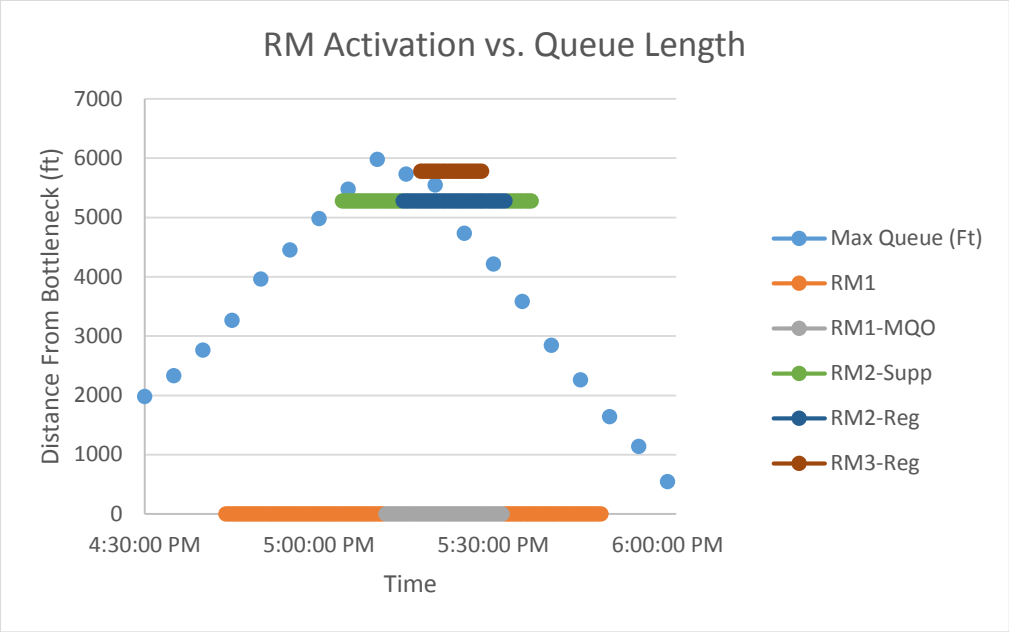

Figure 6-2: Visualization of RM System Utilization

The final step in Component-C requires the determination of ramp meters to deploy based on the results of step 2. Here, the time spent in each mode of operation can be analyzed to assess the justification and operational efficiency of each ramp meter. While a rigorous analysis of the threshold values for control device utilization rates that warrant device implementation was beyond the scope of this study, a decision maker may use the utilization rates for general deployment guidance. In addition, the decision-maker should also be aware of the limitations and potential pitfalls of applying these control strategies. For instance, the length of each on-ramp and associated demand should be considered. Obviously, increased demands and shorter on ramps will tend to have higher potential operating in the ramp queue override mode. Such a finding will be reflecting in the analysis of the operational mode, but suggests that the use upstream ramp meters will likely be needed for efficient congestion mitigation. In addition, if a given on ramp within the congested region has low demand, ramp metering will provide few benefits as the inflow is naturally low. In any case, assume that all of three ramp meters will be deployed at this site.

Having determined the number of required VSL signs and ramp meters, the number of required detectors can be analyzed using Component-D. The first step of this analysis is to determine the number of ingress and egress points within each control sub-segment. Assuming the use of modern roadside detectors, equation 6.9 is applied as this site will deploy VSLRM control. Here, segment 1 contains one on-ramp and one off-ramp, while segment 2 contains two on-ramps and two off-ramps. Thus, 12 detectors are needed to implement VSLRM control at this site.

The final consideration in the deployment guidelines model is the precise location of each control component, covered by Component-E. The first step is to locate each of the VSL signs. Based on the results of Component-B, each control sub-segment will require at least one VSL sign to create a smooth transition from free-flow to the congested conditions. If more than one VSL sign is required to safely control approach speeds into a given sub-segment, then advanced warning sign spacing from the MUTCD should be applied. Using the suggested sign spacing for the original posted speed limit of 55 mph, the distance between VSL signs at each sub-segment control boundary was 990 feet. In addition, for this particular site, one additional VSL sign is required to inform merging motorists at the upstream on-ramp within sub-segment 2. In a similar fashion, the precise location of each ramp meter must allow for safe acceleration to the merging conditions. Here the conservative acceleration length of 960 feet (for design speeds of 55 mph) is selected. Note that this acceleration distance includes the length of the associated ramp acceleration lane. Finally, the location-required detectors are based on data inputs utilized by the control system. As described in above and in detail in Chapter 4, the control system detects congestion by monitoring each point of ingress and egress for each control sub-segment. As congestion grows and then dissipates, the system dynamically shifts the control boundaries to throttle inflow into the congested segment. The visualization of the VSL sign and ramp meter locations is shown in Figure

6-3, while the approximate location of each required detector is presented in Figure 6-4. Figures 6-3 and 6-4 are supplemented by Table 6-5, which describes the function of each of the deployed control components.

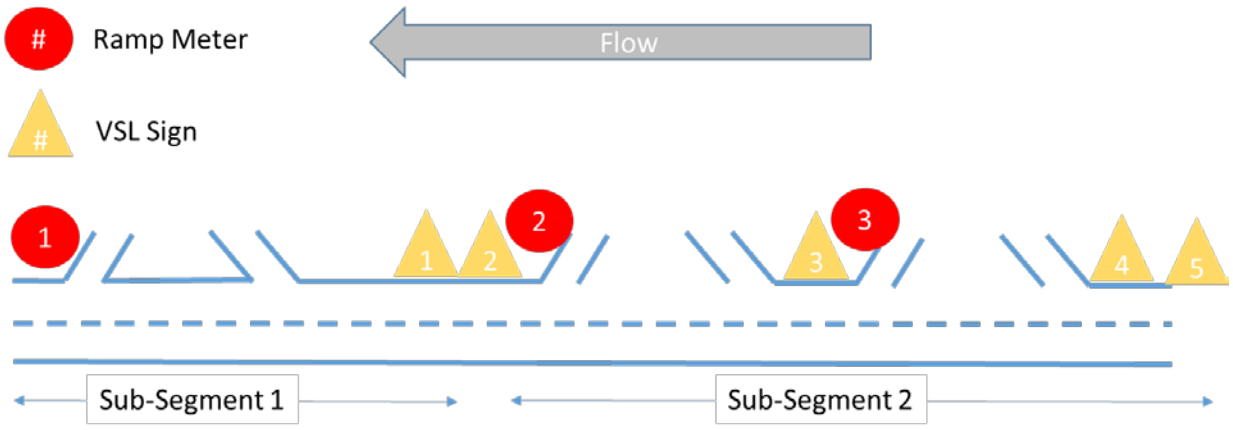

Figure 6-3: Control Device Locations for Example Scenario

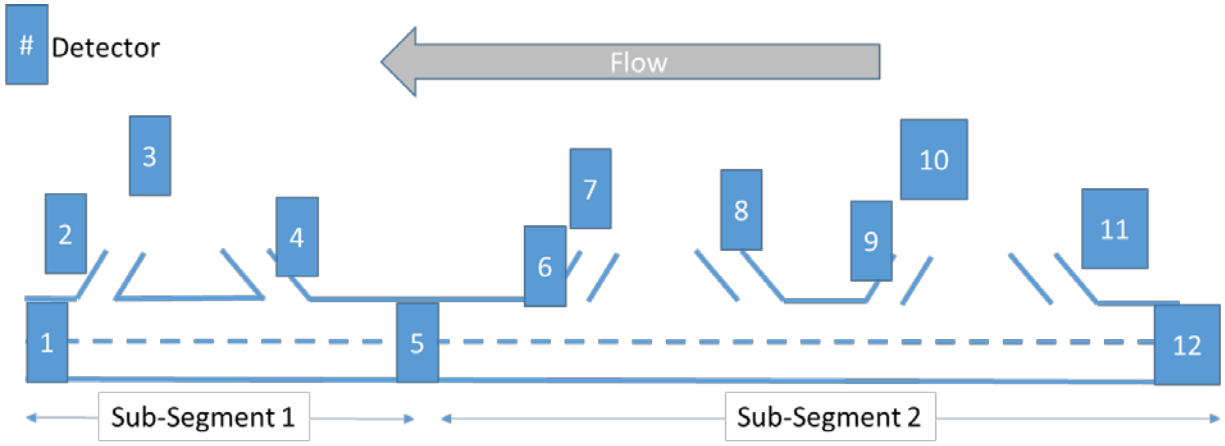

Figure 6-4: Detector Locations for Example Scenario

Table 6-5: Description of Deployed Control System Devices

Device Type	Device ID	Description
Detector	1	Mainline-Downstream Detector for Sub-segment 1
	2	On-Ramp 1 Inflow Detector for Sub-segment 1
	3	On-Ramp 1 Max Queue Detector for Sub-segment 1
	4	Off-Ramp 1 Outflow Detector for Sub-segment 1
	5	Mainline-Upstream Detector for Sub-segment1/ Mainline-Downstream Detector for Sub-segment 2
	6	On-Ramp 1 Inflow Detector for Sub-segment 2
	7	On-Ramp 1 Max Queue Detector for Sub-segment 2
	8	Off-Ramp 1 Outflow Detector for Sub-segment 2
	9	On-Ramp 2 Inflow Detector for Sub-segment 2
	10	On-Ramp 2 Max Queue Detector for Sub-segment 2
	11	Off-Ramp 2 Outflow Detector for Sub-segment 2
	12	Mainline-Upstream Detector for Sub-segment 2
VSL Sign	1	Sub-Segment 1 VSL Sign 1
	2	Sub-Segment 1 VSL Sign 2
	3	Sub-Segment 2 VSL Sign 1
	4	Sub-Segment 2 VSL Sign 2
	5	Sub-Segment 2 VSL Sign 3
Ramp Meter	1	Sub-Segment 1 Ramp Meter 1
	2	Sub-Segment 2 Ramp Meter 1
	3	Sub-Segment 2 Ramp Meter 2

6.8 Summary of Deployment Guidelines

This chapter has presented a procedure for planning the deployment of a VSL or VSLRM control system at a target site, including the number and location of critical control system components. The process began with determining the mainline control boundary. The boundary was determined by estimating the maximum mainline queue length under the suggested control strategy. To do this, regression models were developed using the simulated experiments. Recognizing that VSL control seeks to harmonize speed approaching the queue, the control boundary was determined to be the upstream boundary of the control-sub-segment containing the maximum queue. Next, a procedure for determining the number of required VSL signs within the

control segment was developed. This procedure was based on the dynamic evolution of the congestion pattern and the maximum speed drop within each control sub-segment. A similar procedure was generated for determining the number of required ramp meters. Here, the mode of operation for each ramp meter was evaluated to determine the device utilization and operational efficiency. The next step was to determine the number of detectors required for the control system. This process was based on the control algorithms applied in this study, which monitored each point of ingress and egress for each control sub-segment. The final step of the deployment planning procedure was to determine the location of each control component. The guidelines for the spacing of the VSL signs and exact location of the ramp meters were adopted from FHWA standards. The placement of the detectors was based on the required data inputs defined by the control system logic. In conclusion, the procedures discussed in this chapter can be used to assist the decision-maker in planning for VSL or VSLRM deployment at a specific site by providing guidance on the number and location of the critical control infrastructure components.

Chapter 7: Sample Application of Decision/Deployment Support Tool

7.1 Application Background

To illustrate the use of the developed decision/deployment support tool, this chapter presents a sample application using real-world sites in the state of Maryland. A list of candidate sites for congestion mitigation intervention was generated from the 2014 Maryland State Highway Administration (SHA) Mobility Report (SHA, 2015). Within this report, the top 30 bottleneck locations in the state of Maryland were determined. Upon assessing this list, seven sites were selected as candidate sites for application of VSL or VSLRM control for the purpose of illustrating the use of the developed tool. The selection of these sites was based on data availability, data quality, and the underlying cause of the recurrent congestion (e.g. sites with congestion caused by construction projects were excluded). Figure 7-1 presents the location of the sites used in this sample application and is supplemented by Table 7-1, which provides a description of those locations.

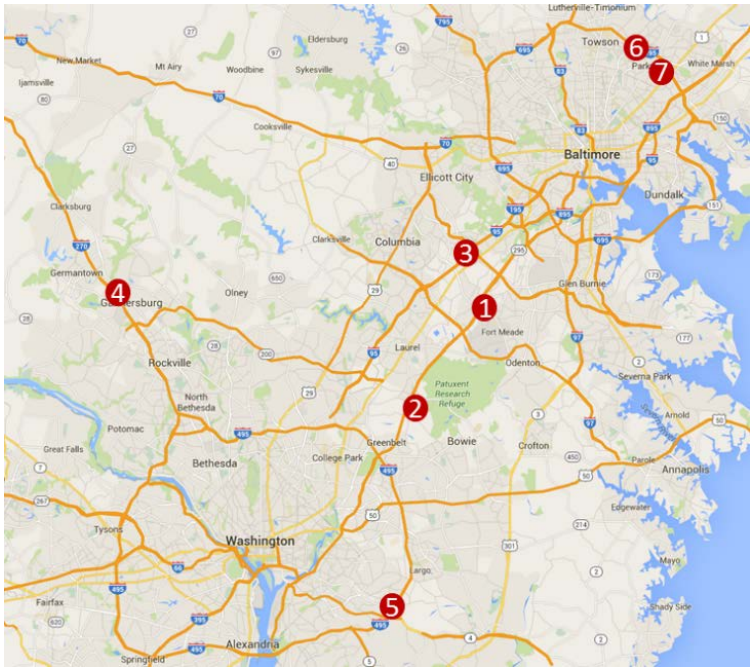

Figure 7-1: Map and Description of Candidate Sites

Table 7-1: Candidate Site Descriptions

Site #	Site Description	Distance to the upstream on-ramp (DistUp)	Percent Trucks (PerTruck)	V/C Ratio (V/C)	Ramp Percentage (PerRamp)	Driver Compliance (DC)
1	MD-295 N @ MD-175	2	2.6	1	24.8	25
2	MD-295 N @ MD-197/Exit 111	1.6	2.6	0.93	12.1	25
3	I-95 N @ MD-100/Exit 43	1.8	12.1	0.89	15.2	25
4	I-270 N Local@ MD 124	1.8	6.3	0.95	12.2	25
5	I-495 CW @ MD-4/Pennsylvania Ave/Exit 11	2	10.1	0.89	12.2	25
6	I-695 CW @ MD-41/Perring Pkwy/Exit 30	1.1	9.2	1	19.2	25
7	I-695 CW @ MD-147/Harford Rd/Exit 31	1.1	8.7	0.85	10.9	25

As presented in Table 7-1, the candidate sites are described by the direction of travel and the nearest interchange to the bottleneck location. For sites 5-7, the abbreviation CW is defined as the clockwise direction of travel for the Capital (I-495) and Baltimore (I-695) beltways. Table 7-1 also summarizes the critical independent variables used in each of the decision/deployment support tool modules. Field traffic data was obtained from the SHA Internet Traffic Monitoring System (I-TMS) (2015). In this application, the assumed driver compliance to VSL control was 25 percent for all sites. For this illustrative example, assume that the decision-maker will deploy the recommended control strategy at only the top-ranked site.

7.2 Results and Analysis of Sample Application

This section describes the step-by-step application of each of the three modules comprising the decision/deployment support tool developed in this study. Section 7.2.1 describes the procedure, results, and analysis of the Decision and Benefits Modules. This section is followed by a detailed discussion on the application of the deployment guidelines module.

7.2.1 Application of Decision and Benefits Module

As presented in Chapter 5, the advanced discrete-continuous model out-performed the base models in terms of model accuracy. Therefore, this sample application adopted the advanced discrete-continuous model for decision guidance and benefits estimation. The application of this model is a four-step process. Recall that the advanced discrete-continuous model applied in this study used the error of the continuous (benefits) component of the model as an input into the discrete (decision) component of the model.

Step 1: Base Decision Calculation- The independent variables for each site are input into the decision portion of the model. For a given candidate site j, the latent decision variable Z, can be computed from equation 5.31 as:

$$Z_j = -13.475 - 0.167 * DistUp_j - 0.042 * PerTruck_j + 0.162 * 100 * VC_j + 0.026 * PerRamp_j \quad (7.1)$$

Note that in this model the V/C ratio variable was multiplied by 100 for scaling purposes. The base decision was computed using the independent variables for each site, summarized in Table 7-1. However, the result *is not the final control decision* as the model must consider the correlation of the error term from the benefits model as calculated in step 2.

Step 2: Benefits Estimation- The independent variables for each site are input into the benefits portion of the model. For a given candidate site j, the expected benefit can be computed from equation 5.36 as:

$$Y_j = -0.711 * DistUp_j - 0.072 * PerTruck_j + 0.047 * 100 * VC_j - 0.064 * PerRamp_j + 0.015 * DC_j + \varepsilon_{TB} \quad (7.2)$$

Again, in this model the V/C ratio variable was multiplied by 100 for scaling purposes. Using the variable values for each candidate site presented in Table 7-1, the results for the expected benefits model (i.e. Benefits Module) are presented in Table 7-2:

Table 7-2: Result of Benefits Module

Site	Benefit
MD-295 N @ MD-175	2.1
MD-295 N @ MD-197/Exit 111	2.6
I-95 N @ MD-100/Exit 43	1.4
I-270 N Local @ MD 124	2.3
I-495 CW @ MD-4/Pennsylvania Ave/Exit 11	1.6
I-695 CW @ MD-41/Perring Pkwy/Exit 30	2.5
I-695 CW @ MD-147/Harford Rd/Exit 31	2.3

Step 3: Final Decision Calculation- Using the correlated error of the benefits estimation, the conditional probability of the latent choice variable Z can be determined from equation 5.40. The result of this application was the final control decision for each candidate site, summarized in Table 7-3.

Table 7-3: Results of Decision Module

Site	Choice
MD-295 N @ MD-175	Over-Congested
MD-295 N @ MD-197/Exit 111	VSLRM
I-95 N @ MD-100/Exit 43	VSL
I-270 N Local @ MD 124	VSLRM
I-495 CW @ MD-4/Pennsylvania Ave/Exit 11	VSL
I-695 CW @ MD-41/Perring Pkwy/Exit 30	Over-Congested
I-695 CW @ MD-147/Harford Rd/Exit 31	VSL

Note that two of the sites, MD-295 N at MD-175 and I-695 CW at MD-41/Perring Pkwy/Exit 30, were found to be over-congested and thus are removed from consideration. Of the remaining five candidate sites, VSL control was suggested for three and VSLRM was suggested for two.

Step 4: Site Ranking- Upon ranking the estimated benefits for each site, the MD-295 N at MD-197/Exit 111 was found to have the most potential benefits with an expected benefit-to-cost ratio of 2.6 after one year of operation. Thus, this site was selected as the deployment site and was passed on to the deployment guidelines module for further evaluation.

7.2.2 Application of Deployment Guidelines Module

The application of the deployment guidelines module uses site-specific inputs to estimate the control boundary, while the expected utilization of specific control devices relies on the outputs from a similar simulated environment under VSLRM control. Here, the most similar site to MD-295 N at MD-197/Exit 111 was the site with a distance to the upstream on-ramp of 1.5 miles, a truck percentage of 2.5, a V/C ratio of 0.95, and the percentage of the V/C ratio originating from the bottleneck on-ramp of 10 percent. The application of the deployment guidelines procedure is presented by explicitly explaining each step of the deployment components described in Chapter 6.

Component-A: Estimation of Control Segment Boundary

Step 1: Applying the inputs for MD-295 N at MD-197/Exit 111 to the VSLRM maximum queue regression equation for site j as:

$$VSLRM\ Max\ Queue_j = -639 * DistUp_j - 48 * PerTruck_j + 7824 * VC_j - 72 * PerRamp_j - 17 * DC_j \quad (7.3)$$

The result of this analysis produced an estimated maximum queue length of 4,892 feet.

Step 2: The next step was used to determine which control sub-segment was associated with the maximum queue using equation 6.1. Using the results of the similar simulated environment, this control sub-segment was determined to the sub-segment originating at the bottleneck location, sub-segment 1.

Step 3: The mainline control boundary was set to match the upstream boundary of sub-segment 1 at a distance of 1.7 miles (~9,000 feet) from the bottleneck location. The map of this site with the control boundary is shown in Figure 7-2.

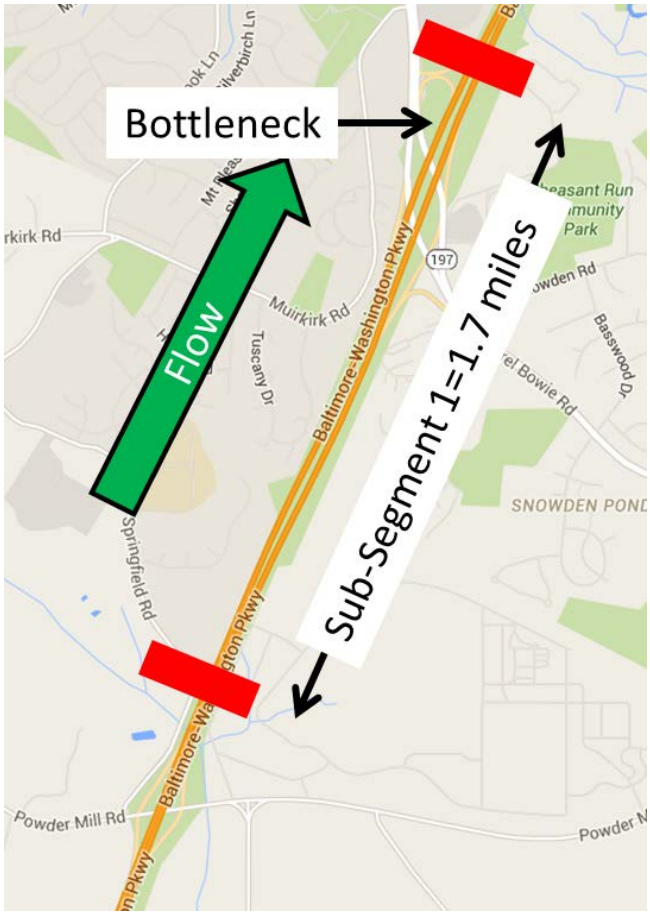

Figure 7-2: Deployment Site Map – MD-295 N at MD-197/Exit 111 (Google, 2015)

Component-B: Number of VSL Signs Required

Step 1: Using equation 6.2 with the outputs of the similar simulated experiment, only sub-segment 1was utilized as a control sub-segment and was activated for 87.2 percent of the analysis period.

Step 2: Applying equation 6.3, the maximum speed drop in sub-segment 1 was 30 mph.

Step 3: Applying equation 6.4 to this maximum speed drop with just one on-ramp ($\mu_i = 1$), **3 VSL signs are required**.

Component-C: Number of Ramp Meters

Step 1: Equation 6.5 was used to create the matrix of the time-dependent mode of operation for each ramp meter.

Step 2: Equation 6.6 was applied to the aforementioned matrix to calculate the percentage of time spent in each mode of operation for each ramp meter.

Step 3: The number of required ramp meters was determined by assessing the utilization and operational efficiency of each ramp meter. Here, **two ramp meters** were utilized. The summary of the ramp meter operational modes is presented in Table 7-4. In the similar simulation environment, the ramp metering system was active for 69.4 percent of the analysis. The ramp meter at the bottleneck location (RM1) was in regular mode of operation for 49.4 percent of the analysis, and was in RQO mode for 20.0 percent of the congested period. On the other hand, the ramp meter upstream of the mainline control boundary was active for 36.1 percent of the analysis, all of which was spent in the upstream supplementation mode.

The visualization of the VSL and ramp meter activation relative to the evolution of the queue is presented in Figure 7-3.

Table 7-4: Summary Ramp Meter Operation Modes

Control Device	TOTAL % TIME ON	%Reg	%Supp	%RQO
RM1	69.4%	49.4%	-	20.0%
RM2	36.1%	0.0%	36.1%	0.0%
RM System	69.4%	-	-	-

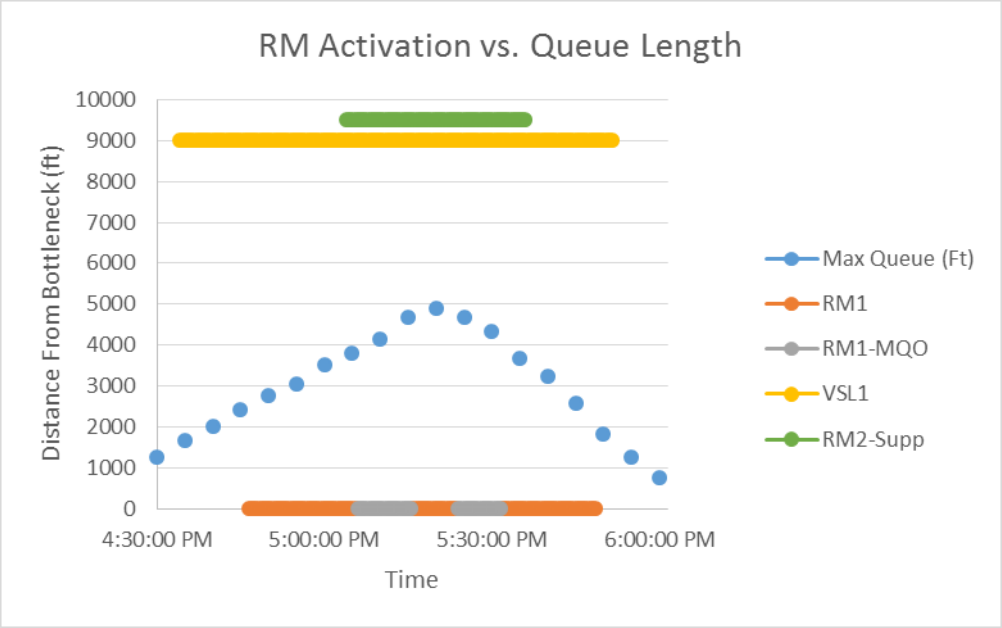

Figure 7-3: Visualization of VSL and RM Utilization

Component-D: Number of Detectors

Step 1: Sub-segment 1 has two points of ingress, the single on-ramp and the upstream mainline boundary. In addition, there are two points of egress, the single off-ramp and the mainline downstream boundary.

Step 2: Equation 6.9 was applied using the parameters from the deployment site. Here, there was a single on-ramp in sub-segment 1 which will be metered. In addition, the upstream on-ramp will also be metered. Thus, the deployment site requires **seven detectors** for VSLRM control.

Component-E: Location of VSL Signs, Ramp Meters, and Detectors

Step 1: Sub-segment 1 is expected to have a maximum speed drop of 30 mph, thus requiring the placement of 3 VSL signs at the upstream boundary. The relative spacing of the signs follows the guidance provided in Table 2C-4 of the 2009 MUTCD for speed and lane changes in heavy traffic. Here the conservative spacing suggested for the free-flow speed of 55 mph was applied. Thus, the **VSL sign spacing is 990 feet**. As shown in Figure 7-4, VSL sign 3 would be placed 990 feet downstream from the upstream boundary of sub-segment 1, VSL sign 2 would be placed 990 feet downstream of VSL sign 1, and VSL sign 3 would be placed 990 feet downstream of VSL sign 2.

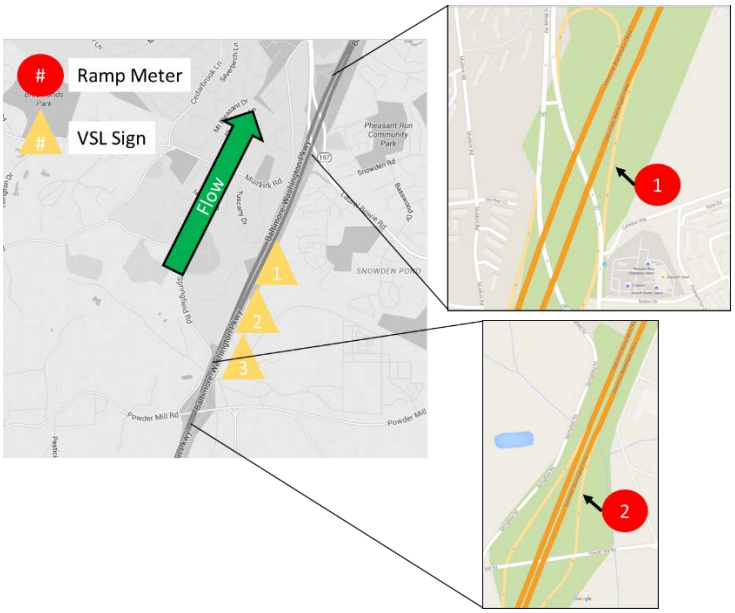

Figure 7-4: Location of VSL Signs and Ramp Meters at Deployment Site

Step 2: Following FHWA guidelines (Jacobson et al. 2010), the location of the ramp meter must allow for motorists to comfortably accelerate to merge condition. Here, the conservative assumption of merging into the free-flow condition (55 mph) was applied. Thus, each ramp meter must give motorists 960 feet to safely merge before the acceleration lane terminates. Figure 7-4 also shows the location of the two required ramp meters.

Step 3: The mainline detectors are placed on the mainline lanes, at the termination of the acceleration lane associated with the on-ramps. The off-ramp detectors shall be placed upstream of the gore of the off-ramp and mainline. The exact location of the off-ramp detector shall consider the potential use of this detector data for other purposes such as the integration of atrial signals with off-ramp demands. Next, in this application, two ramps will be metered, each requiring two detectors. The first detector must be place at the ramp metering location described above. The second detector is placed for maximum queue detection at 75 percent of the on-ramp length, following the guidelines described in Chapter

4. At this site, the length of the bottleneck on-ramp was approximately 1,700 feet and the upstream on-ramp was approximately 1,600 feet. Thus, the **maximum queue detector for each ramp shall be placed at 1,200 and 1,275 feet**, respectively, measured from the gore of the on-ramp and the mainline. The location of the required detectors is shown in Figure 7-5, supplemented by Table 7-4 which describes the function of the detectors.

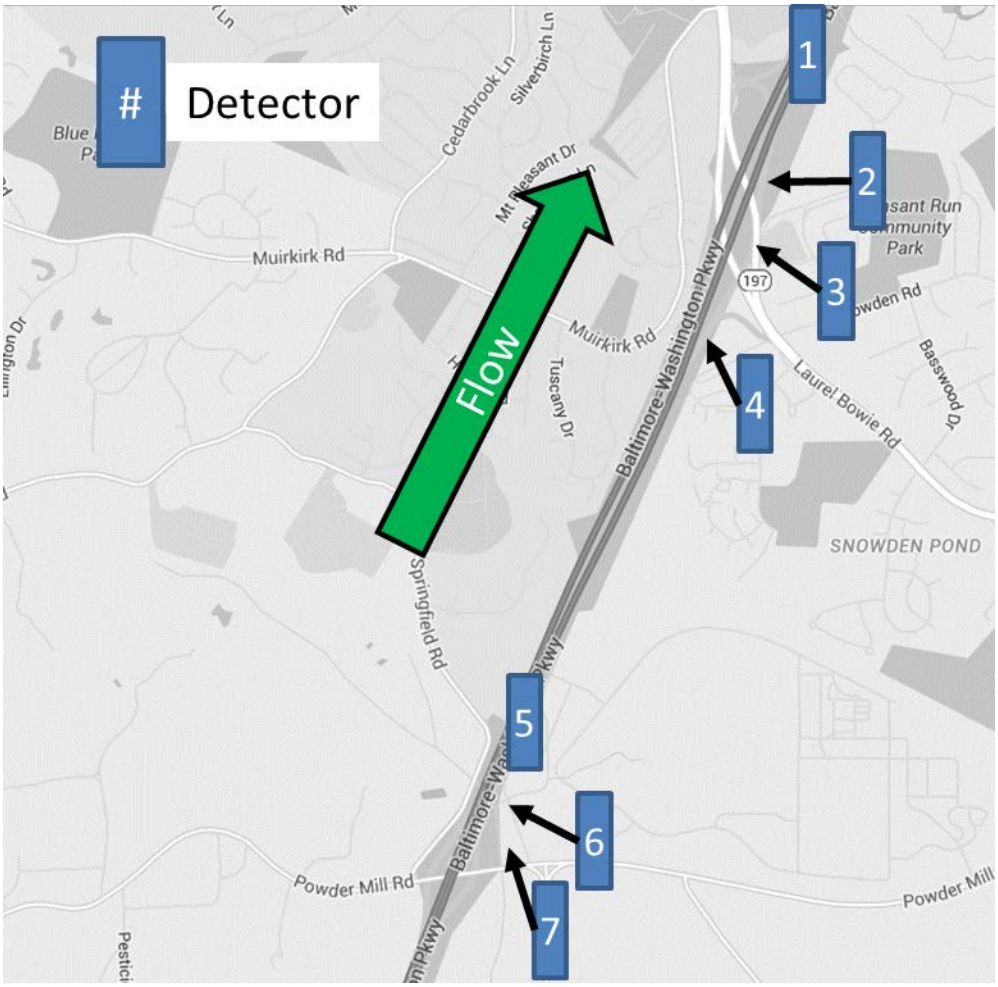

Figure 7-5: Location of Detectors at Deployment Site

Table 7-5: Detector Descriptions for Deployment Site

Detector #	Description
1	Mainline-Downstream Detector for Sub-segment 1
2	On-Ramp 1 Inflow Detector for Sub-segment 1
3	On-Ramp 1 Max Queue Detector for Sub-segment 1
4	Off-Ramp 1 Outflow Detector for Sub-segment 1
5	Mainline-Upstream Detector for Sub-segment1
6	Upstream Supplementary On-Ramp Inflow Detector
7	Upstream Supplementary Ramp Max Queue Detector

7.3 Sample Application Summary

This chapter has illustrated the use of the decision/deployment support tool developed in this dissertation. Using top-ranked bottlenecks from the SHA Mobility Report, a short list of candidate sites was generated for the purpose of demonstrating the application of the tool. Field data for each site was used to calculate the critical traffic flow parameters needed for the tool application. Using the advanced discrete-continuous model, the correlation of the error term in the benefits model was used as an input into the decision model. Here, five of the seven candidate sites were expected to benefit from VSL or VSLRM control. The benefit-to-cost ratios were then used to rank sites. In this application, only the top-ranked site, MD-295 N at MD-197/Exit 111, was considered for VSLRM control deployment. Within the deployment guidelines module, each component was applied using the deployment site data and the output data from the simulated scenario most similar to the deployment site. The resulting analysis provided guidance on the location for each of the VSL signs, ramp meters, and detectors required for VSLRM control. A similar procedure would be followed for VSL control.

Chapter 8: Conclusions and Future Work

8.1 Conclusions and Contributions

To address the need for extensive and consistent planning guidelines for the use of VSL and VSLRM control in recurrent congestion, this dissertation has developed a comprehensive decision/deployment support tool for these ATMS strategies. The structure of the tool was based on the following critical real-world issues related to planning a congestion mitigation project utilizing VSL or VSLRM control:

- *Control Decision:* The first issue in the planning process is to determine if VSL or VSLRM control is expected to provide sufficient benefits to warrant implementation at a given candidate site. When neither strategy is warranted, general explanations should be offered.
- *Site Ranking/Resource Allocation*: Recognizing that most highway agencies will have multiple candidate sites for congestion mitigation projects but not enough available resources to intervene at all of them, guidance is needed to support resource allocation decisions. Specifically, site ranking procedure based on a benefit-cost estimation is required to make informed deployment site selection decisions.
- *Deployment Guidance*: Finally, upon deciding which site(s) will deploy the suggested congestion mitigation strategy, guidance on the location of the VSL signs, ramp meters, and associated detectors is needed to ensure efficient system operation required to achieve the expected benefits.

The effort associated with addressing the aforementioned critical issues related to planning VSL or VSLRM deployment has resulted in the following contributions:

- Generated **1,024** simulated environments to compare the changes in safety and mobility performance measures resulting from VSL and VSLRM control, relative to the no-control case. Using data from a field deployment of VSL control at MD-100, a base scenario was calibrated to reflect observed pattern travel times and bottleneck speeds during the congested period. Upon identifying reasonable ranges of critical variables (i.e. control variables) suspected of influencing the benefits of VSL or VSLRM control, **1,024** potentially congested environments were created. For each environment, simulations were run under no-control, VSL control, and VSLRM control. Then, each control strategy and environment combination was simulated under three random seeds, resulting in **9,216** total simulations. Though other studies have considered the impacts of various parameters such as traffic volume, driver compliance, and control thresholds (Abdel-Aty et al., 2008, Lee et al., 2004, Jiang et al., 2011, etc.), to the best of this author's knowledge, this study has created and evaluated the largest and most diverse dataset for the evaluation of VSL and VSLRM control in recurrent congestion to date.
- Provided valuable insight on the relationship between safety and mobility performance measures under VSL and VSLRM control. Using the outputs of the robust simulated dataset, a general relationship between safety and mobility under VSL and VSLRM control could be investigated. The results of these simulations indicate that there is a positive correlation between safety and mobility performance measures under VSL and VSLRM control. Thus, in general, both measures can be

simultaneously improved under VSL and VSLRM control when the control system is properly implemented and calibrated to the specific conditions of the target site.

- Developed a comprehensive and efficient decision/deployment support tool for addressing the critical issues related to the planning of VSL and VSLRM control. Using the results of the simulated experiments, several models were tested in the development of the Decision Module and the Benefits Module. Ultimately, an advanced discrete-continuous model was found to produce most accurate results for control decisions and estimation of expected benefits. In addition, this study established procedures for planning the deployment of VSL or VSLRM control at a target site, including the location of VSL signs, ramp meters, and detectors.
- Illustrated the application of the decision/deployment support tool. This exercise highlighted the step-by-step process of applying the tool to real-world congestion mitigation candidate sites in the state of Maryland. The output of each of the modules demonstrated the potential of this tool to assist decision-makers in planning for congestion mitigation projects considering the use of VSL or VSLRM control.
- Established a framework for evaluating any ATMS strategy. Though the scope of this study only evaluated VSL and VSLRM control, the general methodology used to build the decision/deployment support may be applied to any ATMS strategy. The results of such research have the potential to streamline the process of analyzing candidate sites for congestion mitigation intervention, thus improving the utilization of limited resources while improving the performance of the transportation network.

- Though this research focused on the planning of VSL and VSLRM control, the outputs of the planning tool can be used to assess the feasibility of independent ramp metering. Obviously, when a particular ramp meter spends a significant amount of time in the ramp queue override mode under VSLRM control, it is reasonable to assume that independent ramp metering will have similar, if not worse, performance. Such results would suggest the need for further investigation of ramp metering at the target site before deploying.

8.2 Future Work

In spite of the significant progress made by this research on the planning of VSL and VSLRM control in recurrently congested environments, several critical issues and challenges remain. Several suggested future research paths are described below:

- In-Depth Statistical Comparison of VSL and VSLRM: Using the dataset generated in this study, a statistical comparison of the safety and mobility benefits of VSL and VLSRM control. These comparisons should analyze the differences in each benefit, between VSL and VSLRM control across the various levels of each of the control variables.
- Advanced VSLRM Coordination Control: The VSLRM control algorithm employed in this study inherently allowed for the ramp metering component to consider the effectiveness of the VSL component by monitoring the conditions within the mainline control sub-segment. However, the VSL component only considered the conditions within the mainline control sub-segment without regard to the mode of operation of the associated ramp meters. In instances where ramp meters are operating in the RQO mode, the VSL component may be able to mitigate the potential for arterial spill-back by allowing for emergency updates to

the VSL system. The potential benefits of such a control strategy, as well as its feasibility for field deployment, should be analyzed.

- Analysis of Spatial Speed Variation under VSL and VSLRM Control: Though the speed variance measure applied in this study offered insight on the safety performance of these ATMS strategies, it did not directly consider the speed difference between each pair of adjacent detectors. Given the speed harmonizing effects of VSL and VSLRM control, this definition of a surrogate measure of safety has the potential to enhance the measured benefits of these control strategies.
- Probe Data-Based Control Strategy: The growing popularity of smart phone-based traveler information systems such as Google Maps and Waze have led to an increased percentage of vehicles serving as probes. This increase in probe data has resulted in higher confidence in the associated real-time performance measures of the highway network. Recognizing the budget constraints of many public transportation agencies, many are turning to innovative data collection technologies to assist in network monitoring and general traffic control that require little or no changes to the infrastructure. To meet this need, many transportation data service providers are conducting research with the objective of developing traffic flow models based on probe data. As this research matures, there is tremendous potential for developing VSL and VSLRM control algorithms based on probe data inputs. Such a system could greatly reduce the cost of implementation and maintenance of an ATMS system by eliminating the need for traditional spot detectors on freeway segments.
- VSL Control in a Connected Vehicle Environment: Acknowledging the potential to improve the safety, mobility, and sustainability of the transportation network, connected

vehicle research is at the forefront of traffic research. Though some early studies (e.g. Wang et. al., 2015) have developed a general framework for a connected vehicle VSL system, more research is needed to validate the results and to inspect the technological and institutional challenges associated with deploying such a control system. This research path should also consider the impact of the critical technology transition period and the impact of human behavior/interaction with connected vehicles. Note that the full potential of connected vehicles depends on motorist adoption/ownership of vehicles equipped with the associated technology. As the overall vehicle fleet transitions to higher percentages of connected vehicles, drivers will need time to become comfortable and confident with the warning messages and automated emergency functions of such vehicles.

References

1. Abdel-Aty, M., Cunningham, R., Gayah, V., and Hsia, L. Dynamic Variable Speed Limit Strategies For Real-time Crash Risk Reduction On Freeways, *Journal of the Transportation Research Board*, No. 2078, pp. 108-116. 2008.
2. Abdel-Aty, M., Dilmore, J., and Hsia, L. Applying Variable Speed Limits and the Potential for Crash Migration, *Journal of the Transportation Research Record*, Vol.1953, pp.21-30. 2006.
3. Abdel-Aty, M., Pande A., and Hsia L. The Concept of Proactive Traffic Management for Enhancing Freeway Safety and Operation, *ITE Journal*, Volume 80, Issue 4, pp 34-41. 2010.
4. Abdel-Aty, M., Pande, A., Lee, C., Gayah, V., and Dos Santos, C. Crash Risk Assessment using Intelligent Transportation Systems Data and Real-time Intervention Strategies to Improve Safety on Freeways. , *ITS Journal*, Vol 11, issue 3, pp. 107-120. 2007.
5. Abouaissa, H., Fliess, M., Iordanova, V., & Join, C. Freeway ramp metering control made easy and efficient. 13th IFAC Symposium on Control in Transportation Systems. Sofia, Bulgaria. 2012.
6. Ahn, K., Trani, A. A., Rakha, H. and Van Aerde, M. Microscopic Fuel Consumption and Emission Models, in Proceedings of the 78th Annual Meeting of the Transportation Research Board, Washington DC, USA. 1999.
7. Alessandri, A., Di Febbraro, A., Ferrara, A. and Punta, E. Nonlinear Optimization for Freeway Control Using Variable-Speed Signaling, IEEE Transactions on Vehicular Technology, vol. 48, no. 6, pp. 2042-2052. 1999.

8. Alessandri, A., Di Febbraro, A., Ferrara, A. and Punta, E. Optimal Control of Freeways via Speed Signaling and Ramp Metering. Control Engineering Practice. vol. 6. pp. 771–780. 1998.
9. Allaby, P., Hellinga, B. and Bullock, M. Variable Speed Limits: Safety and Operational Impacts of a Candidate Control Strategy for an Urban Freeway, IEEE Transactions on Intelligent Transportation Systems, vol. 8, no. 4, pp. 671-680. 2007.
10. Bertini, R., Bogenberger, K. and Boyce, S. Impact of Driver Information System on Traffic Dynamics on a German Autobahn: Lessons for U.S. Applications 12th World Congress on Intelligent Transport Systems. 2005.
11. Bertini, R., Boice, S., and Bogenberger, K. "Dynamics of Variable Speed Limit System Surrounding Bottleneck on German Autobahn." Transportation Research Record: Journal of the Transportation Research Board, No. 1978, Transportation Research Board of the National Academies, Washington, D.C. pp. 149–159. 2006.
12. Bham, G., Long, S., Baik, H., Ryan, T., Gentry, L., Lall, K., Arezoumandi, M., Liu, D., Li, T., Schaeffer, B. Evaluation of variable speed limits on I-270/I-255 in St. Louis. Missouri DOT. Report No. OR 11-014. 2010.
13. Breton, P., Hegyi, A., De Schutter B., and Hellendoorn, H., "Shock wave elimination/ reduction by optimal coordination of variable speed limits," in *Proceedings of the IEEE 5th International Conference on Intelligent Transportation Systems*, Singapore, Sept. 3–6 2002.
14. Buddemeyer, J., Young, R., and Dorsey-Spitz, B. Rural Variable Speed Limit System for Southeast Wyoming. 89th TRB Annual Meeting, Washington D.C. 2010.
15. Caliendo, C., Guida, M., Parisi, A. A crash-prediction model for multilane roads. Accident Analysis and Prevention *vol.*39, pp. 657-670. 2007.

16. Carlson, R., Papamichail, I., Papageorgiou, M. & Messmer, A. Optimal Motorway Traffic Flow Control Involving Variable Speed Limits and Ramp Metering. *Transportation Science*. *vol* 44, pp. 238–253. 2010A.

17. Carlson, R., Papamichail, I., Papageorgiou, M. Local Feedback-Based Mainstream Traffic Flow Control on Motorways Using Variable Speed Limits. IEEE Transactions On Intelligent Transportation Systems. Vol. 12, No. 4, pp.1261-1276. 2011.

18. Carlson, R.C., Papamichail, I.,Papageorgiou, M. and Messmer,A. Optimal Mainstream Traffic Flow Control of Large-scale Motorway Networks. Transportation Research Part C, vol. 18, no. 2, pp. 193-212. 2010B.

19. Chang, G.L., Park, S.Y., and Paracha, J. "ITS Field Demonstration: Integration of Variable Speed Limit Control and Travel Time Estimation for a Recurrently Congested Highway. Transportation Research Board 90th Annual Conference. Washington, D.C. 2011.

20. Chen, D., Soyoung, A., and Hegyi, A.. Variable Speed Limit Control for Steady and Oscillatory Queues at Fixed Freeway Bottlenecks. Transportation Research Part B: Methodological 70: 340-358. 2014.

21. Chien, C., Zhang, Y. and Ioannou, P.A. Traffic Density Control for Automated Highway Systems. Automatica, Vol. 33. No. 7. pp. 1273-1285. 1997.

22. Cirillo, C., Liu, Y., and Tremblay, J.M. Ordered and Unordered Discrete-Continuous Models: A Comparative Analysis for Household Vehicle Holding and Mileage Traveled Decisions. Transportation Research Board 92nd Annual Conference. Washington, D.C. 2013.

23. Cunningham, R. Examining Dynamic Variable Speed Limit Strategies for the Reduction of Realtime Crash Risk on Freeways. Master's Thesis, University of Central Florida, Orlando, FL. 2007.

24. Daganzo, C. The Cell Transmission Model: A Dynamic Representation of Highway Traffic Consistent with the Hydrodynamic Theory. Transportation Research Part B, Vol. 28, No. 4, pp.269-287. 1994.

25. Deryushkina, O. Design and Evaluation of a Probe-based Variable Speed Limit Algorithm in PARAMICS, Master's Thesis, Department of Civil Engineering, University of Calgary. 2012.

26. Dhindsa, A.S. Evaluating Ramp Metering and Variable Speed Limits to Reduce Crash Potential on Congested Freeways Using Micro-Simulation. Master's Thesis. Indian Institute of Technology. 2005.

27. Fang, J. Luo, Y. Hadiuzzaman, M.; Liu, G. Qiu, T.Z. Safety Oriented Variable Speed Limit Control Method with Enhanced Driver Response Modeling. Transportation Research Board 94nd Annual Conference. Washington, D.C. 2015.

28. Fudala, N. and Fontaine, M. Work Zone Variable Speed Limit Systems: Effectiveness and System Design Issues. Virginia Transportation Research Council. Report # FHWA/VTRC 10-R20. Charlottesville, VA. 2010.

29. Goodwin, L., and Pisano, P. Best Practices for Road Weather Management. FHWA Report OP-03-081. 2003.

30. Grumert, E., Ma, E., and Tapani, A. Analysis of a Cooperative Variable Speed Limit System using Microscopic Traffic Simulation. Transportation Research Part C: Emerging Technologies. 2014.

31. Grumert, E., Ma, X. and Tapani, A. Effects of a Cooperative Variable Speed Limit System on Traffic Performance and Exhaust Emissions. Transportation Research Board 92nd Annual Conference. Washington, D.C. 2013.

32. Hadiuzzaman, M. and Qiu, T. Cell Transmission Model Based Variable Speed Limit Control for Freeway. Compendium of papers CD-ROM, Transportation Research Board 2012 Annual Meeting, Washington, D.C. 2012.

33. Hadj-Salem, H., Blosseville, J. and Papageorgiou, M. ALINEA: a local feedback control law for on-ramp metering; a real-life study. Third International Conference on Road Traffic Control. 1990.

34. Haleem, K. M. Exploring the Potential of Combining Ramp Metering and Variable Speed Limits Strategies for Alleviating Real-Time Crash Risk on Urban Freeways. Master's Thesis. University of Central Florida. Orlando, FL. 2007.

35. Harbord, B. M25 controlled motorway-results of the first two years. In: Proceedings of the Road Transport Information and Control, pp. 149-154. 1998.

36. Hasan, M. Evaluation of Ramp Control Algorithms Using Microscopic Traffic Simulation, Master of Science Thesis. Massachusetts Institute of Technology. 1999.

37. Hegyi, A. and Hoogendoorn, S. Dynamic speed limit control to resolve shock waves on freeways –Field test results of the SPECIALIST algorithm. Annual Conference on Intelligent Transportation Systems, Madeira Island, Portugal. 2010.

38. Hegyi, A. Model Predictive Control for Integrating Traffic Control Measures. Doctoral Dissertation. Delft University of Technology, Netherlands. 2004.

39. Hegyi, A., De Schutter, B. and Hellendoorn, J. Optimal Coordination of Variable Speed Limits to Suppress Shock Waves, IEEE Transactions on Intelligent Transportation Systems, vol. 6, no. 1, pp. 102-112. 2005A.

40. Hegyi, A., De Schutter, B., and Hellendoorn, H. Model Predictive Control for Optimal Coordination of Ramp Metering and Variable Speed Limits. *Transportation Research Part B.* Vol 13C. No. 3. pp. 185-209. 2005B.

41. Hellinga, B. and Allaby, P. The Potential for Variable Speed Control to Improve Safety on Urban Freeways. Transportation Association of Canada Annual Conference. Saskatoon, Saskatchewan. 2007.

42. Heydecker, B. G., and Addison, J. D. Analysis and modeling of traffic flow under variable speed limits. *Transportation Research Part C* 19:206–217. 2011.

43. Highway Agency Publications Group. Summary Report: M25 Controlled Motorways. Bristol, UK. 2007.

44. Hoogerndoorn, S.P., Daamen, W., Hoogendoorn, R.G.and Goemans, J.W. Assessment of Dynamic Speed Limits on Freeway A20 near Rotterdam, the Netherlands. Transportation Research Board 92nd Annual Conference. Washington, D.C. 2013.

45. Hou, Z., Xu, JX. And Zhong, H. Freeway Traffic Control Using Iterative Learning Control-Based Ramp Metering and Speed Signaling. IEEE Transactions on Vehicular Technology, Vol. 56. No. 2. pp. 466-477. 2007.

http://www-03.ibm.com/software/products/en/spss-decision-trees

46. IBM. SPSS Decision Trees. Accessed February 1, 2015.

47. Jiang, R., Chang, E., and Lee, J. “Variable Speed Limits: Conceptual Design for Queensland Practice.” Australian Transport Research Forum, Adelaide, Australia. 2011.

48. Jonkers, E. and Klunder, G. Development of an Algorithm for Using Dynamic Speed Limits in Relation to the Weather Situation. 15th World Congress on Intelligent Transport Systems and ITS America's Annual Meeting. New York, U.S. 2008.

49. Kang K. and Chang G. Development of Integrated Control Algorithm for Dynamic Lane Merge and Variable Speed Limit Controls. 11th World Conference on Transport Research 2007.

50. Kang, K, G. Chang and N. Zou, *Optimal Dynamic Speed-Limit Control for Highway Work Zone Operations*, Transportation Research Record: Journal of the Transportation Research Board, No. 1877, TRB, National Research Council, Washington, D.C. pp. 77–84. 2004.

51. Kattan, L. Khondaker, B., Derushkina, and Poosarla, E. A Probe-Based Variable Speed Limit System. Journal of Intelligent Transportation Systems: Technology, Planning, and Operations. 2014.

52. Kianfar, H. Edara, P. and Sun, C. Operational Analysis of a Freeway Variable Speed Limit System- Case Study of Deployment in Missouri. Transportation Research Board 92nd Annual Conference. Washington, D.C. 2013.

53. Kononov, J., Durso, C., Reeves, D., Allery, B. Relationship between traffic density, speed and safety and its implication on setting variable speed limits on freeways. Transportation Research Record. Vol. 2280. pp. 1-9. 2012.

54. Krajzewicz, D. Traffic Simulation with SUMO - Simulation of Urban Mobility. In J. Barceló (Ed.), *Fundamentals of Traffic Simulation.* Vol. 145, pp. 269-293. New York Dordrecht Heidelberg London: Springer. 2010.

55. Kwon, E., Brannan, D., Shouman, K., Isackson, C. and Arseneau, B. Development and Field Evaluation of Variable Advisory Speed Limit System for Work Zones, Transportation Research Record, pp. 12-18. 2007.

56. Kwon, E., Park, C., Lau, D. and Kary, B. Minnesota Variable Speed Limit System: Adaptive Mitigation of Shock Waves for Safety and Efficiency of Traffic Flows. Transportation Research Board 90th Annual Conference. Washington, D.C. 2011A.

57. Kwon, E., Park, C., Lau, D., Kary, B. Development and field assessment of variable advisory speed limit system. Proceedings of the 18th ITS World Congress Orlando. 2011B.

58. Layton, E., Young, R. Effects on speeds of a rural variable speed limit system, Proceedings of the 18th ITS World Congress. Orlando, FL. 2011.

59. Lee, C. and Abdel-Aty, M. Testing *Effects of Warning Messages and Variable Speed Limits on Driver Behavior Using Driving Simulator*, Transportation Research Record: Journal of the Transportation Research Board, No. 2069, Transportation Research Board of the National Academies, Washington, D.C., pp. 55-64. 2008.

60. Lee, C., F. Saccomanno, and B. Hellinga. Analysis of Crash Precursors on Instrumented Freeways. In *Transportation Research Record: Journal of the Transportation Research Board, No. 1784*, TRB, National Research Council, Washington, D.C. pp. 1–8. 2002.

61. Lee, C., Hellinga, B. and Saccomanno, F. Real-time crash prediction model for application to crash prevention in freeway traffic. Transportation Research Record 1840, pp. 67-77. 2003.

62. Lee, C., Hellinga, B., and Saccomano, F. Assessing Safety Benefits of Variable Speed Limits. Transportation Research Record. No. 1897. Washington, D.C. pp.183-190. 2004.

63. Lee, J., Kim, Y., Cho, H. Analysis and evaluation of traffic flow at variable speed limit using the cell transmission model. Proceedings of the 17th ITS World Congress Busan. 2010.

64. Lenz, H., Sollacher, R. and Lang, M. Nonlinear speed-control for a continuum theory of traffic flow. 14th World Congress of IFAC, vol. Q. Beijing, China, pp. 67–72. 1999.

65. Lenz, H., Sollacher, R., and Lang, M. Standing waves and the influence of speed limits. Proceedings of the European Control Conference 2001, Porto, Portugal, pp. 1228–1232. 2001.

66. Lin, P., Kang, P., Chang, G. L. Exploring the Effectiveness of Variable Speed Limit Controls on Highway Work-Zone Operations. Intelligent Transportation Systems. vol. 8, pp. 155–168. 2004.

67. Liu, W., Yin., Y. and , Yang, H. Effectiveness of Variable Speed Limits Considering Commuters' Long-Term Response. Transportation Research Part B: Methodological,. December 2014.

68. Lu, X. Y., Qiu, T. Z., Varaiya, P., Horowitz R. and Shladover, S. E. Combining Variable Speed Limits with Ramp Metering for Freeway Traffic Control, *IEEE American Control Conference*. pp 2266-2271. 2010A.

69. Lu, X.Y., Varaiya, P., Horowitz, R., Su, D. and Shladover, S. A Novel Freeway Traffic Control with Variable Speed Limit and Coordinated Ramp Metering. Transportation Research Board 90th Annual Conference. Washington, D.C. 2011.

70. Lu, X.Y.; Shladover, S. Jawad, I., Jagannathan, R., Phillips, T. A Novel Speed-Measurement Based Variable Speed Limit/Advisory Algorithm for a Freeway Corridor with Multiple Bottlenecks. . Transportation Research Board 94nd Annual Conference. Washington, D.C. 2015.

71. Lu, Xiao-Yun, and Steven E. Shladover. Review of Variable Speed Limits and Advisories: Theory, Algorithms and Practice. Transportation Research Record: Journal of the Transportation Research Board 2423.1 15-23. 2014.

72. Lu, Y., X., Qiu, T.Z., Varaiya, P., Horowitz, R. and Shladover, S.E. Combining variable Speed Limits with ramp Metering for Freeway Traffic Control, American Control Conference, Baltimore, USA. 2010B.

73. Lyles, R.W., Taylor, W.C., Lavansiri, D. and Grosskalaus, J. A Field Test and Evaluation of Variable Speed Limits in Work Zones, Transportation Research Board Annual Meeting. 2004.

74. Malyshkina, N., Mannering, F., Tarko, A. Markov switching negative binomial models: An application to vehicle accident frequencies. Accident Analysis and Prevention, vol.41, pp.217-226. 2009.

75. McLawhorn, N. Variable speed limits signs for winter weather. Transportation Syntheses Report. WisDOT, April 9th, 2003.

76. McMurtry, T., Saito, M., Riffkin, M. and Heath, S. Variable Speed Limits Signs: Effects On Speed and Speed Variation in Work Zones, 88th Transportation Research Board Annual Meeting, Washington, D.C. 2009.

77. MD-100 Segment from Telegraph Road to I-95. Google Maps. http://maps.google.com. Accessed May 4, 2013.

78. Mirshahi, M., Obenberger, J., Fuhs, C., Howard, C., Krammes, R., Kuhn, B., Mayhew, R., Moore, M., Sahebjam, K., Stone, C., and Yung, Jessie. Active traffic management: The next step in congestion management. FHWA-PL-07-012. Washington, D.C. 2007.

79. Nicholson, R.T., Crumley, S.C., Romero, M. and Usman Ali, S. Field Implementation of Variable Speed Limits on the Capital Beltway (I-95/I-495) for the Woodrow Wilson Bridge Project. Transportation Research Board 90th Annual Conference. Washington, D.C. 2011.

80. Nissan, A. Evaluation of Variable Speed Limits: Empirical Evidence and Simulation Analysis of Stockholm's Motorway Control System. Doctoral Dissertation. Royal Institute of Technology. Stockholm, Sweden, 2010.

81. Nissan, A., and Koutsopoulos, H. Evaluation of the impact of advisory variable speed limits on motorway capacity and level of service. 6th International Symposium on Highway Capacity and Quality of Service Procedia Social and Behavioral Sciences, Stockholm, Sweden, pp. 100-109. 2011.

82. Pan, S., Jia, L., Zou, N., Park, S. Design and implement of a variable speed limit system with travel time display – a case study in MD, USA. 17th ITS World Congress Busan 2010. Busan, Korea. 2010.

83. Papageorgiou, M. and Kotsialos, A. Freeway ramp metering: An overview, IEEE Transactions on Intelligent Transportation Systems, vol. 3, no. 4, pp. 271-280. 2002.

84. Papageorgiou, M. Kosmatopoulos, E., and Papamichail, L. "Effects of Variable Speed Limits on Motorway Traffic Flow." Transportation Research Record, No. 2047, Transportation Research Board of the National Academies, Washington, D.C. pp. 37-48. 2008.

85. Papageorgiou, M., Haj-Salem, H., Blosseville, J-M. ALINEA: A local feedback control law for on-ramp metering. Transportation Research Record 1320, 58–64. 1991.

86. Papageorgiou, M., Haj-Salem, H., Middleham, F. ALINEA local ramp metering: summary of field results. Transportation Research Record 1603, 90–98. 1997.

87. Park, B. and Yadlapati, S.S. Development and Testing of Variable Speed Limit Logics at Work Zones using Simulation, Compendium of Papers from the 82nd Transportation Research Board held in Washington D.C. 2003.

88. Placer, J. Fuzzy Variable Speed Limit Device Modification and Testing- Phase II. Arizona Department of Transportation Report 466(2).Flagstaff, AZ. 2001.

89. Placer, John, Sagahyroon, Assim, and Harper, John. “Design of a Fuzzy Variable Speed Limit System for Rural Highways,” Rural Advanced Technology and Transportation Systems 1998 International Conference. University Park, Pennsylvania. Enhancing Safety and Mobility in Rural America. Pennsylvania State University, 1998.

90. Quadstone Limited. PARAMICS Modeler. Edinburgh, UK. 2015.

91. Radwan, E., Zaidi, Z. and Harb, R. Operational Evaluation of Dynamic Lane Merging in Work Zones with Variable Speed Limits. Procedia Social and Behavioral Sciences 16. pp. 460–469. 2011.

92. Rämä, P. Effects of weather-controlled variable speed limits and warning signs on driver behavior. Transportation Research Record: Journal of the Transportation Research Board, Vol.1689, pp.53-59. 1999.

93. Ramazani, H. Benekohal, R., Avrenli, K.Determining Queue and Congestion in Highway Work Zone Bottlenecks. NEXTRANS Project No. 046IY02. 2011.

94. Robinson, M. Examples of Variable Speed Limit Applications. Prepared for the Speed Management Workshop at Transportation Research Board 79th Annual Conference. Washington, D.C. 2000.

95. Saidi, S. and Kattan, L. Coordinated Proactive Ramp Metering Algorithm Based on Probe Vehicle Technology, in Proceedings of the 13th Conference on Intelligent Transportation, Madeira, Portugal. 2010.

96. Schrank, D. Eisele, B., Lomox, T., and Bak, J. 2015 Urban Mobility Scorecard. Texas Transportation Institute and INRIX. 2014

97. Smaragdis, E., Papageorgiou, M.and Kosmatopoulos, E. A flow-maximizing adaptive local ramp metering strategy. *Transportation Research B*, 38:251–270, 2004.

98. Steel, P. and McGregor, R. Application of Variable Speed Limits along the Trans-Canada Highway in Banff National Park. Annual Conference of the Transportation Association of Canada, September 2005 in Calgary, Canada. 2005.

99. Su, D., Lu, XY., Varaiya, P., Horowitz, R., and Shladover, S.E. Variable Speed Limit and Ramp Metering Design for Congestion Caused by Weaving. Transportation Research Board 90th Annual Conference. Washington, D.C. 2011.

100. Transport Simulation Systems (TSS). Aimsun. Barcelona, Spain. 2015.

101. Ulfrasson, G. and Shankar, V. The effect of variable message and speed limit signs on mean speeds and speed deviations. International Journal of Vehicle Information and Communication Systems. Vol. 1, pp. 69-87. 2005.

102. United States Department of Transportation. Intelligent Transportation Systems Cost Database. Accessed July 11, 2015. http://www.itscosts.its.dot.gov/

103. Van den Hoogen, E. and Smulders, S. Control by variable speed signs: results of the Dutch experiment, in 7th International Conference on Road Traffic Monitoring and Control, IEE Conference Publication No. 391, London, England, pp. 145-149. 1994.

104. Waller, S., Ng, M., Ferguson, E., Nezamuddin, Sun, D. Speed harmonization and peak-period shoulder use to manage urban freeway congestion. FHWA. 2009.

105. Wang, M. Daamen, W. Hoogendoorn, S.P., and Van Arem, B. Connected Variable Speed Limits Control and Vehicle Acceleration Control to Resolve Moving Jams. Transportation Research Board 94nd Annual Conference. Washington, D.C. 2015.

106. Wang, Y. and Ioannou, P. A New Model for Variable Speed Limits. Compendium of papers CDROM, Transportation Research Board 2011 Annual Meeting, Washington, D.C. 2011.

107. Wang, Y., Papageorgiou, M., Gaffney, J., Papamichail, I., & Guo, J. Local ramp metering in the presence of random-location bottlenecks downstream of a metered on-ramp. In *Intelligent Transportation Systems (ITSC), 2010 13th International IEEE Conference on* (pp. 1462-1467). IEEE. 2010.

108. Xu, C. Wang, X. and Chen, X. Urban Expressway Speed Spatial Inconsistency and its Effect on Safety. Transportation Research Board 91st Annual Conference. Washington, D.C. 2012.

109. Yang, Y., Lu, H., Yin, Y. and Yang, H. Optimizing Variable Speed Limits for Efficient, Safe and Sustainable Mobility. Transportation Research Board 92nd Annual Conference. Washington, D.C. 2013B.

110. Ying, L. and Chow, H.F. Optimization of Motorway Operations via Ramp Metering and Variable Speed Limits. Transportation Planning and Technology. 38.1: 94-110. 2015.

111. Yu, R. and Abdel-Aty, M. Bayesian random effect models incorporating real-time weather and traffic data to investigate mountainous freeway hazardous factors. Accident Analysis and Prevention 50: 371-6. 2013.

112. Zegeye, S.K., De Schutter, B., Hellendoorn, H. and Breunesse, E. Reduction of Travel Times and Traffic Emissions Using Model Predictive Control, Proceedings of the 2009 American Control Conference, St. Louis, Missouri, pp. 5392-5397. 2010.